



Melanie Mayr

THE DELTA E VALUE AS A PREDICTOR FOR
SILICONE COVERAGE IN RELEASE PAPER
PRODUCTION

Master thesis

Thesis supervisors:

Univ.-Prof. Dipl.-Ing. Dr.techn. Wolfgang Bauer
Josef Glawogger

Graz University of Technology
Institute for Paper Pulp and Fiber Technology

Graz, 28.11.2013

STATUTORY DECLARATION

I declare that I have authored this thesis independently, that I have not used other than the declared sources / resources, and that I have explicitly marked all material which has been quoted either literally or by content from the used sources.

.....
date

.....
(signature)

ABSTRACT

Release base paper production is the first step in the manufacturing process of self-adhesive laminates. A silicone layer is applied to the release base paper surface functioning as a barrier layer between the paper and the self - adhesive label. It is of utmost importance to obtain a closed silicone layer to prevent the adhesive from contact with the release base paper. Especially in industrial applications of self – adhesive laminates it is important that the labels can be released from the release liner (release base paper and silicone) uniformly. Silicone coverage is tested by a colour stain test, colouring the defects in the silicone layer. The more defects and the larger the defects are the higher is the colour difference ΔE , between the unstained and stained release liner, evaluated by a colorimetric measurement. The ΔE results as a measure for silicone coverage show only a poor correlation with the measured quality parameters describing the release base paper. The first possible reason for this observation is that a parameter is missing in the quality control of the release base paper, which cannot be described by other standard quality parameters. The second possibility is, that the ΔE value does not explain silicone coverage only. In this thesis these two possibilities are discussed. New methods allowing a more detailed description of relevant release base paper properties are presented. The ΔE test is evaluated in detail and the results are compared with a newly developed method for the detection of defects in the silicone layer. A model for the prediction of silicone coverage by release base paper quality parameters is determined using multiple linear regression analysis and these quality parameters and their relation to local paper properties are discussed.

KURZFASSUNG

Trennbasispapierherstellung ist der erste Schritt in der Produktion von selbstklebenden Etiketten. Eine Silikonschicht dient als Barriere zwischen dem Kleber der Etikette und dem Basispapier. Es ist von größter Bedeutung, dass diese Silikonschicht das Basispapier geschlossen überzieht, um den Kontakt zwischen Kleber und Basispapier zu verhindern. Vor allem in industriellen Anwendungen von selbstklebenden Etiketten ist es wichtig, dass die Etiketten vom Trennpapier (Basispapier mit Silikonschicht) gleichmäßig abgezogen werden können. Die Bestimmung der Silikonabdeckung erfolgt durch die Färbung von Defekten in der Silikonschicht. Je mehr Defekte auftreten und je größer diese Defekte sind, desto höher ist die Farbdifferenz ΔE , zwischen dem ungefärbten und dem gefärbten Trennpapier, die mit einer farbmetrischen Messung bestimmt wird. Die ΔE Werte als Maß für die Silikonabdeckung weisen nur eine geringe Korrelation mit den gemessenen Qualitätsparametern des Basispapiers auf. Das Fehlen eines wichtigen Qualitätsparameters zur Beschreibung der Silikonabdeckung ist eine mögliche Erklärung. Eine weitere Möglichkeit wäre, dass der ΔE Wert nicht nur die Silikonabdeckung erklärt, sondern auch von anderen Faktoren beeinflusst wird. In dieser Arbeit werden diese beiden Möglichkeiten diskutiert. Neue Methoden, die eine detailliertere Beschreibung von relevanten Basispapiereigenschaften ermöglichen werden vorgestellt. Der ΔE Test wird im Detail untersucht und die Ergebnisse werden mit einem neu entwickelten Verfahren zum Nachweis von Defekten in der Silikonschicht verglichen. Ein Modell für die Vorhersage der Silikonabdeckung mit den Qualitätsparametern des Basispapiers wird durch multiple lineare Regressionsanalyse ermittelt und diese Qualitätsparameter und deren Verhältnis zu lokalen Papiereigenschaften werden diskutiert.

ACKNOWLEDGEMENTS

I would like to thank Prof. Dr. Wolfgang Bauer for his great support, for helping me with problems, for his encouragement and for the supervision of my master thesis. I also want to thank Josef Glawogger for the possibility to write my thesis for the Dunafin paper mill in Hungary, where I spent the first month of my work. Because of my nice colleges there I immediately felt at home.

At this point I would like to thank Ágnes Pinter, who helped me with the administrative procedures and also thank you for the nice chats. I want to thank all my colleagues from Dunafin for their support, where I would like to mention particularly Ildiko Dutkova, who provided me with information and material from the time on I continued my thesis in Graz, Tuomas Turtola for the interest he showed in the technical discussions about my work and Fabrizio Gaiero for the support with background information to release base papers, which was a completely new topic for me.

Back at the Institute for Paper, Pulp and Fibre Technology at TU Graz, thanks to Ass.Prof.Dr. Ulrich Hirn for his advice and explanations for the regression analysis part of my thesis. I am grateful to Adelheid Bakhsi, for the support in the laboratory, Harald Streicher for the help with the EDV and Michael Dauer for the help with MATLAB. Thanks to all my colleagues on the institute for the great working atmosphere and helping me out when I had a question.

Finally I would like to thank my family my parents Marianne and Karl for their support and their understanding, my grandmother Maria and my brothers Philipp and David and my sister Sarah. At last I would like to thank my boyfriend Michal, who listened to my problems and for his great patience.

Melanie Mayr
Graz, 28.11.2013

CONTENTS

1.	Introduction:	1
1.1.	Scope of this thesis	1
1.2.	Self - adhesive laminates	1
2.	Release liner for industrial applications:	3
2.1.	Production of the silicone base paper:	3
2.1.1.	Production process:	3
2.1.2.	Functional chemicals:	4
2.1.3.	PVA function and chemistry	4
2.2.	Silicone application on release base papers:	5
2.2.1.	Chemistry of the silicone and additives:	5
2.2.2.	Silicone systems:	7
2.2.3.	Reactions and inhibition:	8
2.2.4.	Application machines and converting process:	11
2.3.	Base paper requirements and quality parameters:	13
2.4.	Release liner requirements and quality parameters:	15
3.	Description of the delta E test:	18
3.1.	Introduction of the colorant and the colour space:	18
3.2.	Differentiation in the test parameters:	20
3.3.	Delta E test procedure:	22
3.4.	Evaluation of additional parameters using image analysis:	23
3.4.1.	Description of structure size analysis:	23
3.4.2.	Parameters generated from image analysis:	26
4.	Overview of measurement methods and analysis routines:	30
4.1.	Development of a method to characterize PVA coverage and distribution:	30
4.2.	Method and field of application for silicone negatives from base paper and release liner surfaces:	31
4.2.1.	Method of taking silicone negatives:	31
4.2.2.	Infinite focus measurement:	32
4.3.	Local comparison of various paper properties:	33

4.3.1.	Marking of the samples:.....	34
4.3.2.	Registration using the markings:.....	34
4.4.	Multiple linear regression:.....	35
4.5.	Additional quality parameters:	35
4.6.1.	Surface pH:.....	35
4.6.2.	Contact angle:.....	36
4.6.	Standard methods to describe the quality of release base papers:.....	36
5.	Results and discussion:	37
5.1.	Evaluation of the delta E test:.....	37
5.1.1.	Possible influential factors on the delta E test results:.....	37
5.1.2.	Release base paper - colorant interaction:.....	40
5.1.3.	Stability of the colorant.....	47
5.1.4.	L*a*b* colour space and L*a*b* measurement:	51
5.1.5.	Execution of the delta E test.....	52
5.2.	Discussion of variability of measurement data for the use in multiple linear regression analysis.....	60
5.3.	Prediction of the delta E value and silicone coverage using multiple linear regression analysis:.....	65
5.3.1.	Prediction of delta E:.....	66
5.3.2.	Prediction of silicone coverage:.....	71
5.3.3.	Additional response variables:	78
5.4.	Evaluation of silicone coverage by the comparison of 2D data maps:....	81
6.	Conclusions:.....	86
6.1.	Delta E value:	86
6.2.	Silicone coverage:	87
7.	Outlook.....	89
A.	Appendix:.....	91
A.1.	New methods: detailed test procedure:.....	91
A1.1.	method to characterize PVA coverage and distribution:.....	91
A1.2.	Method for silicone negatives from base paper and release liner surfaces:	93
A.2.	Release base paper colorant interaction:.....	96
A.3.	Stability of the colorant:	97
A.4.	Standard error and sample volume:	97
A.5.	Variability of measurement data and process fluctuations:	98

A.6. Prediction of silicone coverage and delta E using multiple linear regression analysis:.....	100
A.7. Evaluating quality issues of silicone coverage by the comparison of 2D data maps:	102
Bibliography.....	104

LIST OF FIGURES

Figure 1-1: Components of a self adhesive laminate ([14])	2
Figure 2-1: Polymerisation of vinylacetate.....	4
Figure 2-2: Alcoholysis of polyvinylacetate.....	4
Figure 2-3: Structure and chemical formula of polydimethylsiloxane ([1]), ([9]).	6
Figure 2-4: Chemical formulas of a crosslinker (1) and a Pt – catalyst (2), ([9]), ([4]).	6
Figure 2-5: Structure and chemical formula of dimethyl silicone resins ([1]), ([2])...	7
Figure 2-6: Silicone systems.....	7
Figure 2-7: Reactions of silicone and crosslinker ([3]).	9
Figure 2-8: Side reactions of the silicone with the substrate ([3]).....	10
Figure 2-9: Silicone application machines ([14]), ([12]).....	12
Figure 2-10: The functional role of the release base paper in the subsequent converting steps ([14])	14
Figure 2-11: Release force test ([14]).....	17
Figure 3-1: Malachite green ([18])	19
Figure 3-2: L*a*b* colour space and determination of L*a*b* ([20])	20
Figure 3-3: Differences in the delta E test	21
Figure 3-4: Separation and binarisation of stained and non – stained areas.....	23
Figure 3-5: Corelation of the stained area, evaluated with image analysis and the delta E value for one delta E test series.	24
Figure 3-6: Correlation of colored area determined using a bandpass filter and the delta E value.....	25
Figure 3-7: Density distribution for a base paper with different silicone coat weights	27
Figure 3-8: Development of the delta E value	28
Figure 3-9: Development of the ratio (stained spot size).....	29
Figure 4-1: Examples showing differences in PVA coverage	31
Figure 4-2: Infinite Focus Measurment device (Alicona) ([28])	33
Figure 4-3: Marked 2D – datamap with identified coordinate system	34
Figure 5-1: Influence of the surface pH on the delta E result.....	40
Figure 5-2: Differences in the spreading properties of malachite green.....	43
Figure 5-3: Spectra of unstained and stained white and yellow grades.....	45
Figure 5-4: Difference in light absorbtion of a yellow and a white grade with different silicone coat weights	45
Figure 5-5: Differences in the spectra, within a multiple use of the colorant solution	49
Figure 5-6: Differences in the spectra of a release base paper and a release liner ...	51

Figure 5-7: Different device settings	52
Figure 5-8: Development of the delta E test result with the penetration time	53
Figure 5-9: Development of coloured area for different colorants with increasing penetration time	55
Figure 5-10: Comparison of spreading and absorption properties of different colorantants for different penetration times	56
Figure 5-11: Variability of the delta E values: Comparison of two siliconizing trials	59
Figure 5-12: Comparison of Cobb values from different laboratories	61
Figure 5-13: Relative measurement range and variability of measurement data	63
Figure 5-14: Prediction of delta E with MLR (all parameters).....	67
Figure 5-15: Prediction of delta E with MLR (final model).....	68
Figure 5-16: Correlation and coefficient of determinations (MLR delta E).....	69
Figure 5-17: Prediction of delta E with MLR (Final Model) including P_{total}	70
Figure 5-18: Area distribution of the scanned delta E test image and the defects of the silicone negatives (same base paper)	72
Figure 5-19: Area distribution of the scanned delta E test image and the defects of the silicone negatives (same base paper)	72
Figure 5-20: Prediction of P_{total} with MLR (all parameters).....	73
Figure 5-21: Prediction of P_{total} with MLR (final model)	74
Figure 5-22: Correlation and coefficients of determination (MLR P_{total})	75
Figure 5-23: Determination of a model valid for all silicone coatweights between 0.7 g/m ² and 1.3 g/m ² based on Dunafin data	76
Figure 5-24: Correlation for the prediction model (equation (5-3))	77
Figure 5-25: Prediction of P_{total} with MLR (Final Model) including delta E	78
Figure 5-26: Correlation between P_{total} and the Durlac value for Dunafin and Tervakoski data.....	80
Figure 5-27: Distribution of PVA coverage based on grey levels of the silicone negative images.....	82
Figure 5-28: Images from silicone negatives (base paper and liner (4x4mm))	83
Figure 5-29: Local surface area	84
Figure 6-1: Influences on the delta E value	86
Figure A-1: Schematic drawing of the experimenatal setup.....	92
Figure A-2: Examples showing differences in PVA coverage	93
Figure A-3: Counter plate and sample frame.....	94
Figure A-4: Addition: Differences in the spreading properties of malachite green ..	96
Figure A-5: Standard errors of delta E values (five measurements per sample)	97
Figure A-6: Variability of measurement data (large scale variations).....	99

Figure A-7: Prefix change caused by the interaction Cobb*surface pH (MLR delta E)	100
Figure A-8: Prediction of S_{cov} with MLR (all parameters).....	101
Figure A-9: Prediction of the Durlac value with MLR (all parameters)	101
Figure A-10: Topography maps from silicone neagatives base paper (4x4mm).....	102
Figure A-11: Comparison of roughness (max structure size 100 μ m)	102
Figure A-12: Comparison of waviness (structures between 500 – 2500 μ m)	103
Figure A-13: Distribution of roughness, waviness and total topography	103

LIST OF TABLES

Table 2-1: Silicone recipe	12
Table 2-2: Properties and testing methods related to the siliconability of release base papers	15
Table 5-1: Quality parameters (M098 and M025).....	42
Table 5-2: Comparison of spot areas	43
Table 5-3: Comparison of the stained area and the delta E result	46
Table 5-4: Comparison of the L*a*b* differences between white and yellow grades	46
Table 5-5: Mean relative and absolute difference of delta E values comparing different trials with trial x.0	48
Table 5-6: Comparison of the coloured area, delta E results using an area equation and measured delta E	50
Table 5-7: Expected error for a penetration time difference of 5 seconds.....	53
Table 5-8: Area development with penetration time, using different colorants.....	55
Table 5-9: Comparison of the stained area for different silicone coat weights	57
Table 5-10: Basis for the evaluation of variability of measurement data (small scale)	60
Table 5-11: Measurement range and variability of measurement data (small scale)	62
Table 5-12: Variability of measurement data (large scale variations).....	64
Table 5-13: Resulting influence parameters on the Durlac value (stepwise regression)	80
Table 5-14: Average parameters calculated from 2D maps	85
Table A-1: Determination of mean relative and absolute differences of delta E values	97
Table A-2: Determination of the measurement range including 31 papers (Dun Lab)	98
Table A-3: Determination of the measurement range including 21 papers (Toy Lab).....	99

1. INTRODUCTION:

1.1. SCOPE OF THIS THESIS

Release base paper production is the first step in the manufacturing process of self-adhesive laminates. A silicone layer is applied to the release base paper surface functioning as a barrier layer between the paper and the self - adhesive label. It is of utmost importance to obtain a closed silicone layer to prevent the adhesive from contact with the release base paper. Especially in industrial applications of self – adhesive laminates it is important that the labels can be released from the release liner (release base paper and silicone) uniformly. Silicone coverage is tested by a colour stain test, colouring the defects in the silicone layer. The more defects and the larger the defects are the higher is the colour difference delta E, between the unstained and stained release liner, evaluated by a colorimetric measurement. The delta E results as a measure for silicone coverage show only a poor correlation with the measured quality parameters describing the release base paper. The first possible reason for this observation is that a parameter is missing in the quality control of the release base paper, which cannot be described by other standard quality parameters. The second possibility is, that the delta E value does not explain silicone coverage only. In this thesis these two possibilities are discussed. New methods allowing a more detailed description of relevant release base paper properties are presented. The delta E test is evaluated in detail and the results are compared with a newly developed method for the detection of defects in the silicone layer. A model for the prediction of silicone coverage by release base paper quality parameters is determined using multiple linear regression analysis and these quality parameters and their relation to local paper properties are discussed.

1.2. SELF - ADHESIVE LAMINATES

Self-adhesive laminate consist of four layers. To introduce important terms Figure 1-1 shows the compound. The release base paper is the first component, where all other layers are built on. The release base paper itself, is the paper with a PVA layer on top. The PVA coating is necessary to anchor the silicone release coating and the silicone release coating is responsible for an easy release of the self-adhesive label that consists of the label face stock and the adhesive. Therefore, the silicone release coating must form a uniform layer without any defects and holes. This requirement can only be reached when the release base paper meets the highest quality standards.

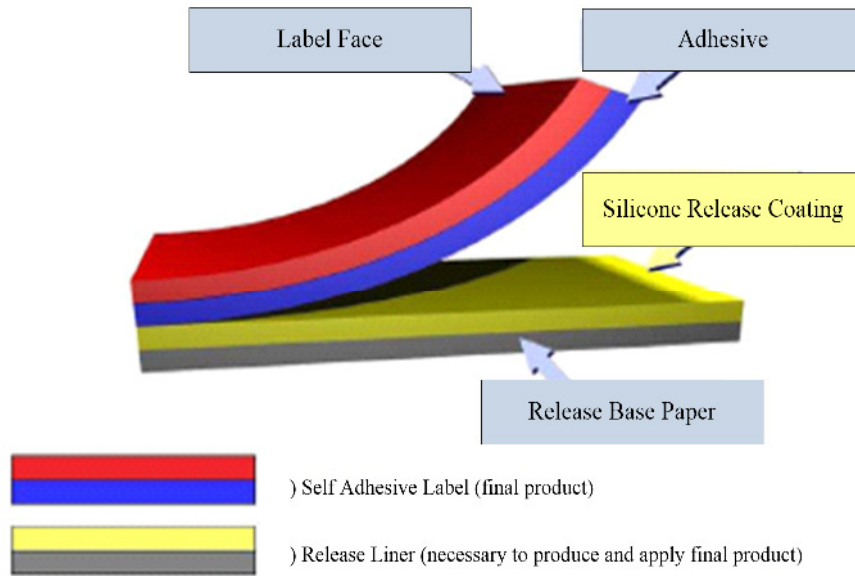


FIGURE 1-1: COMPONENTS OF A SELF ADHESIVE LAMINATE ([14])

Laminate manufacturers constantly aim at reducing the silicone amount, as silicone causes about 6 % of the whole product costs ([11]). Silicone costs are between 15 and 20 €/kg. The basis weight of the silicone layer applied on a 60 g/m² release base paper is about 1.0 to 1.3 g/m². Application of 1.0 g/m² silicone leads to costs of 330 €/ton of silicone release coating. A reduction of 0.1 g/m² silicone thus means a saving of 33 €/ton. The amount of silicone that has to be applied depends on the chemical and surface properties of the release base paper.

2. RELEASE LINER FOR INDUSTRIAL APPLICATIONS:

2.1. PRODUCTION OF THE SILICONE BASE PAPER:

2.1.1. PRODUCTION PROCESS:

Base papers to be siliconized can be pigment coated papers, vegetable parchment, glassine and greaseproof paper ([15]). Coated papers have at least one coating layer, consisting of pigments and binders. The coat weight applied is in the range of 5 to 12 g/m². The coating has the function to close the surface and to obtain good silicone hold out. Coated papers for silicone applications needs to be calandered. Vegetable parchment and greaseproof papers are not discussed in detail, as they are not used as label release papers and do have mostly different applications.

The focus of this thesis is on glassine release paper. Compared to pigment coated paper, glassine paper furnish has a higher level of refining. Another difference is in the surface treatment, whereas glassine coating is mainly containing binder and little to no pigments. The applied coat weights of 1.0 to 2.0 g/m² are much lower than for conventional coated papers. In glassine production the coating is applied in a conventional size press or in a metering size press. The glassine is calendered in a supercalender offline. This is the reason why glassines are denser than pigment coated papers. Furnish recipes and stock preparation are usually different between the mills that make these papers. Glassines are produced as white or colorantd yellow grades. The basis weight ranges between 30 and 90 g/m² ([13]). Paper machines for glassine production usually have a width of two to five meters and run at a speed ranging from 200 to 1000 m/min. Often Fourdrinier machines retrofitted with a top former are used in glassine production. Press and drying section design varies.

The applied coating, consists of pure polyvinyl alcohol (PVA), mixtures of PVA and carboxymethylcellulose (CMC) or mixtures of PVA and starch. They can also be pigmented with clays. Coat weights range from 1 to 2 g/m² and are limited by coating rheology. Solid content depends on the application system and the coating formulation that can be up to 15 wt% solids and more. After the drying of the coating, the paper web has to be remoistened to provide ideal conditions for the calendering process at the supercalender. Remoistening can be done directly at the paper machine, before winding or at the supercalendar. The advantage of remoistening in the paper machine is a longer dwell time and therefore a more uniform moisture profile in the z – direction of the paper web. Problems at the reel after remoistening can occur because of layers sticking together, caused by the tackiness of the coating.

The speed of the supercalender should be as low as possible to achieve good smoothness and uniformity, but has to be about ten per cent higher than the machine speed to ensure a continuous production. Because of these conflicting requirements

sometimes two supercalenders are used. After rewinding the glassine production process is finished.

2.1.2. FUNCTIONAL CHEMICALS:

As with many paper grades chemical additives are used to control and modify paper properties in the release liner base paper production. Internal sizing decreases water uptake and alkyl succinic anhydride (ASA) or resin size is used, depending on the pH of the system. Alkyl ketene dimer (AKD) is weed out, since it can cause inhibition of the platinum catalyst that is used in the silicone release coating. Inhibition plays an important role which is why the choice of chemicals and possible sources of contamination must be considered in the base paper production. Inhibition will be discussed in detail in chapter (2.2.2).

The use of retention systems is depends on the pulp and the refining level. Some paper mills use a retention aid just in the fibre recovery system. Release base papers are produced as white and yellow grades. For yellow release base papers it is necessary to use colorants. Usually PVA is applied to the surface of the base paper using a film press. As PVA plays a unique role in release paper production it will be discussed separately (2.1.3.).

2.1.3. PVA FUNCTION AND CHEMISTRY

Polyvinyl alcohol (PVA or PVOH) is a synthetic polymer. It is not possible to polymerize PVA directly as the monomer is not stable. For this reason the polymerisation takes place in two steps. First vinyl acetate is polymerized by a radical chain polymerisation mechanism in an organic solvent (usually Methanol) (Figure 2-1). In the second step polyvinyl acetate reacts with the residual methanol, under the presence of caustic soda, working as catalyst, to polyvinyl alcohol ([17]) (Figure 2-2).

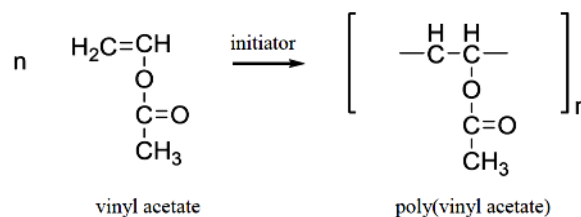


FIGURE 2-1: POLYMERISATION OF VINYLACETATE (FIRST STEP IN PVA PRODUCTION) ([16])

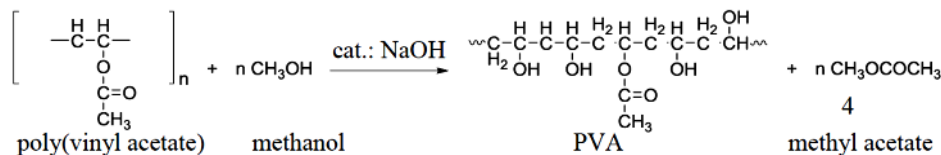


FIGURE 2-2: ALCOHOLYSIS OF POLYVINYLACETATE (SECOND STEP IN PVA PRODUCTION) ([16])

The functions of PVA in release base paper production are:

- To act as a barrier against silicone penetration into the base paper
- To form a film
- To reduce surface roughness
- To enable the adhesion between the silicone and the release base paper.
- To ensure that no inhibition of the platinum catalyst, takes place, by shielding the base paper from the silicone applied afterwards.

The most important parameters of PVA controlling its functional properties are the molecular weight and the degree of hydrolysis. Water resistance of dried PVA films, increase with the mean molecular weight of the polymer and the degree of hydrolysis. The water resistance of PVA can be further improved with acids, ammonium chloride and aldehydes ([16]). Fully hydrolysed PVAs with high molecular weight are mainly used in glassine paper production, although for a better closing of pores and compensation of roughness, partly hydrolysed PVAs with lower molecular weight are recommended ([16]). In this case the resulting lower water resistance can be increased with cross linkers. A drawback of the lower degree of hydrolysis is the poor adhesion of PVA to the cellulose fibres.

2.2. SILICONE APPLICATION ON RELEASE BASE PAPERS:

2.2.1. CHEMISTRY OF THE SILICONE AND ADDITIVES:

The silicone composition for thermally curing systems consists of

- Silicone polymer
- Crosslinker
- Platinum based catalyst

The silicone is a polydimethylsiloxane (PDMS), which is liquid at room temperature for this application, but can have a gum like consistency at higher molecular weight. The helical polymeric structure consists of an inorganic Si-O-Si backbone and linked methyl groups. The fact that the energy required for rotation of the bonds is near zero and the high surface energy of the backbone (while the surface energy of the methyl groups is low) allows the silicone to wet nearly every surface. The structure and the chemical formula of PDMS are shown in Figure 2-3.

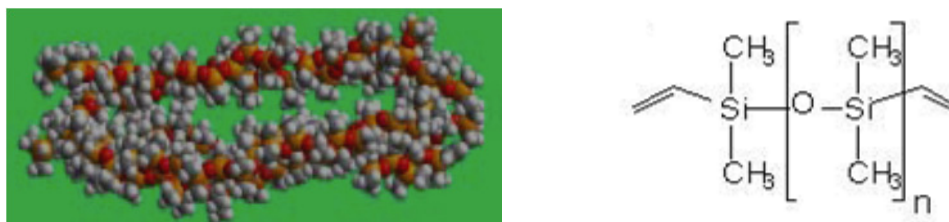


FIGURE 2-3: STRUCTURE AND CHEMICAL FORMULA OF POLYDIMETHYLSILOXANE ([1]), ([9]).

Although PDMS has low solubility and is inert to most chemicals, reactions with the crosslinkers and the substrate is necessary to form a stable non-flowable silicone film on the surface of the release base paper. The cross linker consists of dimethylsiloxanes too, but the end groups are methyl groups instead of vinyl groups. For the crosslinker the chain length, n , is lower than with the PDMS. The catalyst is platinum based and can be acidic or alkaline. The structure of the cross linker is shown in Figure 2-4 (1) and the catalyst in Figure 2-4 (2).

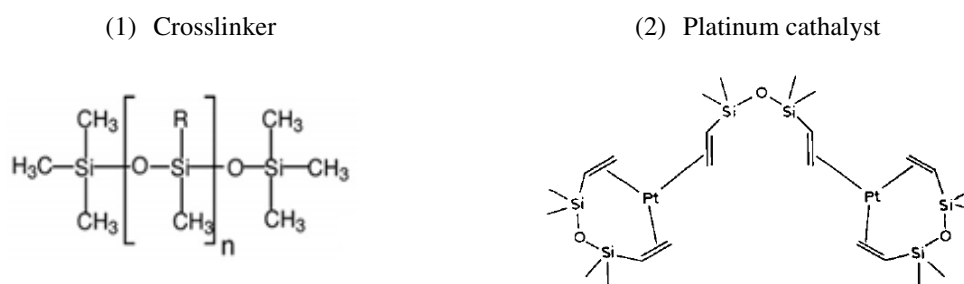


FIGURE 2-4: CHEMICAL FORMULAS OF A CROSSLINKER (1) AND A PT - CATHALYST (2), ([9]), ([4]).

Although the catalyst only lowers the activation energy for the crosslinking reaction and is not consumed during the reaction, the catalyst cannot be recovered. As platinum is very expensive, there are efforts to reduce the quantities or to substitute it with other metals. The advantage of the platinum catalyst is its selectivity; the drawback is the sensitivity against catalyst poisoning, which may be caused by many different substances. The effect of catalyst poisoning is that the silicone layer cannot build up enough adhesion to the base paper and the silicone layer itself will remain rubber like. The resistance against the adhesive of the label migrating through the silicone layer is also reduced, which affects the time stability of the final laminate product. Also, the release force which cannot be adjusted to an appropriate level that does not fluctuate in its height. The effect is less significant at low release speed, but becomes important at higher speed levels which are standard in industrial labelling processes.

To control the release force, dimethylsilicone resins are added. They increase the release force which is usually too low. Dimethylsilicone resins are also referred to as

“high release additives” (HRA), which describes their function. The structure and chemical formulas are depicted in Figure 2-5.

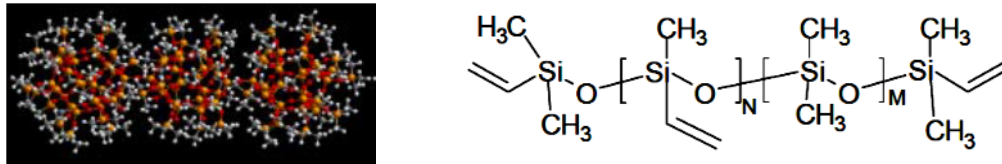


FIGURE 2-5: STRUCTURE AND CHEMICAL FORMULA OF DIMETHYL SILICONE RESINS ([1]), ([2]).

2.2.2. SILICONE SYSTEMS:

Silicones have a high range of applications and also the curing mechanism of silicones varies. An overview concerning the various silicone curing systems is given in Figure 2-6. The main groups can be divided into thermally cured silicones and radiation cured silicones. Thermally cured systems can be further subdivided in condensation or addition curing systems ([3]). Another differentiation within the thermally curing silicone systems is to group them in solvent based, solventless (100% systems) and emulsion systems ([6]). Originally solvent based silicones have dominated the market, while today 70 % of the pressure sensitive market volume are solventless systems ([8]). From this market segment, approximately 90 % are thermally curing ([7]).

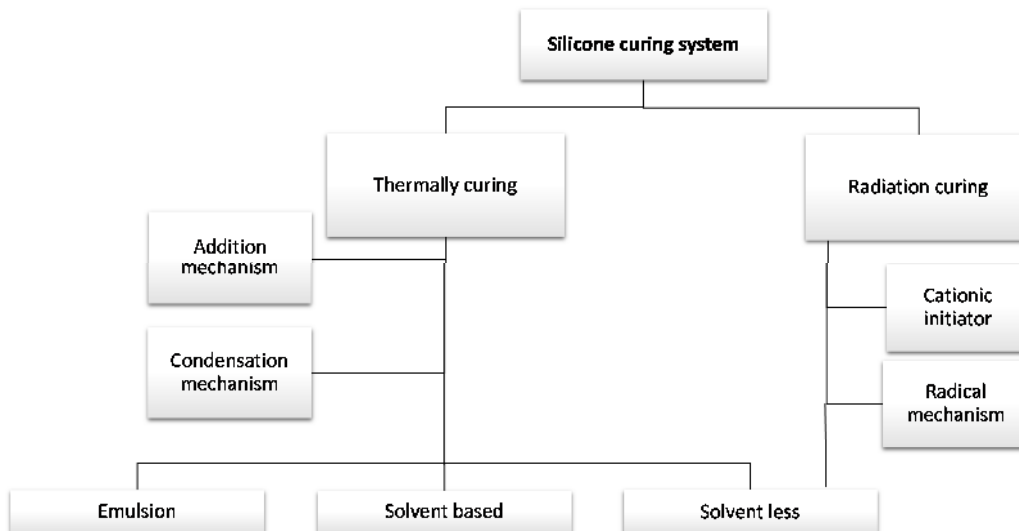


FIGURE 2-6: SILICONE SYSTEMS

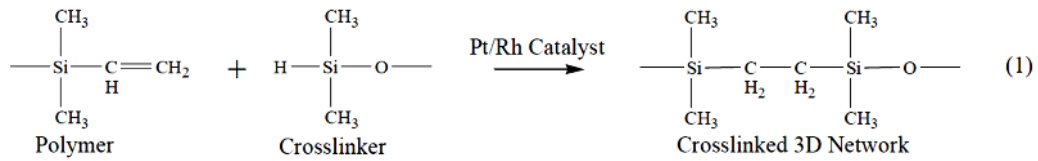
Although solvent less thermally curing systems are preferred, these systems are the most difficult to control, since the catalyst (mostly platinum catalysts) is sensitive to

poisoning. The whole curing reaction can be stopped or slowed down (2.2.2) which affects the function of the silicone layer and the adhesion of the silicone to the base paper. Release force, an important property for laminate products, is difficult to control with thermally curing systems. To set the release force on a defined level, silicone resins (2.2.1) have to be added. Solventless systems have the important advantage of non-toxicity and save energy, as water or solvents do not need to be evaporated. The development goes further in the direction of low temperature curing systems (LTC systems) and systems which require a lower amount of catalyst, since platinum costs are high. Crosslinking of LTC systems takes place at a temperature range from 60°C to 100°C rather than 110°C to 150°C used for conventional silicones. The main disadvantage of LTC silicones is the low anchorage of the silicone to the base paper ([15]). The group of radiation curing systems includes electron beam and UV light. This group includes free radical curing systems and systems curing in the presence of cationic initiators. UV curing systems need no heat for the cure. Therefore, no changes in mechanical or dimensional properties of the paper occur. The radical curing systems need a nitrogen purge of the UV drying unit. Given the fact that radical curing systems are very stable and not affected by inhibition caused by contamination, chemicals or humidity, the advantages compared to the more sensitive cationic systems is evident ([7]). In this thesis thermal curing, solventless systems at conventional curing temperatures (110°C to 150°C) were used for siliconizing. Silicone chemistry and application machines are discussed for this system.

2.2.3. REACTIONS AND INHIBITION:

The crosslinking reaction between the PDMS and the crosslinker has to be separated from the mechanism to build up adhesion between the silicone layer and the base paper. The crosslinking reaction takes place in two steps. The primary reaction is between the crosslinker and the silicone, building up a crosslinked 3D network (Figure 2-7 (1)). Secondary reactions also occur, especially when an excess of crosslinker is used (Figure 2-7 (2-4)) ([3]). The primary reaction is referred to as “cure” and happens spontaneously during the silicone application process, while secondary reactions, which are subsumed under the term “post cure”, are much slower and occur as the material ages after the coating.

Primary Reaction



Secondary Reactions (Post-Cure)

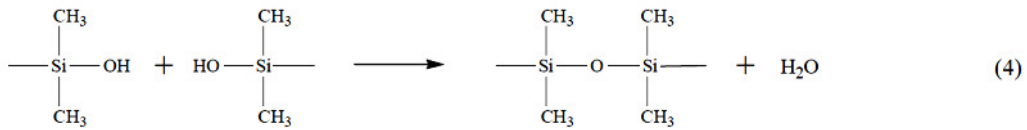
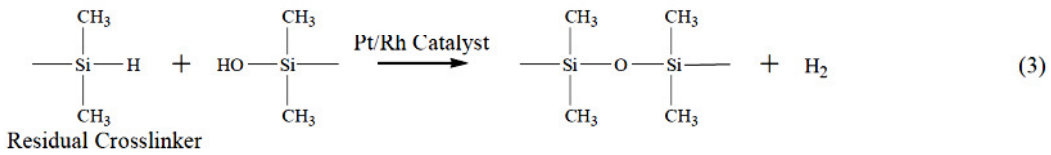
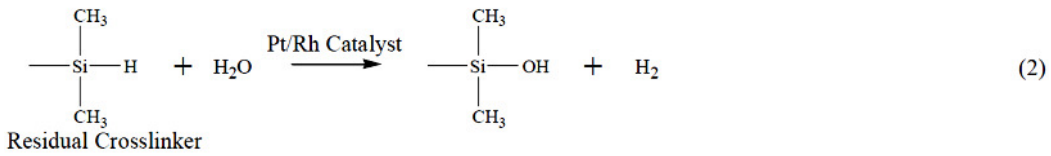


FIGURE 2-7: REACTIONS OF SILICONE AND CROSSLINKER ([3]).

A silicone resin, which functions as high release agent, reacts with the crosslinker via hydrolysis of the vinyl groups of the resin. It is recommended that the crosslinking density is the most important factor affecting release force ([2]). Crosslinking density is defined as the number of polymer crosslinks per unit volume. It is dependent on the molecular weight of the PDMS and the active parts of the crosslinker. High crosslinking density results in a rigid coating layer which has a flat release force profile. A release force profile illustrates the force needed to release the self-adhesive label with increasing peeling speeds. Low crosslinking density networks are more flexible and yield an elastic coating. At low peeling speeds the release force profile of a less cross-linked network behaves similar than for a high cross-linked network. At higher peeling speeds, the release force of low density networks increases while high density networks shows a flat profile over the whole peeling speed range. This increase of release force at higher peeling speeds is caused by the higher penetration of the adhesive and the interaction of the silicone layer with the adhesive polymer, of less cross-linked networks. Long chain siloxane networks have an entanglement effect, resulting in energy dissipation and absorption during the application of the peeling force. The crosslinking density together with the entanglement and the anchorage of the silicone to the base paper are the factors regulating release force.

Release force can be increased further with the addition of a high release agent (HRA). HRAs are changing the siloxane network structure and its physical properties. The resins reduce the mobility of the network and have an energy dissipating function.

The chemical mechanisms responsible for the adhesion of the silicone to the base paper are similar to the reactions in the silicone network. Silicone anchorage to the substrate is caused by two reasons:

- 1.) Mechanical interlocking with the substrate
- 2.) Chemical reactions with the substrate

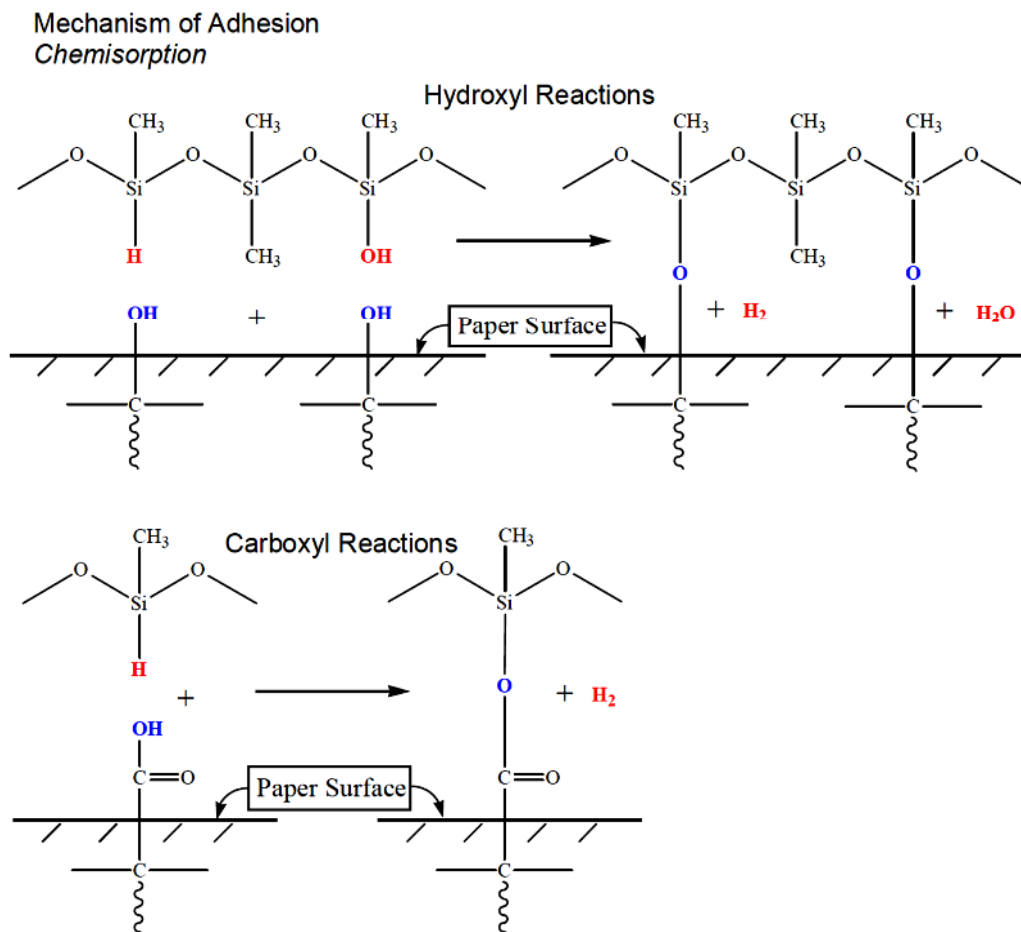


FIGURE 2-8: SIDE REACTIONS OF THE SILICONE WITH THE SUBSTRATE ([3]).

Mechanical interlocking with the substrate happens when the substrate has a porous and rough surface. Although glassine release papers have a smooth and closed surface, some mechanical interlocking still takes place. For long term stable anchorage, chemical interactions of the silicone with the base paper are most important. As mentioned already, PVA is applied to the surface of the release base paper. PVA

provides different functionalities. Beside its function as surface size to accomplish water resistance, surface levelling, closing of pores and acting as a barrier for catalyst poisons from the base paper, PVA provides the reactive groups for the reaction with the silicone. The main reaction occurs between a terminating vinyl group of the PVA and the silicone crosslinker, similar to the reaction of PDMS and crosslinker in Figure 2-7 (1). As cellulose and PVA contain unreacted –OH and –COOH groups, side reactions occurs (Figure 2-8), which are important for anchorage too, despite forming weaker bonds. Bonds between the substrate and the silicone might break, affecting long term stability. For example the reaction of –COOH groups with –SiH may be reversed in the presence of an alcohol at neutral pH. Glycol, which provides a hydroxyl functional group, is often used in the adhesive. When glycol penetrates through the silicone layer to the substrate - silicone interface, the bonds between silicone and the substrate are weakened and cause a loss of adhesion ([3]). High temperature and high moisture can also affect long term stability of adhesion, especially when the silicone is not cured completely. A patent from Ahlstrom proposes better results for release liner properties with the use of modified PVA in the coating ([15]). The PVA is modified, by a reaction of an organic molecule consisting of an aldehyde and a vinyl function with the –OH groups of the PVA. The anchorage increases because of additional reactive vinyl groups.

Long term stability can also be negatively affected by catalyst poisoning. Catalyst poisoning is caused by impurities coming from the base paper. This is another reason, why it is important to have a closed PVA layer on the paper surface, as PVA is chemically inert to the catalyst. A wide range of chemicals inhibiting silicone curing exists. The most problematic ones are alcohols, amides, ammonia and thiocompounds, which can slow down the curing rate or totally stop the curing process. Most of these chemicals can be present in the process water in paper manufacturing. Impurities in the water of the remoistening unit are especially critical, because the PVA shielding the base paper from the direct contact with the silicone can be contaminated with this water. Avoiding inhibition is an important issue in glassine production. Chemical additives have to be tested, before they are applied in the papermaking process. Differential scanning calorimetry (DSC) is a test method that is used for screening new additives ([5]).

2.2.4. APPLICATION MACHINES AND CONVERTING PROCESS:

An exemplary silicone recipe consisting of the polydimethylsiloxane (PDMS), crosslinker, high release agent (HRA) and platinum based catalyst is provided in Table 2-1. PDMS has the highest concentration in the formula. The components are mixed together shortly before the application, as the mixture is only stable for approximately one hour. The mixing can be done continuously or in batches.

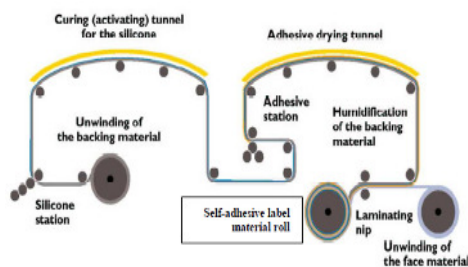
component	parts of component
polydimethylsiloxane (PDMS)	10
high release agent (HRA)	1,5
crosslinker	1
platinum based catalyst	1

TABLE 2-1: SILICONE RECIPE

After mixing the components are in a liquid state and are stored at a constant temperature of about 60 °C.

Silicone coating machines in the pressure sensitive industry run at speeds of up to 1000 m/min. Line width is up to about 2.20 meters ([11]). Silicone coating machines can either produce the release liner only or apply the adhesive and the face stock too, finishing the laminate product in an inline process. The whole process is shown in Figure 2-9. In the left picture an example of the application process for manufacturing the finished laminate product is shown. At the right a pilot silicone coater, which only applies the silicone to the paper substrate is depicted.

(1) outline of the application process for the laminate product



(2) Pilot coater for the production of release Liner



FIGURE 2-9: SILICONE APPLICATION MACHINES ([14]), ([12]).

The silicone coating unit consists of four to five counterrotating cylinders. The first cylinder dips into the silicone bath and picks up an excess of silicone. This cylinder has the slowest speed from all the cylinders of the coating unit. The second roll counterrotates at higher speed and takes off part of the silicone via a film splitting mechanism. Due to the speed increase which thins the silicone film and the film splitting mechanism, the silicone film on the cylinder gets thinner by passing each nip. The paper web runs between the last cylinder and a counter cylinder where the silicone is transferred to the paper. To adjust the required coat weight, two of the cylinders are movable. Directly after the silicone application the web runs through a drying section, where the silicone layer is thermally cured and the crosslinking reaction and the reaction with the base paper takes place. After the drying unit two process steps are possible depending on whether only the release liner or the whole laminate product is manufactured. The production of the release liner alone ends with a winding unit after

the drying section. For the laminate product two additional steps are necessary before winding. The adhesive is applied on the release liner over a rotating cylinder unit and has to be dried afterwards. Then face stock material, which can be a polymer or paper is brought into contact with the adhesive in the laminating nip.

Further converting processes take place on separate machines. The laminated product has to be printed, as the final product is the self-adhesive label. After the printing step the labels have to be cut out via die cutting. The face material surrounding the printed label, mentioned under the term “matrix” is stripped from the release liner and rewound in the machine. The force at which the face material is removed from the release liner is known as release force.

To achieve appropriate printing and most important die cutting, the release liner has to have uniform strength properties and thickness. If the release base paper is thicker, the die will cut through the silicone layer. With a thinner release liner the face material will not be cut completely and the labels are torn off with the matrix.

The last step in the production chain is the label application process. To apply the labels on the product at the required speed, automatic dispensers are used. The release force is the most important parameter regarding this process.

Summarizing, the release base paper is the key for a good performance of the final product and has to fulfil different requirements in each converting step. In the next chapters a closer look at quality parameters and the functional role of the base paper and the release liner is taken.

2.3. BASE PAPER REQUIREMENTS AND QUALITY PARAMETERS:

Starting from the release base paper until the application of the label on a product, five converting steps are necessary. In each step the release base paper has to fulfil different functional properties, which are illustrated in Figure 2-10. At first, the release base paper's function is support the self-adhesive label, to prevent the labels from sticking together and to protect them from other defects during transportation at the end. Additionally, it has to be siliconized and should have a good quality in terms of siliconability, which includes three aspects: The silicone should cover the release base paper uniformly without any defects or holes. The silicone coat weight should not vary. The release base paper should have no impurities in order to guarantee good adhesion of the silicone. Uniform coverage is achieved by having a uniform base paper with a closed surface. Therefore, smoothness and absorption properties of the base paper are important characteristics. Smoothness of the base paper is measured with a Bekk instrument. Absorption properties are evaluated with the Cobb Unger measurement, using castor oil and IGT – Ink absorption. To ensure a uniform silicone coat weight, the cross direction profiles, especially basis weight, smoothness and absorption profiles have to be controlled to very low variability. Impurities are determined using

an online measurement system and crosschecked by visual inspection in the quality laboratory. For good runability in the different converting steps, the release base paper has to have an even profile in cross direction and sufficient strength properties to prevent breakage during production. Although the release base paper is just the carrier for the final product, the paper has to be free from any visual dirt spots or stickies, which can easily be introduced into the system during paper production. Besides the poor optical properties, impurities can affect the siliconability of the base paper.

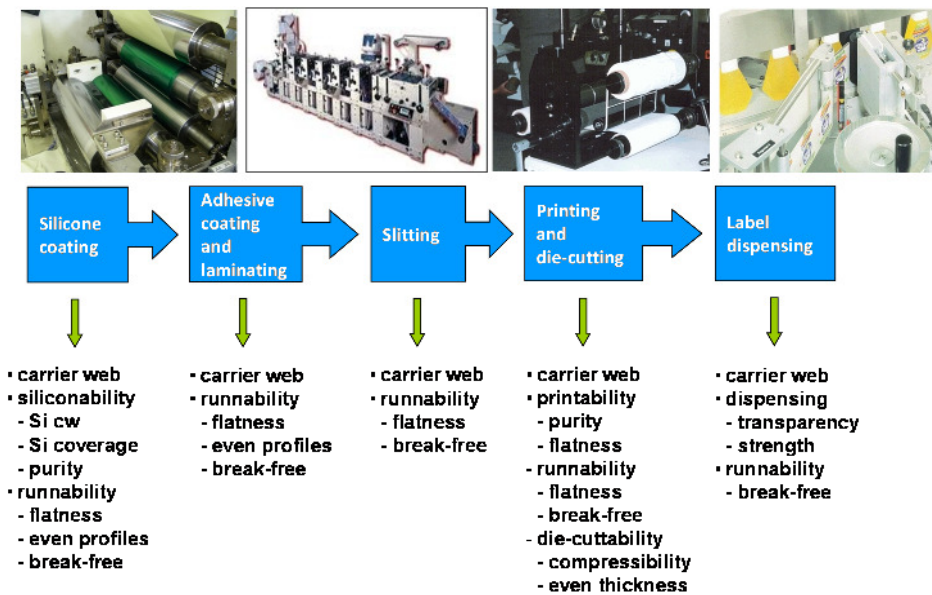


FIGURE 2-10: THE FUNCTIONAL ROLE OF THE RELEASE BASE PAPER IN THE SUBSEQUENT CONVERTING STEPS ([14])

Especially in the diecutting process, an even thickness profile and the compressibility of the release base paper is of utmost importance. The thickness that a base paper of a certain grammage has to have is specified by the customers. The die cutter has to be adjusted to this thickness and therefore the uniformity of the thickness over the whole web is another issue. If the compressibility of the paper web is too high, this can cause an insufficient cut through the whole face stock. The automatic dispensing unit in label application is equipped with a photocell, which detects the label position reading through the paper web. The positions where the face stock material is located, are distinguished via transparency difference from spaces where only the more transparent liner is located. When the transparency of the release liner is too low, the photocell does not recognize the label position and stops the process. As the tension of the web changes continuously in a stop and go process, mechanical strength properties and dimensional stability are also an issue ([14]).

2.4. RELEASE LINER REQUIREMENTS AND QUALITY PARAMETERS:

The release liner functions as a carrier web for the real product, which is the self-adhesive label. The silicone layer should guarantee a uniform release from the carrier web. If insufficient silicone coverage occurs, the label will not be released, or parts of the release liner will tear off. Even if the defects are not large enough to cause this type of problems, migration of the adhesive through the silicone layer may still affect long term stability. Long term stability is also required, as the laminate product should retain the same properties over one year storage. Some case studies done by Orlych ([3]), show that migration of the adhesive affects long term stability. Extreme storage conditions under high humidity and temperatures have a negative effect on migration. Glycol, a component of the adhesive, can disturb the bonds between the PVA and the silicone. Another issue is insufficient curing of the silicone, which appears as a rubbery like consistency of the silicone. Insufficient curing can be caused by impurities which inhibit the catalyst and slow down the curing reaction. This has an effect on the release force, which has to be set to a specified level. The silicone coverage can also be influenced as the anchorage to the base paper cannot be provided at all. Migration occurs more easily, as the silicone network is less dense, because of a smaller amount of crosslinks per unit volume.

In Table 2-2, testing methods to measure the quality of the release liner in the aspect of siliconability are shown. A wider range of methods, which are not included in this thesis can be found on the homepage of FINAT ([29]).

Property	Testing method	Quality parameter
silicone coat weight	Silicone coat weight by energy-dispersive X-ray fluorescence spectrometry	silicone coat weight [g/m ²]
silicone coverage	Evaluation of silicone coverage of coated papers by use of a water based stain test	delta E [-]
silicone adhesion	Rub off test	amount of silicone rubbed off manually [1 to 6]
silicone adhesion	Automatized rub off test, with measurement of silicone coat weight.	Durlac value [-]
silicone curing/inhibition	Differential Scanning calorimeter	heat flow rate
release force	Low/high speed release force	release force in [N/m]
migration	extract with isobutylmethylketone	extract value [-]

TABLE 2-2: PROPERTIES AND TESTING METHODS RELATED TO THE SILICONABILITY OF RELEASE BASE PAPERS

In the measurement of silicone coat weight, energy-dispersive X-ray fluorescence spectrometry (XRF) is used. Special XRF devices have been designed which are able to display silicone coat weight directly using a three point calibration. The extent of silicone coverage is evaluated with stain tests, where a colorant solution remains in contact with the release liner for a specified period of time. After removing the solution, the stained spots show the defects in the silicone layer. The coverage is then measured by the colour difference between the untreated liner and the stained release liner. The change in colour is based on the geometric colour difference, ΔE , within the $L^*a^*b^*$ colour space. The various testing conditions and measurement methods differ significantly, which will be discussed in detail in chapter (3.1). Silicone adhesion can be tested using a manual rub off test. This is a very subjective method and depends on the person conducting the test. Silicone is removed from the base paper by rubbing with the thumb over the surface. Depending on how easily the silicone is removed, values from one to six are given, with six meaning a poor adhesion and easy rub off. This method is often used as direct quality measurement by the release liner producers. For a more objective analysis of adhesion, the Durlac value can be determined. For this procedure the silicone coat weight is measured from a circular sample using the XRF method which is then glued with the back side to a defined weight. The weight is pushed over a felt at a defined speed by a mechanical device for two times. The silicone coat weight is measured once again. The coat weight of the silicone after abrasion is divided by the initial weight which gives the Durlac value. This test is considered critical, as only the top layer of the silicone is rubbed off, by the felt. The test results for poorly cured coatings, which have a rubbery like consistency, are very unreliable. For such cases the silicone layer is more flexible and can withstand the abrasion better. Therefore, better results may be observed, although the adhesion to the base paper is usually worse than for well cured silicones. Silicone curing and a possible inhibition of the catalyst can be analysed with differential scanning calorimetry (DSC). Silicone is applied on the paper surface and cured thermally in an oven. With DSC it is possible to evaluate the energy which is developed or absorbed during the chemical and physical reactions of the curing process. The variation of energy necessary for the reactions allows a conclusion about the base papers compatibility ([5]). This test is used primarily for the examination of new chemicals in paper production, for the evaluation of glass transition temperature, crystallisation and melting points.

Release force plays a role in the diecutting process and finally in the label dispensing. The silicone layer and the adhesive are responsible for this parameter. The force level is controlled with the silicone composition, affected by the crosslinking density of the silicone and the addition of high release agents (HRA). Crosslinking

density depends on the amount of crosslinker, catalyst, curing conditions and inhibition of the catalyst. The adhesive also plays a role in release profiles. The release force increases with the peel rate using acrylic based adhesives, while rubber based adhesives shows a decrease in force at higher peel rates ([8]). The measurement is performed at low peel rates (0.3 m/min) and high peel rates (10-300 m/min) and under different angles, mostly 90° and 180°. The release force test is illustrated in Figure 2-11.

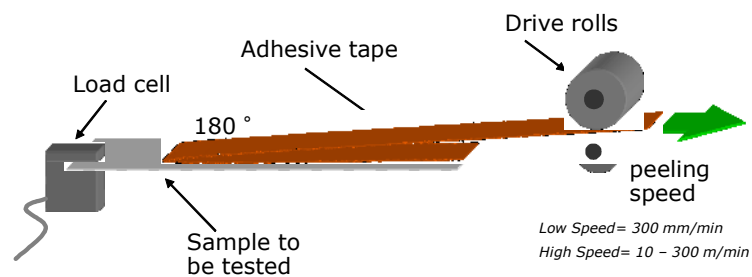


FIGURE 2-11: RELEASE FORCE TEST ([14]).

The laminate sample to be tested is fixed in a load cell. The adhesive tape is locked between the driving rolls, which apply a certain peel speed. The force, which is needed to release the adhesive tape from the release liner is detected via the load cell.

3. DESCRIPTION OF THE DELTA E TEST:

In this chapter the delta E test will be introduced in detail. The delta E test is performed to determine the silicone coverage of release liners, staining defects in the silicone layer with a colorant solution. The colour difference, delta E, between the liner before and after the staining of the defects, is determined using L*a*b* values. Background information regarding the colorant used in this procedure and the L*a*b* colour space is given in chapter 3.1. In chapter 3.2 variations in the test conditions are discussed, as there are large differences in the possible conduction of the delta E test. The delta E test procedure, which is performed in this thesis is described in chapter 3.3. Besides the measurement of the L*a*b* values and the calculation of the delta E value, the stained samples can be analysed further, using an image analysis routine implemented in MATLAB for the analysis of the scanned delta E test samples. The image analysis provides additional information regarding the stained spot size distribution and allows to derive further parameters, which describe the performance of release liners in the delta E test.

3.1. INTRODUCTION OF THE COLORANT AND THE COLOUR SPACE:

Malachite green:

Malachite green is a synthetic colorant, which appears in a green crystalline form. It is a polyaromatic with conjugated primary amine functional groups (Figure 3-1). It absorbs visible light principally at 420 nm and 623 nm wavelength. Malachite green is soluble in water, methanol and ethanol and was used as a colorant for dyeing textiles. However, malachite green has deficiencies in its lightfastness, i.e. it fades under the exposure to light. The low lightfastness of malachite green is explained by the mechanism how it attaches on cellulose fibres. In comparison to colorants of the group of reactive colorants that are able to form covalent bonds with the substrate, malachite green is only bonded by weaker bonding mechanism. Malachite green is belonging to the group of direct colorants, which are able to attach to the substrate directly, caused by the higher affinity to the substrate. Direct colorants can be further classified in substantive, anionic and cationic colorants. The classification in substantive and ionic colorants is indistinct, as substantive colorants also can have ionic groups. Differences are in the spatial orientation of the molecules which are usually orientated planar and in the higher molecular weight of substantive colorants, compared to ionic colorants. Malachite green is not orientated planar and is a rather small molecule. Further it has a positively charged functional group. Therefore malachite green can be classified as a direct cationic colorant. The colorant attach to fibres in the void volume of the cell

wall and is fixed chemically or physically. Malachite green can be fixed by electrostatic forces, Van der Waal's forces and water bridges to cellulose fibres. As malachite green has a positive charge it is affine to anionic groups. Salts are added to substantive colorants to increase the aggregation of the molecules in the voids of the cellulose fibres. The molecules needs less space, when they are present as aggregates and therefore more colorant is capable to be fixed in the voids of the fibre. Under the assumption that to some degree this phenomenon will also occur with cationic colorants, the quantity of colorant in the pores and voids of the cell wall will increase with the addition of salts to the colorant solution. ([19]). The colour of a malachite green solution depends on the pH. At strongly acid pH, malachite appears yellow and changes to green with increasing pH. In a wide range from pH 2 to 11.5 the colour is bluish green. It change at higher pH levels to turquoise, before the colour starts to fade at a pH of 13.

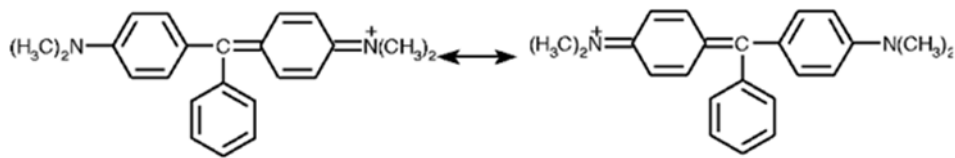
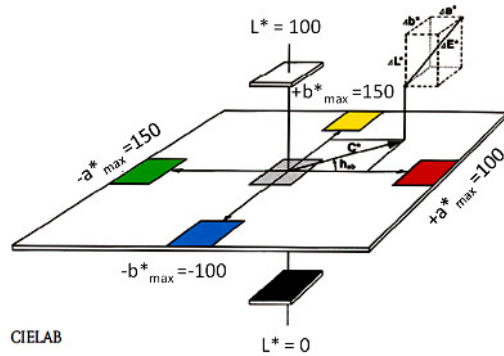


FIGURE 3-1: MALACHITE GREEN ([18])

L*a*b* System and delta E

L*a*b* defines the coordinates of a three dimensional Cartesian coordinate colour space. a* represents the colours red and green, while b* indicates yellow and blue for the positive and negative axis in xy - direction. L* is the parameter for lightness and is orientated in z-direction. The L*a*b* system is based on the XYZ colour space, where X and Z represent the colours red and blue. Y describes the green colour aligned with the dominant sensitivity of the human eye and the lightness. Transformation of the XYZ system to the L* a* b* system is possible by a nonlinear transformation of the XYZ colour system (see Figure 3-2). The parameter Y is part of L* a* and b*, while X is only needed for the calculation of a*, which leaves Z for the determination of b* values. Compared to other colour spaces as RGB or XYZ, L*a*b* was designed to approximate human sensation of colours. A change of the same amount in a colour value produces a similar change in visual impression. Printers use the L*a*b* system to evaluate the colour position. Furthermore the delta E value is used to determine the difference between two colours and is the three dimensional distance between two points in the L*a*b* colour space (see Figure 3-2). This allows printers to evaluate the quality of the printed product and to adjust the colours. An equal delta E value independent of the colour positions, is meant to represent the same change in colour for a human's eye.



$$L^* = 116 \cdot \sqrt[3]{\frac{Y}{Y_n}} - 16$$

$$a^* = 500 \cdot \left(\sqrt[3]{\frac{X}{X_n}} - \sqrt[3]{\frac{Y}{Y_n}} \right)$$

$$b^* = 200 \cdot \left(\sqrt[3]{\frac{Y}{Y_n}} - \sqrt[3]{\frac{Z}{Z_n}} \right)$$

FIGURE 3-2: L*A*B* COLOUR SPACE AND DETERMINATION OF L*A*B* ([20])

3.2. DIFFERENTIATION IN THE TEST PARAMETERS:

As discussed in chapter 2.4 the delta E test is a method used for the evaluation of silicone coverage of release liners. It is a very simple method, using a water based colorant solution to stain defects in the silicone layer of the release liner.

The L*a*b* values of the unstained sample must first be measured. Then the siliconized side of the sample is brought in contact with the colorant solution, which is remaining in contact with the release liner for a defined time period. After removing the liquid, the paper sample is cleaned from the excess colorant. L*a*b* values are measured again. The delta E value is then calculated as the geometric distance between the points in the three dimensional L*a*b* colour space (3-1), which is depicted in Figure 3-2.

$$\Delta E = \sqrt{\Delta L^{*2} + \Delta a^{*2} + \Delta b^{*2}} \quad (3-1)$$

Despite the simplicity of this method there are large variations in the test conditions that can affect the results. The procedure to determine the delta E value is valid for all variations of the method, although sometimes the delta E value is not measured, but only evaluated by visual inspection to categorize silicone coverage.

The procedure is differentiated into three parts which are:

- Type of colorant and preparation
- Laboratory test conditions
- L*a*b* measurement

Figure 3-3 indicates how the delta E value can be determined using different testing conditions. The five colorants which are used are vastly different. “Shirlastain A” is a dilute aqueous colorant solution prepared with G150 chlorazol blue, 3BS crocein scarlet and picric acid. The different chemicals all have colouring properties, but differ

in the mechanism. The silicone layer is coloured yellow, while fibres will turn red to brown after the application. “Shirlastain A” is supplied as liquid ready for use. The other colorants are received as crystalline powders which have to be diluted. The concentrations of the colorant solutions vary from 1 to 5 g/l. Compared to “Shirlastain A”, malachite green stains only the fibres, which appear bluish green. The other colorants are not discussed in detail, as they were not used in the research described in this thesis.

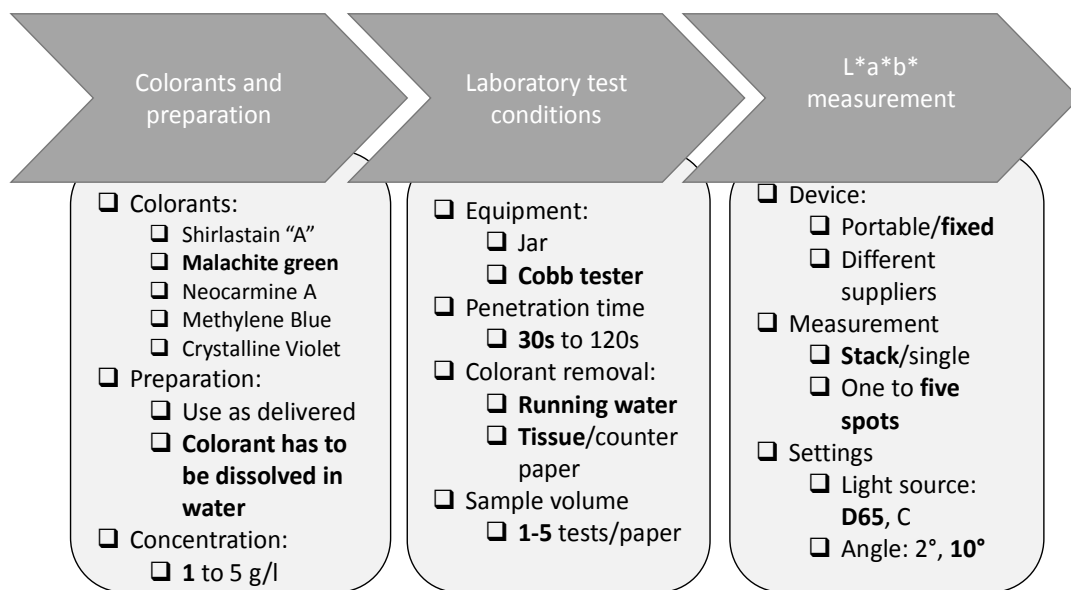


FIGURE 3-3: DIFFERENCES IN THE DELTA E TEST

The test equipment needed to conduct the laboratory test, can be a jar filled with the colorant or a Cobb tester. The colorant solution wets the paper from the top in the Cobb tester while the jar method is used with the paper placed on top of the colorant solution. Penetration times vary from 30 seconds to 120 seconds, depending on different procedures and on the colorant used. The visual difference between the stained spots and the silicone is greater with malachite green than with “Shirlastain A”, since “Shirlastain A” also colours the silicone layer. The penetration time is therefore often shorter for malachite green. The colorant which has not been attached to the paper is removed by blotting with a tissue or a counter paper. The sample surface is sometimes rinsed under running water, before blotting the sample dry, since not all of the colorant that remains on the silicone can be removed with the tissue only. The number of tested samples is often low in order to save time. Typically only one sample is taken for the test. Colorimetric measurement systems are provided by many different suppliers, which could result in a variability in the L*a*b* values. However, since only the colour difference, delta E, is important, the effect on the result should be minimal.

In some cases a stack of the same paper is put under the sample during colorimetric measurement, while in other cases only the single sample is measured. The stained area is usually much larger than the measurement spot of the colorimeter and the stain density varies over the entire stained area. Therefore it is advisable to measure several spots and determine a mean value. Light source and measurement angle for the $L^*a^*b^*$ measurement are sometimes not defined and different settings can also introduce small differences. Concerning all the variations in the execution of the delta E test, the only option is to define a procedure, keeping all parameters constant. In this thesis the method used in Dunafin ([26]) was selected. The parameters used in this study are written in bold letters in Figure 3-3.

3.3. DELTA E TEST PROCEDURE:

For the preparation of the colorant solution 1.0 g of malachite green oxalate crystals was diluted with distilled water in a 1 l flask at ambient temperature. The solution is stored in darkness as the colorant is not resistant to light.

The procedure starts with the measurement of $L^*a^*b^*$ values of the unstained sample, measured with a standard colorimeter (Colour touch 2) using the D65 light source and 10° . During the measurement the sample is placed on a stack of white copy paper, to prevent variation in opacity from influencing the results. Five spots are measured on each sample and the mean value is used for a result. In the Dunafin procedure, a stack of the same paper was used instead of a white backing paper, but since only the colour difference is needed it will not make a difference, as long as the same paper is used as backing paper. For the laboratory test an oil Cobb tester is used instead of the standard Cobb ring. Results from the Cobb tester and the oil Cobb were compared and no significant differences were found. The sample size is 14 x 14 cm and the area of contact of the colorant with the paper surface is a circle with a diameter of 10 cm for the Cobb and the oil Cobb. The advantage of the oil Cobb is the simplified handling and especially the faster removal of the colorant after the time span of 30 seconds. For the laboratory test, 50 ml of the 1 g/l malachite solution are measured in a flask and emptied into the oil Cobb. The sample is placed on the ring with the silicone side down and fixed with the top of the oil Cobb tester. The device is flipped over. After 30 seconds it is flipped back to the original position and the top is quickly removed. The sample is then rinsed under running water, until the water appears colourless. Afterwards the sample is blotted dry with a tissue. The $L^*a^*b^*$ values from the stained area are measured in five spots, with the same settings as described for the unstained sample. The delta E value is determined from the mean $L^*a^*b^*$ values using formula (3-1).

3.4. EVALUATION OF ADDITIONAL PARAMETERS USING IMAGE ANALYSIS:

3.4.1. DESCRIPTION OF STRUCTURE SIZE ANALYSIS:

Besides the measurement of the $L^*a^*b^*$ values and the calculation of the delta E value, the stained samples can be further analysed. The stained samples are scanned using an “Epson Perfection 4990 4” scanner, at a resolution of 1200 dpi, which is equal to a pixel size of $21.17 \mu\text{m}$. A square area with a side length of 7.46 cm (3524 pixels) is selected inside the stained area image and used for further image analysis implemented in MATLAB. This sample area was chosen for the analysis, in order to obtain a maximum area from the stained sample, but to avoid bringing in an error from the sample edges. To ensure a high overlapping of the area used in image analysis with the colorimetric measurement was an additional aspect. The best option would have been to scan a circular area, which was not possible with the software of the scanner and would also cause further difficulties in the image analysis. The images are decoded on three levels (RGB – values) and displayed as a numerical data matrix in MATLAB. Each level represent a colour filter (red, green, blue). The addition of the three levels displays the full colour information of the image. The numerical information obtained for the stained spots, differs from the non-stained areas. Using a threshold value the stained areas are segmented from the non-stained areas. The applied threshold value has to be adjusted when other settings of the scanner or a different scanner is used. Another way to separate stained and non–stained areas would be via gradients, which is not as sensitive against different scanner settings, but could not be implemented in the available time during this thesis.

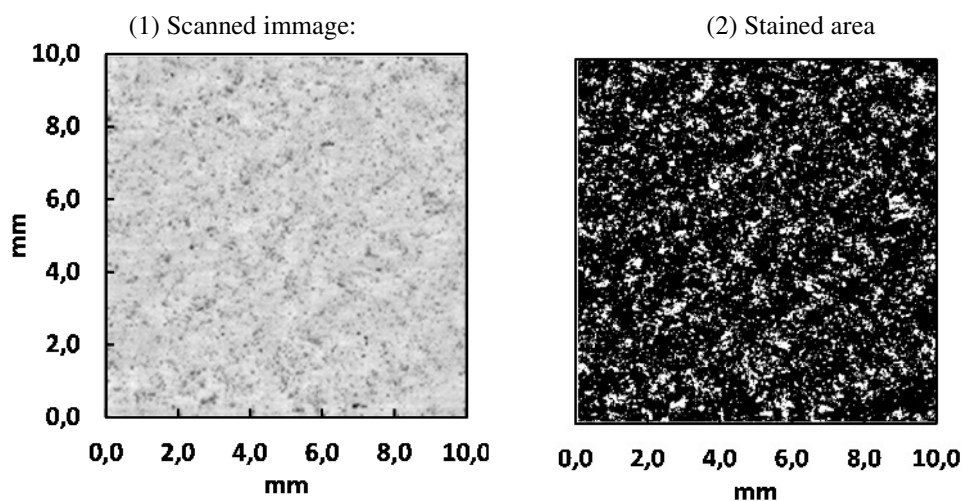


FIGURE 3-4: SEPARATION AND BINARISATION OF STAINED AND NON – STAINED AREAS

After the segmentation all stained spots are set to a single value. This is depicted in Figure 3-4 (2), where the stained areas are white and the rest is black. The aim was to compare the size of the stained area with the whole area, which was done by summing up the area of all stained spots. The sample size was held constant, which would not make it necessary to calculate a percentage of the stained area. Nevertheless this was done in order to obtain clearly transparent values.

This analysis makes it possible to compare the results from the colorimetric measurement, the delta E value, with the size of the stained area which is shown in Figure 3-5 for a number of release liner samples measured in a measurement series.

Small deviations are caused, because colour intensity was neglected in the determination of the stained area. Further it is not possible to cover exactly the same area for the image analysis as with the colorimetric measurements, measuring the L*a*b* values on five spots of the same delta E test paper.

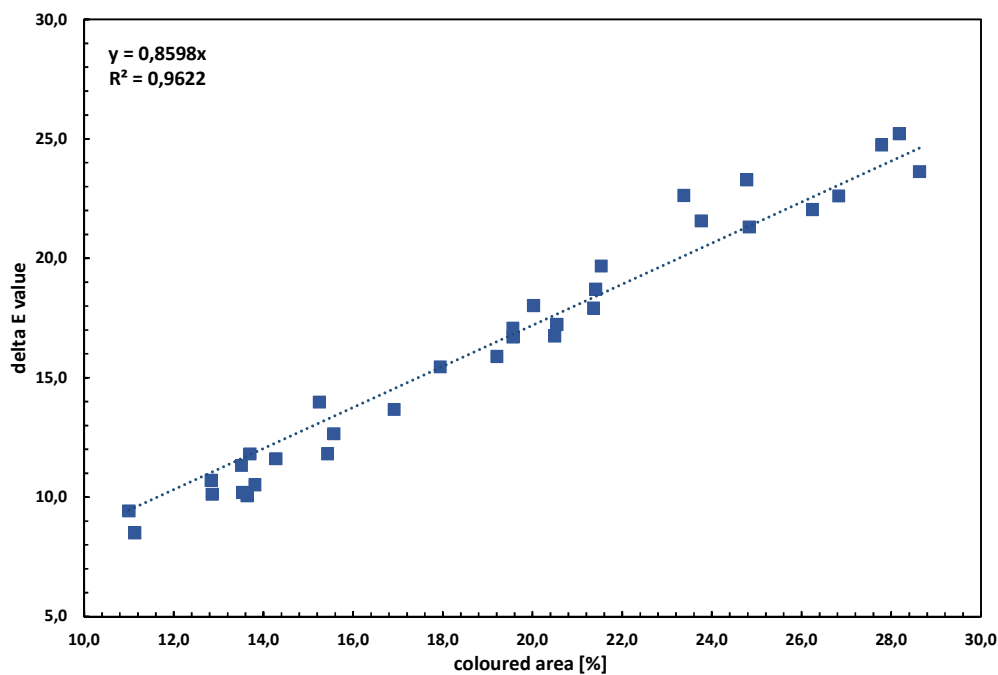


FIGURE 3-5: CORRELATION OF THE STAINED AREA, EVALUATED WITH IMAGE ANALYSIS AND THE DELTA E VALUE FOR ONE DELTA E TEST SERIES.

A further step is to separate the size of the stained spots. In Figure 3-4 it is clearly visible that there are smaller and larger spots. Using a bandpass filter, structure sizes can be separated. With a bandpass filter a band, e.g. from 42.34 μm to 84.68 μm is set. All spots within this range are kept, while spots out of this range are rejected. 28 classes, each class with a band width of 42.34 μm were calculated. The class width was chosen to be twice the scanned resolution of 21.17 μm . For mathematical reasons

it is not possible to filter structures smaller than the doubled resolution. It has to be taken into account that therefore no structures below $42.34\ \mu\text{m}$ are determined for these scanned images. Nevertheless the summation of the areas in all classes shows a high correlation with the delta E values (see Figure 3-6). All measurements are included in the figure, which implements 180 data points. At the left edge of the graph, release liners with a low delta E value and therefore good silicone coverage are depicted. These liners have a high percentage of stained spots smaller than the detection limit of $42.34\ \mu\text{m}$ that is why the correlation between stained area and delta E value is poorer at low delta E values. In the linear equation an offset is present, also caused by the detection limit. All in all this correlation shows, that it is reliable to determine the stained area by the summation of area classes produced with a bandpass filter. Further parameters are determined based on structure size distribution of the stained spots. The procedure will be explained in detail in chapter 3.4.2. The whole stained area will be used in the following chapters for different comparisons. A separation in structure sizes is not necessary for this comparisons and only brings in an error by the limitation at $42.34\ \mu\text{m}$. Therefore the whole stained area is determined without the use of the bandpass filter.

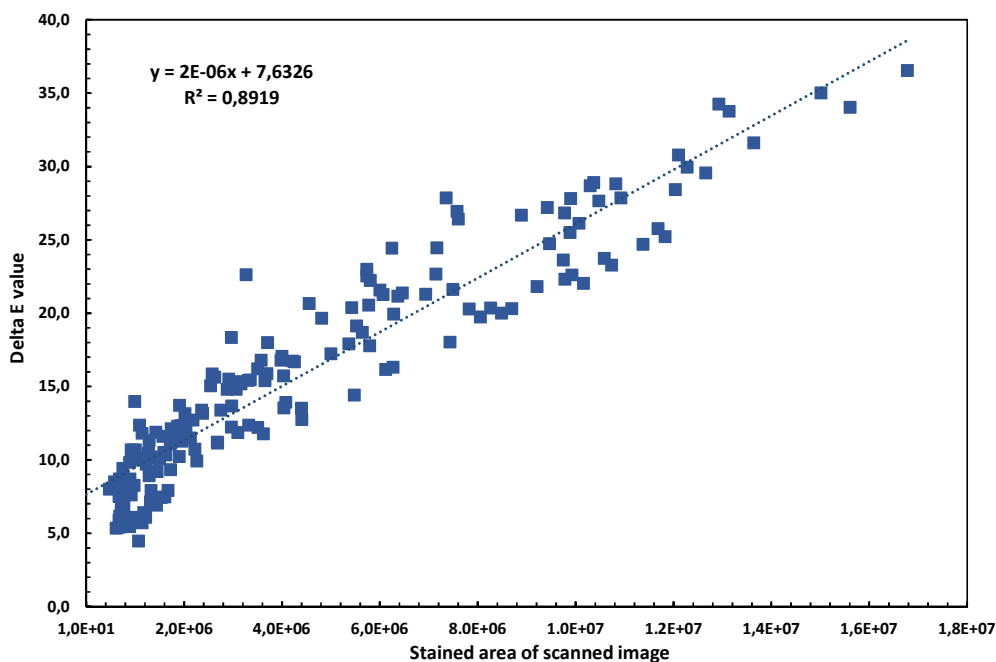


FIGURE 3-6: CORRELATION OF COLORED AREA DETERMINED USING A BANDPASS FILTER AND THE DELTA E VALUE

3.4.2. PARAMETERS GENERATED FROM IMAGE ANALYSIS:

After the separation of the spot sizes in 28 classes, with a class width of 42.34 μm a determination of spot size distribution is performed. For each class the stained area can be calculated, by the summation of the stained spots within each class, using the same method as described for the calculation of the entire stained area. The calculation of the area for each class is generating an area distribution (q_2 distribution). Under the assumption that the spots have the shape of circles, a length (diameter) distribution (q_1 distribution) can be calculated from the area distribution, using formula (3-2). The length calculated is the sum of the mean length of the class i . The mean class length (L_i) is divided by the mean size of the class ($\frac{s_i+s_{i+1}}{2}$) to obtain a point distribution (q_0 distribution) (see formula (3-3)). The points indicates how many spots are stained in any class i .

$$L_i = \sqrt{\frac{4 * A_i}{\pi}} \quad (3-2)$$

$$P_i = \frac{L_i}{\left(\frac{s_i + s_{i+1}}{2}\right)} \quad (3-3)$$

After the calculation for each class, the sum over all classes is determined. To make the distribution functions comparable, they have to be normalized, so the sum of each distribution is always one ((3-4)(3-5)(3-6)).

$$A_{total} = \sum_{i=1}^n A_i \quad L_{total} = \sum_{i=1}^n L_i \quad P_{total} = \sum_{i=1}^n P_i \quad (3-4)$$

$$a_i = \frac{A_i}{A_{total}} \quad l_i = \frac{L_i}{L_{total}} \quad p_i = \frac{P_i}{P_{total}} \quad (3-5)$$

$$\sum_{i=1}^n a_i = 1 \quad \sum_{i=1}^n l_i = 1 \quad \sum_{i=1}^n p_i = 1 \quad (3-6)$$

In Figure 3-7 an example for the density distribution is given for the same base paper with silicone coat weights of 0.7 and 1.3 g/m^2 respectively. Details of the scanned delta E test images are added. The curves terminate at a structure size of 42.34 μm on the low side of the structure sizes, because of the resolution limitation of the scanned sample. The point distributions have their maximum at the lowest structure

size, while the frequency in the area distribution reaches the highest level at higher structure sizes. Therefore it can be concluded, that most of the defects in the silicone layer are located at a minimum structure size, but they have less impact on the final result of the delta E value, as this value correlates with the stained area. A comparison of the two silicone coat weights, shows a steeper distribution for 1.3 g/m² silicone, which just says, that the defects in silicone coverage have a smaller size for the higher coat weight. This tool will be used for the comparison of the quality of silicone coverage in chapter 5.3.

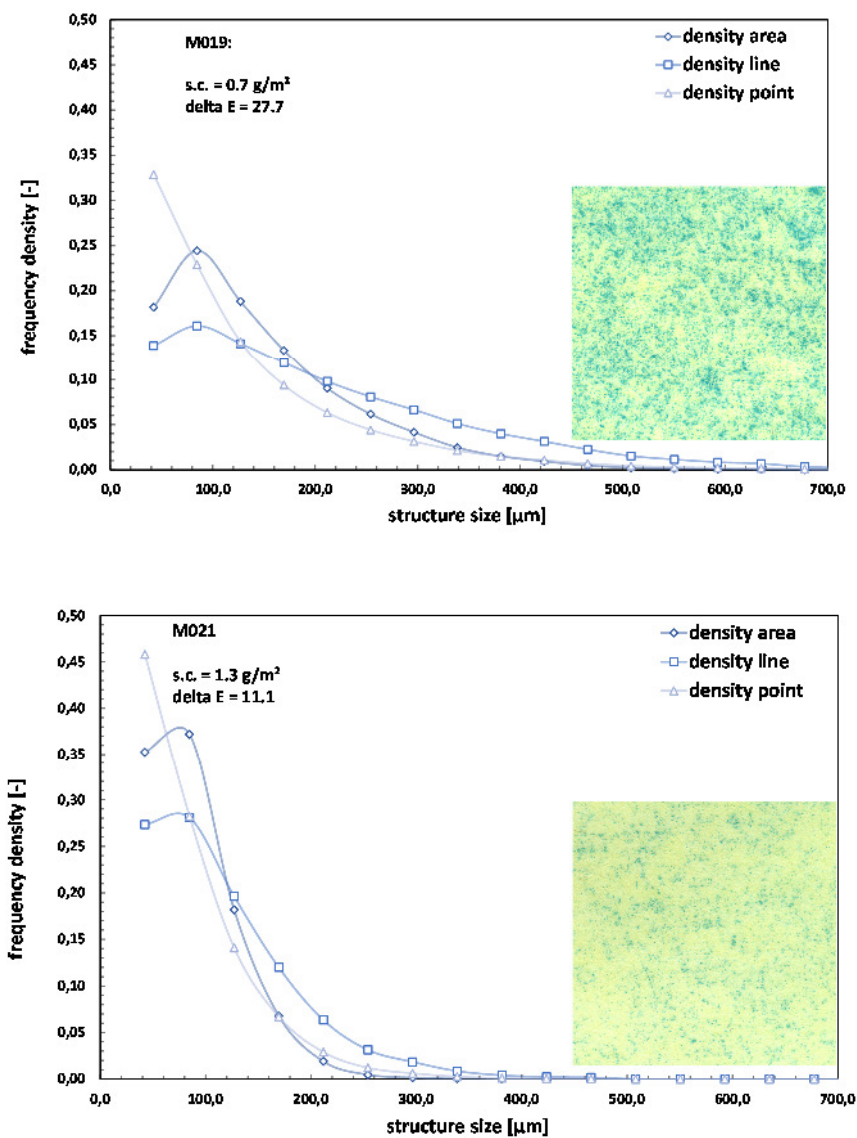


FIGURE 3-7: DENSITY DISTRIBUTION FOR A BASE PAPER WITH DIFFERENT SILICONE COAT WEIGHTS

To facilitate a comparison between different papers, a further parameter is generated from the structure size analysis. This parameter describes the mean size of defects in silicone layer is defined by the ratio R expressed by the total number of points divided by the total area (3-7).

$$R = \frac{P_{total}}{A_{total}} * 10^6 \quad (3-7)$$

This parameter is determined for the three silicone coat weights (0.7 g/m², 1.0 g/m² and 1.3 g/m²), applied to the identical base paper. A higher ratio indicates smaller holes in the silicone layer in the average, for the applied silicone coat weight. Plotting the ratio against the applied coat weights the slope (S_{cov}) occurs, indicates the ability of closing defects. A higher slope of the ratios is therefore an indicator for the ability to close defects with increasing silicone coat weight better. As the slope is calculated from parameters determined from the scanned delta E test image, truthfully not the closing of defects, but the reduction of the size of the stained spots with increasing silicone coat weight is described. Four different release base papers siliconized with the three different coat weights are shown exemplarily. In Figure 3-8 the development of the delta E value with the silicone coat weight is plotted for a comparison. Figure 3-9 shows the increase of the rate with the silicone coat weight.

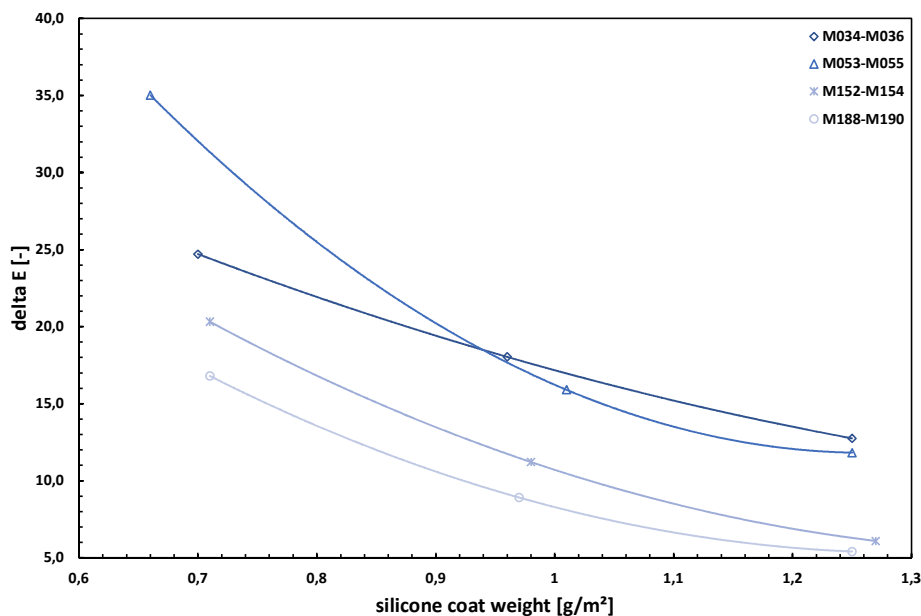


FIGURE 3-8: DEVELOPMENT OF THE DELTA E VALUE

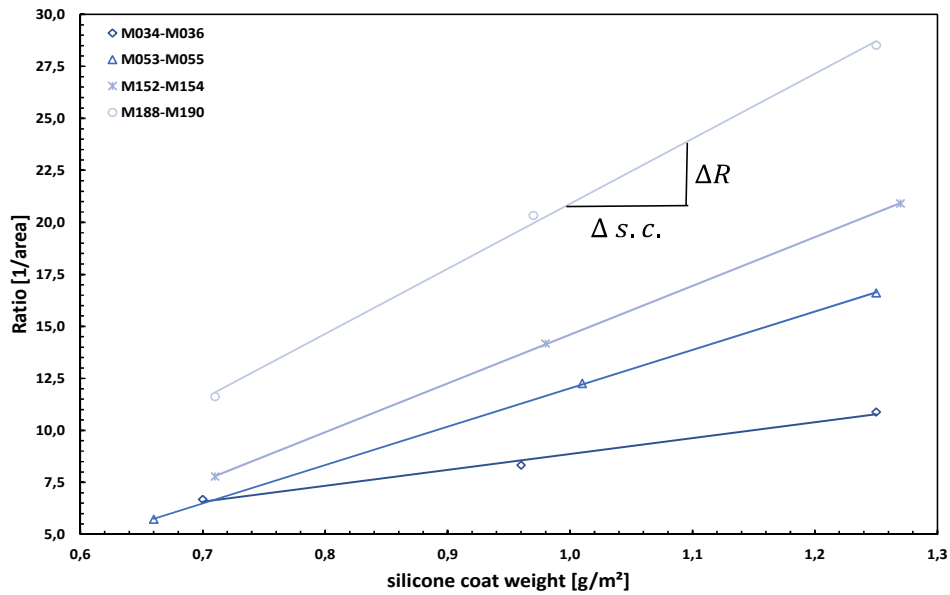


FIGURE 3-9: DEVELOPMENT OF THE RATIO (STAINED SPOT SIZE)

Summarizing the parameters P_{total} and S_{cov} are used in chapter 5.3 in multiple linear regression analysis. P_{total} describes the number of stained spot of the scanned delta E test image. S_{cov} is an indicator for the ability of closing defects with increasing silicone coat weights. A higher slope S_{cov} means a faster closing of the silicone layer.

4. OVERVIEW OF MEASUREMENT METHODS AND ANALYSIS ROUTINES:

The development of new measurement methods was performed in order to be able to provide additional information on the quality of release base papers, which might describe the influence on the delta E value and silicone coverage. In chapter 4.1 a method for the characterization of PVA coverage on the release base paper is introduced. Chapter 4.2 describes a method which enables a topographical and image analysis of the transparent release base papers and release liners, using the optical infinite focus measurement (IFM). This is possible by taking silicone negatives of these papers.. A method and an analysis routine used for the local comparison of images and other 2D maps is explained in chapter 4.3. Multiple linear regression provides a tool for the prediction of influences on a response variable (see chapter 4.4). In this thesis multiple linear regression was used to predict silicone coverage and the delta E value (see chapter 5.3). Chapter 4.5 and chapter 4.6 are describing methods used as standard methods and additional methods for the quality evaluation of release base papers. The parameters coming from these methods are used as prediction parameters in multiple linear regression analysis.

4.1. DEVELOPMENT OF A METHOD TO CHARACTERIZE PVA COVERAGE AND DISTRIBUTION:

PVA forms a transparent layer on the surface of the release base paper. PVA coverage is important for the further siliconizing process, for various reasons discussed in chapter 2.1.3. A method to evaluate the uniformity of PVA application on the base paper was developed, therefore. This method is a modification of a qualitative method for PVA identification, based on a Tervakoski test method ([27]). Under presence of boric acid, a colour reaction of PVA with a potassium iodide (KI) – iodide (I₂) solution appears. Bluish color indicates the presence of pure PVA. In the case that PVA is used together with starch, the colour shifts to a more purple region, while starch alone is indicated only by a purple coloration. This shift allows to determine PVA coverage also for PVA and starch coated samples (see Figure 4-1).

A 40 g/l boric acid solution was prepared. For the preparation of the KI – I₂ solution 2.5 g KI and 0.1 g I₂ is crushed and mixed in a mortar. To dissolve the crushed KI – I₂ mixture, 5 ml of distilled water are added in the mortar slowly. 2 ml of this solution are pipetted in a 100ml flask and filled up with distilled water. The KI – I₂ solution, is applied to the release base paper surface via a spray can, followed by the boric acid

solution, which is applied the same way. A more detailed description of the test method is added in the appendix (see appendix A1.1). Due to the colour reaction with the PVA this test allows an evaluation of PVA coverage and uniformity of PVA distribution.

The treated paper samples were scanned with an “Epson Perfection 4990 4” scanner at a resolution of 21.17 μm per pixel. An area of 3.4 cm x 3.4 cm is selected for further analysis. The whole sample cannot be analysed as it is not possible to apply the chemicals uniformly to a larger area. The coloured and non - coloured areas are separated via a threshold value the same way as described for the papers from the delta E test (see chapter 3.4.1). A value for the PVA covered area (PVA_{cov}) is determined dividing the coloured area (representing the presence of PVA) by the total sample area.

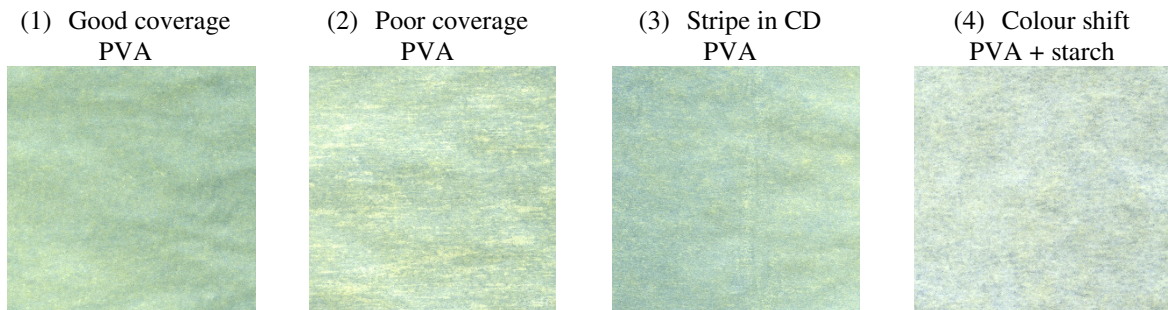


FIGURE 4-1: EXAMPLES SHOWING DIFFERENCES IN PVA COVERAGE

4.2. METHOD AND FIELD OF APPLICATION FOR SILICONE NEGATIVES FROM BASE PAPER AND RELEASE LINER SURFACES:

4.2.1. METHOD OF TAKING SILICONE NEGATIVES:

ESCA (electron spectroscopy for chemical analysis) and AFM (atomic force microscopy) are usually used to detect the topography and the silicone coverage of release liners. These methods have their advantages in the high resolution that can be achieved, but only very small areas can be analysed with a rather high effort. Optical topography methods for release base papers and release liners are generating questionable results, as these papers are transparent and vary in their local opacity. Mechanical topography methods can be used, but are time consuming when high resolutions are required and the measuring head is in direct contact with the paper sample. This can cause variances from the real topography, as it is necessary to apply a minimum force on the paper. Taking a negative of the paper surface, using silicone, creates an optical homogeneous surface, which can be analysed using optical topography methods. Due to its low surface energy and its freedom of rotation, silicone

is capable to creep into small pores and to wet all kind of surfaces. These properties are needed to achieve a negative which includes all the topographical information from the original. The silicone is weight in a plastic beaker together with 10 % hardener (based on the mass of silicone) and homogenized with a spatula. A small quantity of the black paste is mixed with the already homogenized components with a spatula until the mixture reaches a homogeneous black colour. The liquid silicone compound is then poured onto the paper sample (backed with a counter plate) in a sample frame. The counter plate provides an even and smooth backing for the paper sample. The sample frame functions as a boarder for the silicone. For the counter plate and the sample frame a polymer board was used. After a curing time of three hours the silicone negative can be separated from the frame and the paper. The silicone negative replicates the topography of the paper, which cannot be evaluated directly via optical topography systems due to the transparency of the paper, of the applied PVA and, in case of the release liner, due to the transparency of the silicone layer. The black silicone negative however can be analysed using optical methods. Topographical mapping of quite large areas compared to the methods working on the basis of the chemical composition of the silicone or the PVA is possible for the silicone negatives using e.g. the optical infinite focus method (IFM). A detailed description of the method is added to the appendix (see appendix A1.2)

4.2.2. INFINITE FOCUS MEASUREMENT:

Infinite focus measurement (IFM) is based on the principle of focus variation. The low depth of focus of the optics of a microscope makes it possible to extract topographical information. Variation of the distance in z - direction between the objective and the specimen generates images, where some regions are sharp and other regions are out of focus. Determination of the topographical information is performed with a software using the information regarding the focus (sharpness of image) and the variation of focus in z – direction ([22]). Figure 4-2 illustrates the IFM measurement device.

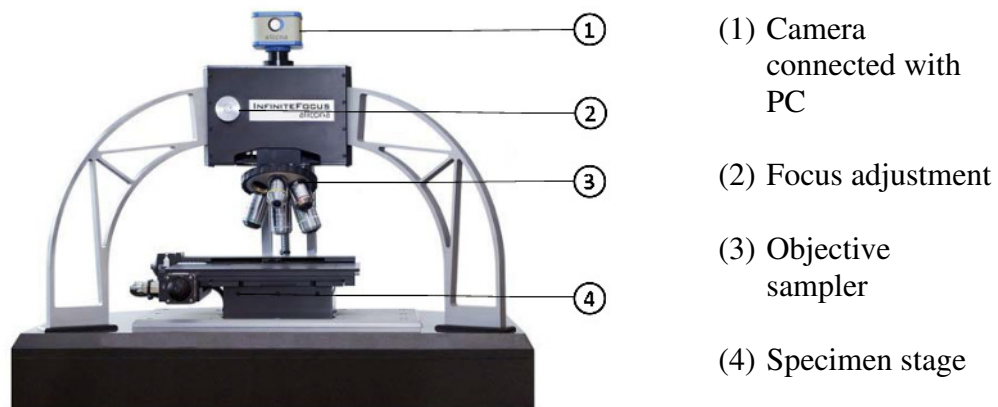


FIGURE 4-2: INFINITE FOCUS MEASUREMENT DEVICE (ALICONA) ([28])

The specimen stage is movable in xy - direction and can be operated with a joy stick, or via the user interface provided by the software. Magnifications of 2.5x, 5x, 10x, 20x, 50x can be selected. With a 5x magnification a resolution in the xy - plane of 12.8 μm per pixel and for a 50x a magnification of 1.28 μm per pixel is achievable for the topographical map. Measurement time is dependent on the surface roughness and the magnification of used. The resolution in z - direction can be adjusted from 2 μm to 10 nm, depending on the magnification. In addition to the topographical information the software provides the optical image and tools for topographical analysis. For the topographical mapping a 10x magnification is used in further tests. With the resolution of 6.4 μm per pixel it is ensured that the topography of single fibres and small defects in the silicone layer are detected in the measurement. The resolution in z - direction was chosen with 333nm.

4.3. LOCAL COMPARISON OF VARIOUS PAPER PROPERTIES:

This method developed at the Institute for Paper, Pulp and Fibre Technology at Graz University of Technology, is used to compare 2D paper property maps obtained with different devices at different resolutions using image registration. The procedure is described in detail by Hirn et.al. ([21]). The method consists of three steps:

- Marking of the sample.
- Registration of the 2D maps
- Local comparison and image analysis.

The first two steps are described in more detail in this chapter. The third step will be discussed in chapter 5.4.

4.3.1. MARKING OF THE SAMPLES:

The paper samples are marked with a high precision laser cutter. The marks are small holes of approximate 0.4 mm in diameter and define the coordinate system for the registration. In earlier applications a rectangular piece of adhesive tape was used for this purpose.

4.3.2. REGISTRATION USING THE MARKINGS:

A software for the registration of 2D datasets was developed at the Institute for Paper, Pulp and Fibre Technology at TU Graz. The data maps are imported as image files, txt/csv files or xls files. The image registration consists of three steps. First, the coordinate system of the images has to be identified, using the laser marks (see Figure 4-3). Aligning of the images is the second step. When different measurement devices are used in the determination of local paper properties, the obtained 2D maps usually do not have the same resolution. In the third step the software therefore recalculates the resolution of all 2D maps to an identical resolution. The target pixel size and the region of registered samples is defined in a database, which includes the registered maps.

The registered data are available as images, or as csv data file for further analysis.

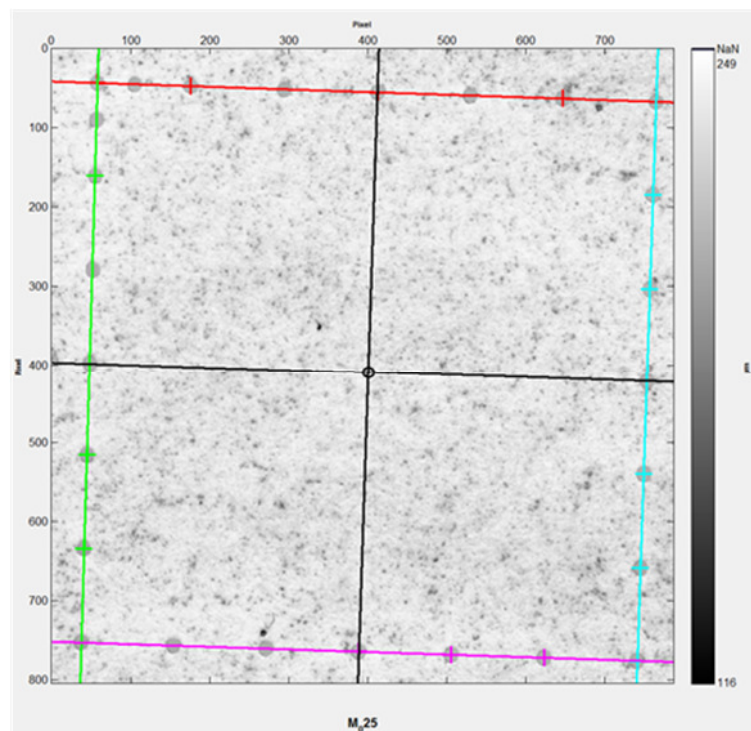


FIGURE 4-3: MARKED 2D – DATAMAP WITH IDENTIFIED COORDINATE SYSTEM

4.4. MULTIPLE LINEAR REGRESSION:

Multiple linear regression provides a tool for the prediction of influences on a response variable (Y) (see formula (4-1)), where p_1, p_2, \dots, p_n are the supposed predictors for the response variable (Y). The aim is to determine the coefficients ($\beta_{0,1,\dots,n}$), which are predicting the scale of influence of each variable and the direction of the influence. Y and p_i are vectors with the same length. Each row ($i = 1 \dots n, j$) is representing a measurement set of one defined paper sample, where all predictor variables and the response variable are included. The length of the vector is therefore the number of measurement sets, which has to be at least the number of predictor variables. Accuracy increases with the number of measurement sets.

$$Y_j = \beta_0 + \beta_1 * p_{1,j} + \beta_2 * p_{2,j} + \dots + \beta_n * p_{n,j} \quad (4-1)$$

Predictor variables can interact with each other. Picking for example, Cobb Unger and Cobb₆₀ are an example for predictors that are not independent from each other. Using them separately as the only predictor for the response variable Y in a simple linear regression model (SLR), they might have both a coefficient of determination $r^2 = 0.5$. If they would be completely independent from each other, these two predictor variables, used together in a multiple linear regression model would describe the response variable with an $r^2 = 1$. This is not the case, as the Cobb Unger already describes a high percentage of the Cobb₆₀, which make them dependent from each other. Therefore it is necessary to determine the exclusive and the redundant share of the coefficient of determination (r^2) for each predictor variable in the model to be able to evaluate the quality of the predictor variable (see ([23])). Multiple linear regression analysis can be applied in the comparison of local paper properties, produced with 2D mapping methods and for the prediction of the impact of paper quality parameters on a response variable. In this thesis the second application is in the focus.

4.5. ADDITIONAL QUALITY PARAMETERS:

4.6.1. SURFACE pH:

Surface pH measurements were performed in order to proof the hypothesis, that the pH of the release base paper is affecting the final result of the delta E value, in terms of the colour intensity of the stained fibres and absorption properties.

The measurement is carried out according to TAPPI method T 529 om-99 ([25]). A surface pH – electrode (WTW, SenTix® SUR) is used for the measurement. The surface pH – electrode has a flat membrane, to ensure a uniform contact with the paper

surface. The paper has to be backed with a non - absorbent, elastic material. A drop of distilled water is put on top of the paper with a pipette and the electrode is placed on the wetted spot, remaining ten minutes, before reading the pH value.

4.6.2. CONTACT ANGLE:

Contact angle is measured with the Fibro 1100 DAT dynamic absorption tester. The test liquid is silicone oil, which is applied onto the sample as a drop formed at the end of a 0.9 mm hose. Difficulties appear as the silicone oil tends to cling to the surface of the hose. The hose was cut diagonal to reduce this property. The distance between the paper sample and the hose exit and the stroke pulse are the parameters to set the time for the release of the drop from the hose. The drop size was set to 5.5 μ l. Ten measurements were performed for each paper sample. The initial contact angle (A_04), gives an indication for the surface energy of the paper. A lower initial angle means a higher wettability of the base paper by the silicone oil. The difference between the initial contact angle and the contact angle after 2.6 s (d_A), should describe spreading and absorption together. The difference between the initial drop volume and the drop volume after 2.6 s (d_V) indicates absorption properties only.

4.6. STANDARD METHODS TO DESCRIBE THE QUALITY OF RELEASE

BASE PAPERS:

The parameters and methods used in the quality control of release base papers are explained briefly in this chapter. Parameters of interest are basis weight, thickness, density, smoothness, porosity, water absorption, oil absorption and ink absorption. Together with the additional parameters described in chapter 4.1 and 4.5, which are PVA coverage, surface pH, contact angle, contact angle difference and drop volume difference, these parameters will be used later as predictor variables in multiple linear regression analysis attempting to find a model to explain the delta E value and silicone coverage (see chapter 5.3). Smoothness measurement is done with a Bekk device, which is an indirect air leakage method. The results are given in Bekk seconds. Porosity is determined in Gurley seconds. A Cobb value for the time of 60 s is used to describe water absorption. For Cobb Unger oil absorption measurement castor oil is used and the contact time is 120 s. For the ink absorption the IGT method is used. A delta E value determined using “Shirlastain A” on the release base paper is measured for some of the papers. The data for these measurements are provided by Dunafin and Tervakoski. Cobb₆₀ (ISO 535), Bekk smoothness (DIN 53107), basis weight (ISO 536) and thickness (ISO 534), where measured in the laboratory of TU Graz in order to evaluate the variability of measurement data (see chapter 5.2).

5. RESULTS AND DISCUSSION:

In chapter 5.1 influences on the result of the delta E test, besides silicone coverage are discussed. The subchapter 5.1.1 provides an overview considering possible influences which are evaluated in chapter 5.1.2 to chapter 5.1.5. Multiple linear regression analysis (MLR) was used in chapter 5.3 for the prediction of the delta E value and of silicone coverage. Some statistical background concerning the variability of measurement data of the prediction variables used in MLR are evaluated in chapter 5.2. Chapter 5.4 discusses possible analysis routines for a local correlation of silicone coverage with local release base paper properties.

5.1. EVALUATION OF THE DELTA E TEST:

Possible influential factors on the results of the delta E value will be discussed in this chapter. It has to be considered that the delta E value in release liner production is an important measurement for the evaluation of silicone coverage. The colour difference between the release liner before and after the stain test with malachite green, which detects uncovered spots, is measured using the L*a*b* colour space (see chapter 3.3). Errors can be produced due to various reasons. Possible sources of errors can be categorized in the following groups:

- Release base paper - colorant interaction
- Stability of the colorant solution
- L*a*b* colour space and L*a*b* measurement
- Execution of the delta E test

5.1.1. POSSIBLE INFLUENTIAL FACTORS ON THE DELTA E TEST RESULTS:

Release base paper - colorant interaction:

The aqueous colorant solution comes in direct contact with the release base paper, where the silicone layer does not cover it. Taking into account the chemical nature of the colorant and the mechanism it attach to cellulosic fibres, differences in colour intensity and in the absorption spectra of visible light may result. As malachite green is a direct colorant, which attach to the fibres, forming aggregates in the void volume of the cell structure, there has to be a difference depending how large the available volume is. This void volume is affected by the *fibres treatment and the papermaking process* and the pulp recipe itself. In the papermaking process parameters as density,

drying conditions and sizing level are expected to change the colour uptake of the base paper. Due to the fact that paper components other than fibres also influence the colour uptake, the colorant uptake of the PVA coating may be different from the cellulosic fibres. In addition to the lower amount of colorant PVA is capable to absorb, the *maxima of light absorption* for stained PVA compared to cellulosic fibres shifts to a higher wavelength ([19]). The *pH value* of the release base paper might have an effect on the amount of colorant attached to the fibre as the colorant is bonded partly via electrostatic bonding mechanism. Therefore cellulosic fibres which provides more negatively charged groups are capable to bind more colorant. A theory claims that with increasing amount of water bridges, which would be in an alkaline area, less colorant is capable to attach to the fibre ([19]). No proof for this theory has been found in the literature. The *absorption properties* of the release base paper are the sum of influences of the papermaking process and is affected by the degree of internal sizing, PVA coverage, density of the paper, the pulp recipe and also the pH of the base paper. At a higher absorption capacity of the paper more colorant solution can be attached, therefore also more of the aqueous colorant solution might penetrate into the paper causing *darker spots*. Another aspect is the influence of the absorption properties of the base paper on the *spreading* of the colorant at the base paper - silicone interface. In other words: Having two papers, different in the absorption properties, with the same size of defects in the silicone layer, the stained spots on the paper with the higher absorption capacity should be larger. Silicone release liner is produced as a white grade or *dyed yellow*. The yellow colour is realized by the combination of three dyes, which may interact with the cellulose fibres similar to the malachite green colorant solution used for the delta E test. This can have possible effects on the absorption spectra of visible light, by a change in the mechanism the colorant is attaching to the fibres.

Stability of the colorant solution

The age of the colorant solution does play a role as the colorant can *oxidise*, which changes the chemical composition of the colorant. The colorant uptake of the release base paper is low and the surplus colorant solution is often reused. With each test *ions* coming from the paper are transferred to the colorant solution. In an article concerning the adhesion of substantive colorants to cellulosic fibres ([19]) it was shown that with the quantity of salts the amount of colorant attached to the fibre increases. The *pH* value of the colorant solution is also changing, when reusing the colorant solution. This effect should be negligible as the colorant should not changing the colour over a wide pH range.

L*a*b* colour space and L*a*b* measurement

The *L*a*b* colour space* is a non-linear transformation of the XYZ colour space and represents the position of colour and variances of colour positions in a way a human eye would see it. Especially the green component of colours is compressed in the L*a*b* system. Using the L*a*b* system for the measurement of the colour difference, leads not to the physical difference in colour, but represents the subjective difference in colour, how the human eye is seeing it. *Siliconizing* is changing the L*a*b* result compared to the release base paper. Filling up pores with silicone the refractive index and thus scattering changes which is causing the difference. Considering that only spots get stained, which are not covered with silicone, it is not correct to subtract the L*a*b* values of the stained paper from the L*a*b* values of the unstained paper as the unstained paper is also a compound of silicone areas and non – silicone areas, where only the non – silicone areas are changed by the stain test. The *device settings* as light source and angle should also play a role.

Execution of the delta E test

Further possible errors are caused by the execution of the test. The colorant solution is in contact with the paper for 30 seconds and is then removed from the Cobb ring. The *time* to remove the colorant solution surplus, to get the paper out of the Cobb tester and to finally remove the excess of the colorant under running water is dependent on the experience of the laboratory staff. It is therefore not possible to keep the contact time constantly at 30 seconds. In most cases only *one sample* is taken for the analysis, which of course is not sufficient, given the inhomogeneous nature of the paper. *Different colorants* can interact differently with the release base paper, depending on the speed of colorant uptake, the intensity of colorant and its spreading properties at the base paper - silicone interface. Executing the test under non *climatised conditions* could also influence the uptake of the colorant solution. A paper with higher humidity will absorb less colorant. The temperature can have effects on the kinetics of colorant uptake.

In the following subchapters some of the influential factors that might lead to errors are evaluated for the release liners produced in Dunafin. Different methods as absorption spectra, structure size distribution, evaluation of the whole stained area and local comparison of 2D maps, are used in these investigations.

5.1.2. RELEASE BASE PAPER - COLORANT INTERACTION:

pH – value:

To investigate the influence of the pH value on the delta E result the surface pH of 31 release base papers from siliconizing trials in Dunafin is measured. Three measurements per paper sample were performed. The mean values are calculated from these three tests and plotted against the delta E value determined on the corresponding release liner samples with a silicone coat weight of 1.3 g/m² (see Figure 5-1). The delta E values at 1.3 g/m² silicone coat weight is preferable, as the effect of other properties, as e.g. the Cobb value, on base paper properties should be low at higher silicone coat weights. In theory with an increasing pH value a lower amount of colorant is capable to attach to the fibres, which would result in a lower delta E value. Figure 5-1 seems to prove this theory. But considering that there are other influential factors on the delta E result, e.g. the silicone coverage itself, this conclusion has to be taken with care. Different regions in the plot can be referred to the differences in base paper production, which are responsible for the pH of the paper. A delta E value of the release base papers using “Shirlastain A” as a colorant was also compared with the surface pH, but no correlation could be found. As the delta E value using “Shirlastain A”, do not correlate with the delta E values from the release liners, with the silicone coat weight of 1.3 g/m², there might be another mechanism which is responsible for the colour intensity of “Shirlastain A”.

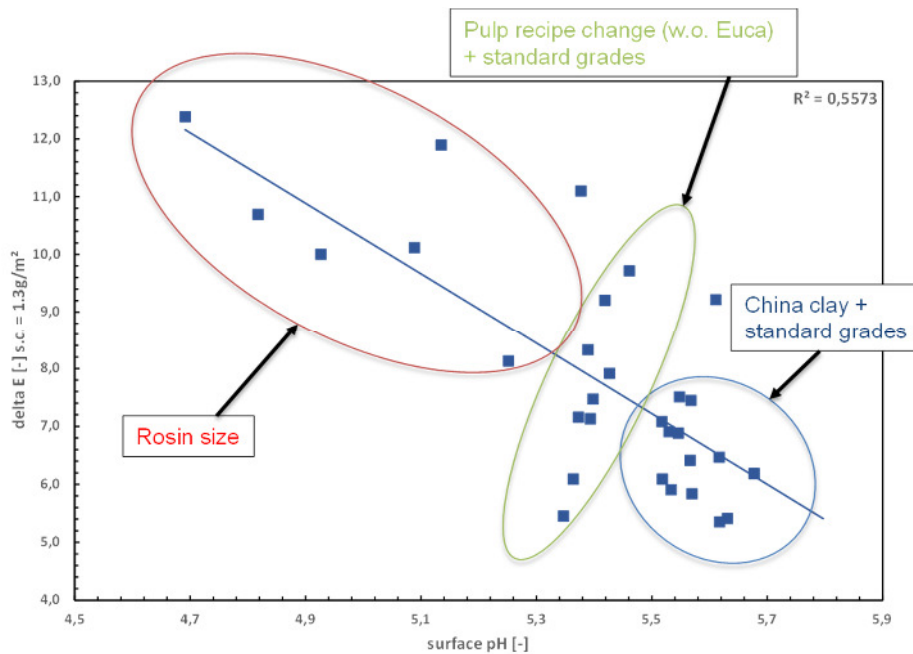


FIGURE 5-1: INFLUENCE OF THE SURFACE PH ON THE DELTA E RESULT

Evaluation of spreading and absorption properties

To prove the influence of spreading and absorption properties of the base paper on the delta E test result a scanned image of the release liner after a delta E test (see chapter 3.4) is compared with the image of the silicone negative analysed with the IFM (see chapter 4.2). To be able to localize the same spots on the samples, they were marked and registered (see chapter 4.3). The sample size is 1.5 cm x 1.5 cm. Two release liner samples (M025, M098) with a similar delta E value (measured at TU Graz) at a silicone coat weight of 1.32 g/m², are discussed. In Figure 5-2 selected areas of these two release liners with the same silicone coat weight of 1.32 g/m² are compared. Only the stained spots from the scanned delta E test images and the defects from the images of the silicone negatives are visible in this figure to enhance the contrast. The original images, where non stained spots (or silicone covered areas) are visible too, are shown in the appendix together with the quality parameters, measured for the two release base papers (see Figure A-4, Table 5-1).

Comparing the 2D maps, the scanned image of the delta E test and the image of the silicone negative, for sample M025, the smaller spots being visible in the negative image cannot be located in the scanned delta E test image. The penetration of the colorant solution through these small holes in the silicone layer seems to take more time than the defined contact time of 30 s. Spots visible in the scanned delta E test image and in the silicone negative image are larger in the scanned delta E test image. That is an indication that the colorant solution spreads at the release base paper - silicone interface. If there is a higher amount of small spots in a narrow area, the spots grow together and demand more space, than the single spots would do. This property is visible comparing the silicone negative and the scanned delta E test image, especially for paper M098. As spreading occurs the question is, whether the Cobb value does have an influence and how big this influence is. The images of the silicone negatives of both papers show a similar distribution and size of defects. Comparing the scanned delta E test images of these two samples, quite some differences are noticed. The effects of the spreading of colorant and the fusion of stained spots is more pronounced for sample M098. Determination of the spot area in relation to the whole sample area for the samples displayed in Figure 5-2 makes the colorant spreading difference in these papers more obvious (see Table 5-2). The spot area of the negatives is 50 % higher in sample M025 compared to sample M098. Which means silicone coverage is worse in sample M025. The result of the scanned delta E test samples, exactly tells the opposite, with a 50 % lower spot area determined for sample M025. This numbers are determined neglecting the colour intensity. The regions where spreading occurs are therefore overestimated as these regions are lighter. A comparison of the quality parameters from the release base papers, related to these

release liners, shows differences in the Cobb value and the IGT ink absorption. The quality parameters can be found in Table 5-1.

The other issues are different absorption properties of the colorant, which should result in colour intensity differences of the stained spots of delta E test papers. It was not possible to directly relate the Cobb value to differences in absorption of the colorant. In theory at higher Cobb values, darker spots should appear, due to the higher water absorption capacity of these papers. As the intensity of colour is dependent on the spot size too, this may be an indicator for a difference caused by the absorption capacity.

Release base paper		
parameter	M 098	M 025
Basis Weight	62,2	58,3
Thickness	53,8	51,0
Density	1,2	1,2
Porosity	42300	42300
Bekk W.S.	2214	2087
Unger	0,6	0,8
Cobb60 PVA side	19,4	16,8
Cobb60 starch side	19,2	17,5
IGT	131	167

TABLE 5-1: QUALITY PARAMETERS (M098 AND M025)

The regions where spreading of the colorant solutions at the silicone base paper interface occurs appears lighter, than the spots, where the actual defects are located. Summarizing it can be said that:

- The colorant solution is spreading at the silicone base paper interface
- Differences in the spreading of the two compared papers might be explainable by differences in the Cobb value and the IGT ink absorption
- Spreading of the colorant leads to a fusion of small dots, which increases the stained area.
- Penetration of the colorant through small holes in the silicone layer seems to need more time than 30 seconds.
- The colour intensity of larger defects is higher than for smaller ones, which might be caused by a lower colorant absorption capacity of small defects.
- The colour intensity at the silicone base paper interface is lower than for the actual defects in the silicone layer

	Spot area [%]	
	Silicone negative	Scanned delta E test image
M025	7,4	13,1
M098	4,9	27,2
Relative difference (M025:M098)	1,50	0,48

TABLE 5-2: COMPARISON OF SPOT AREAS

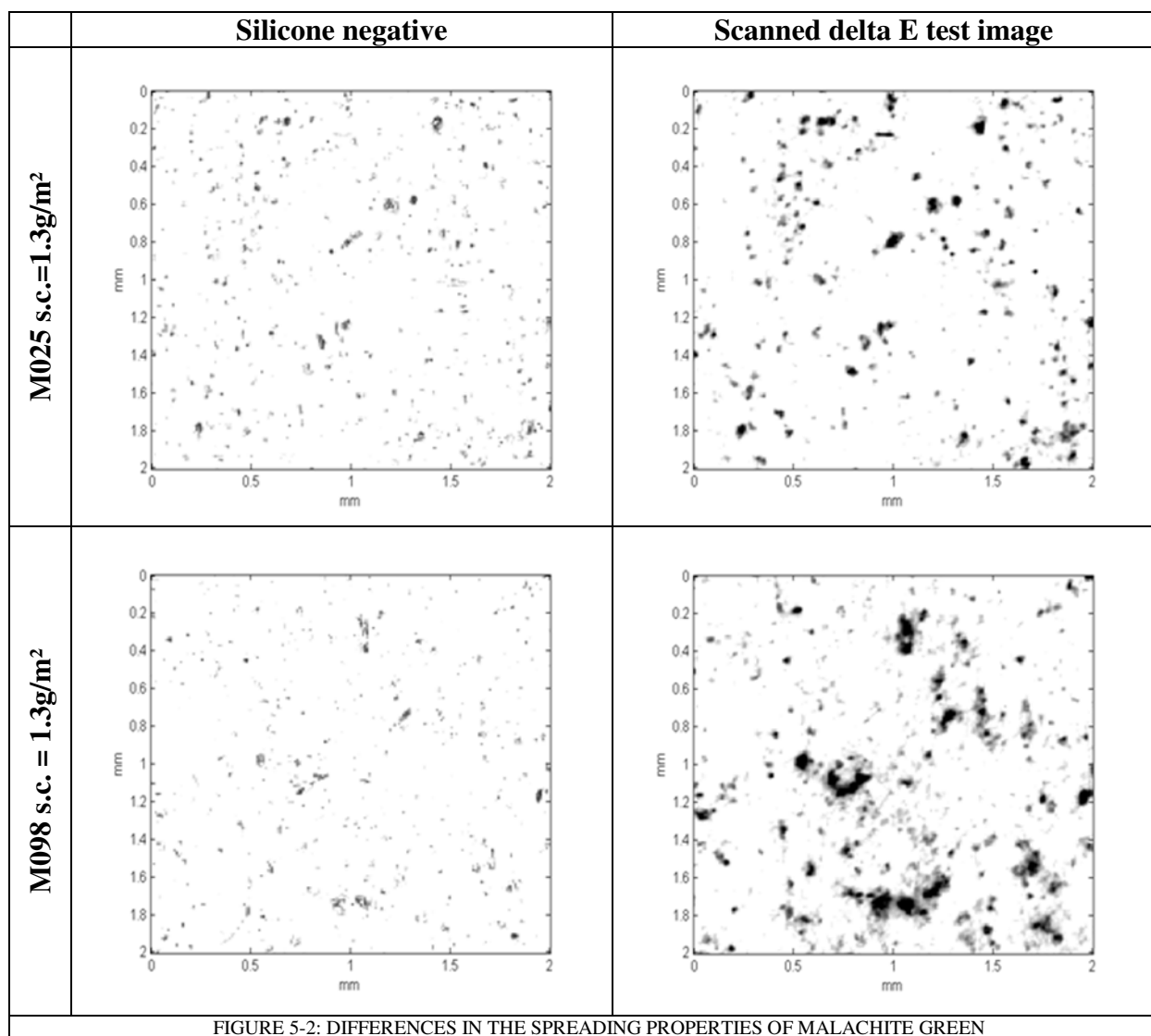


FIGURE 5-2: DIFFERENCES IN THE SPREADING PROPERTIES OF MALACHITE GREEN

Colour of papers:

An influence of the colour of glassine paper grades, yellow or white, on the final result of the delta E test can be demonstrated by the comparison of light absorption spectra. A white and a yellow paper grade from the siliconizing trials are compared.

In Figure 5-3 the spectra of a white and a yellow grade for the unstained paper (suffix R) and the stained delta E test paper (suffix C) is plotted. M548 represent the white grade indicated by the light blue lines. M061 shows the yellow grade with the dark blue lines. The thicker lines are the spectra of the unstained papers. The vertical lines represent the theoretical and actual absorption maxima. The black dashed lines shows the theoretical absorption maxima of malachite green at the wavelength of 420 nm and 623 nm, while the light and the dark blue lines in the area of 400 nm to 450 nm indicates the real absorption maxima of the white and the yellow paper grade. The first local absorption maximum of the white grade is lower than for the yellow grade and close to the theoretical maximum of 420 nm. The maximum of the yellow grade is shifted to a higher wavelength compared to the theoretical maximum. The second local absorption maximum is equal for both grades at approximately 630 nm. Comparing the unstained papers (M548_R and M061_R), the yellow grade additionally absorbs light in the area of 400 nm to 550 nm. The spectra of the stained delta E test papers (M548_C and M061_C) have a similar shape, although the spectrum of the yellow grade (M061_C) is shifted to a higher wavelength in the area of 400 nm up to 550 nm, caused by the additional absorption of light by the yellow colour of the paper.

As the $L^*a^*b^*$ values are originally determined from these spectra, the hypothesis is that the difference of the unstained paper and the stained paper spectrum should have the same shape for white and yellow grades. In Figure 5-4 the difference between the stained and unstained reflectance spectra is determined for a white grade (M548_RC, M546_RC) and a yellow grade (M061_RC, M059_RC) with the silicone coat weights of 0.7 g/m² and 1.3 g/m². This difference in the reflectance spectra is taken as a measure of absorption of light by the coloration of the paper. White grades shows a lower absorption at higher wavelength and a higher absorption at lower wavelength, compared to the yellow grades. The crossing point of the spectra appears at a lower wavelength for a paper with a silicone coat weight of 0.7 g/m². The yellow grades have a higher absorption maximum as the theoretical absorption maximum at 420 nm.

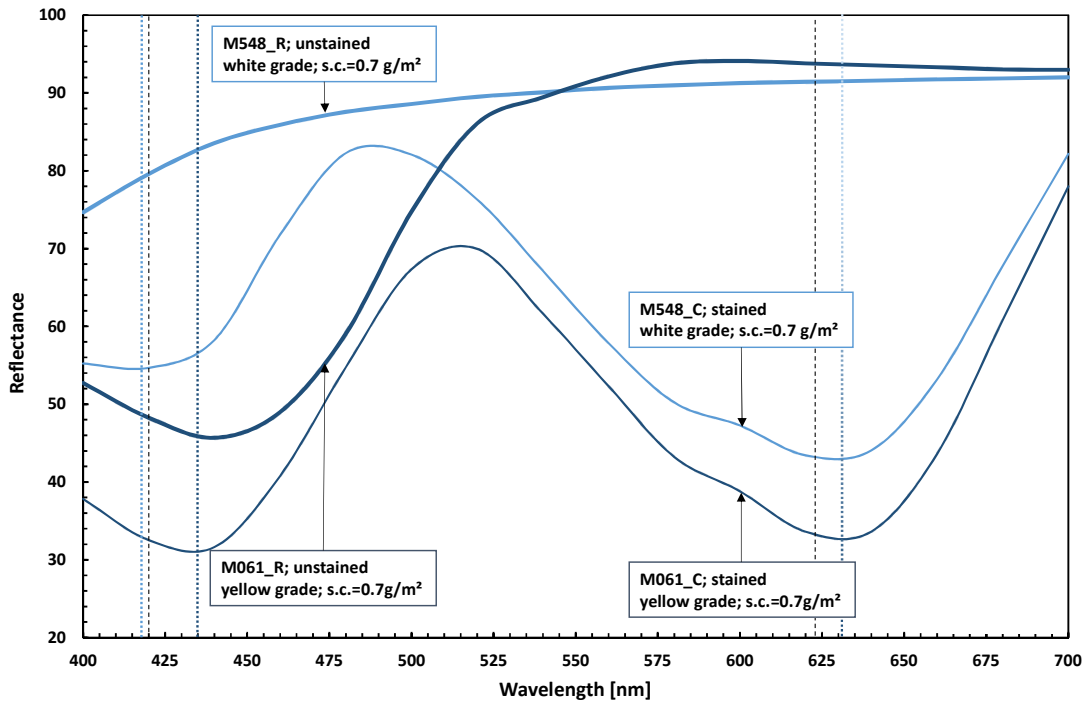


FIGURE 5-3: SPECTRA OF UNSTAINED AND STAINED WHITE AND YELLOW GRADES

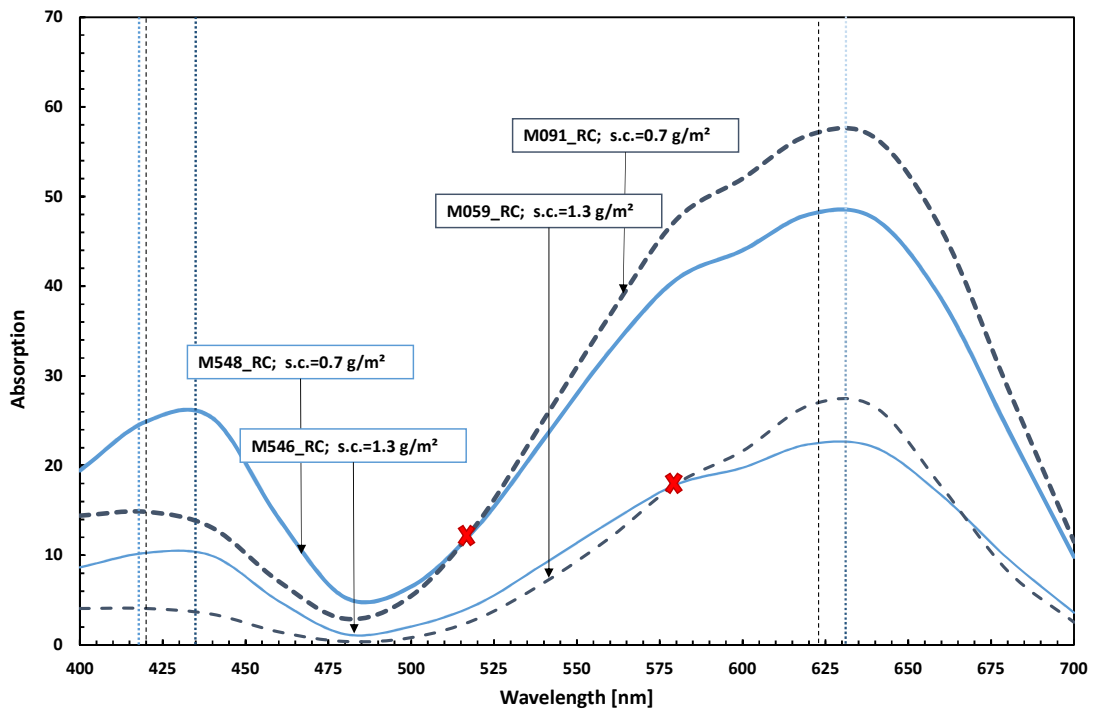


FIGURE 5-4: DIFFERENCE IN LIGHT ABSORPTION OF A YELLOW AND A WHITE GRADE WITH DIFFERENT SILICONE COAT WEIGHTS

Another possibility to point out the differences between white and yellow grades, is to compare the delta E values for a white and a yellow grade with the coloured area, determined from the scanned delta E test images (see Table 5-3). Determination of the coloured area percentage from the scanned delta E test images for a white and a yellow grade with different silicone coat weights, gives similar results for the silicone coat weights of 1.3 g/m² and 1.0 g/m², which lets you expect similar results in the delta E value for these two papers. But the delta E values are much lower for the white grades, which is explainable by the comparison of the L* a* b* differences calculated by the L*a*b* values before and after staining, which are used to determine the delta E value (see Table 5-4). The delta L* and delta a* values for a white grade are both about 20 % lower than for a yellow grade at a similar coloured area. The delta b* value shows an even higher difference compared to the delta L* and delta a* values. Therefore the lower delta E value of white grades is not just explained by a linear dependency of colour intensity, but especially by higher differences for the yellow grade in the blue and yellow region of light, which is represented by the delta b* value.

s.c. [g/m ²]	white	coloured area [%]	delta E
1.3	M546	17,93	10,1
1.0	M547	23,61	15,3
0.7	M548	29,94	24,5
s.c. [g/m ²]	yellow	coloured area [%]	delta E
1.3	M059	18,01	13,7
1.0	M060	23,32	20,3
0.7	M061	33,37	34,2

TABLE 5-3: COMPARISON OF THE STAINED AREA AND THE DELTA E RESULT

s.c. = 1.3 g/m ²	dL*	da*	db*	dE
M546_w	5,10	7,92	3,60	10,08
M059_y	6,09	10,08	7,08	13,74
Ratio (M546:M059)	0,84	0,79	0,51	0,73
s.c. = 1.0 g/m ²	dL*	da*	db*	dE
M547_w	7,95	11,91	5,28	15,26
M060_y	9,51	14,86	10,07	20,31
Ratio (M547:M060)	0,84	0,80	0,52	0,75

TABLE 5-4: COMPARISON OF THE L*A*B* DIFFERENCES BETWEEN WHITE AND YELLOW GRADES

Summarizing it can be said that:

- The resulting delta E value is affected by the colour of the base paper.
- Yellow grades show higher delta E results although a comparison of the stained area would not lead to this conclusion.
- The difference in the delta b* value of white grades is higher than the difference in the delta L* and delta a* values, which is an indication for a possible interaction between the paper colour and the colorant solution used for the delta E test.
- The absorption maxima are different, for the white and yellow grades, which is an additional indication for an interaction of the colour of the base paper and the colorant used for the delta E test.

Fibre treatment and papermaking process:

The possible effect of fibre treatment and the papermaking process on the delta E value was not investigated, as pilot or mill trials with subsequent siliconization would have been necessary, which was not within the scope of this thesis.

5.1.3. STABILITY OF THE COLORANT

Salt content and oxidation of the colorant:

In this section the hypothesis, that the colouring intensity of coloured spots and thus the delta E value increases, with the reuse of the same colorant solution for the measurement of a high quantity of papers is discussed and underlined with an experiment. Delta E tests executed on two different test dates are compared. The applied colorants had different ages and were already used for delta E tests on other paper samples. The test series are the combination of two numbers (Test x.y). The first number (x = 1 - 3) indicates different siliconizing trials in which the release base papers were siliconized. The second number (y = 0 - 2) is categorizing different test series of the delta E test for the specific papers of silicone trial x. Delta E tests performed at TU Graz (x.1) or at Dunafin (x.2) are compared with the delta E tests performed at Wacker (x.0) directly after siliconizing of the release base papers. In Dunafin 3 tests per release liner were performed using a freshly prepared colorant solution and a mean delta E value was determined. The mean values are used in the following comparisons. At Wacker and TU Graz only one test per release liner was carried out. The age of the solution used at Wacker is not known. The colorant solution used at TUGraz had already aged for three month. All tests performed at TUGraz, discussed in this section

were carried out within three days. The comparisons are determined separately for the different silicone coat weights, which are 0.7 g/m², 1.0 g/m², 1.3 g/m².

The relative and absolute differences of two test series are compared for delta E tests performed at TU Graz (x.1) or at Dunafin (x.2) with the delta E tests at Wacker (x.0) (see Table 5-5). The determination of mean relative and absolute differences is performed in detail for the comparison of trial 3.1 and trial 3.0 (see Table A-1). For the first three comparisons in Table 5-5, where the number of tests per paper is equal, the mean absolute difference is similar for the three different silicone coat weights. This results in the highest relative difference for a silicone coat weight of 1.3 g/m², as the absolute delta E values have the lowest numbers for this coat weight. Why the comparison of test series 3.2 with test series 3.0 is acting differently might be explained by a different number of delta E tests per release liner. The fact, that the absolute difference is not affected by the silicone coat weight, can only be explained by intensity changes of the colorant on the paper and not by fluctuations of spreading properties, as this influence depends on the number and size of defects.

The mean differences in the delta E test results between Wacker (x.0) and TU Graz (x.1) for the three siliconizing trials (1.y-3.y) are not equal. The siliconizing trials at Wacker were carried out over a time span of four month, while the tests on TU Graz were carried out in three days. Therefore the aging of the colorant, might be an influence.

	mean relative difference (Trial x.y : Trial x.0)			mean absolute difference (Trial x.y - Trial x.0)		
	delta E (s.c.=1.3 g/m ²)	delta E (s.c.=1.0 g/m ²)	delta E (s.c.=0.7 g/m ²)	delta E (s.c.=1.3 g/m ²)	delta E (s.c.=1.0 g/m ²)	delta E (s.c.=0.7 g/m ²)
Test 1.1:Test 1.0	1,76	1,35	1,17	4,24	4,20	4,16
Test 2.1:Test 2.0	1,59	1,30	1,16	3,40	3,20	3,13
Test 3.1:Test 3.0	1,19	1,07	1,04	0,95	0,70	0,82
Test 3.2:Test 3.0	1,11	0,96	0,87	0,59	-0,40	-2,66

TABLE 5-5: MEAN RELATIVE AND ABSOLUTE DIFFERENCE OF DELTA E VALUES COMPARING DIFFERENT TRIALS WITH TRIAL X.0

A direct comparison of delta E measurements on the same release liner carried out at the beginning and the end of a period of three months was done. During the first test series five tests were performed for this release liner. The papers with the lowest and the highest delta E test result of these five tests are used in this comparison. In the second test series only one delta E test was performed on this release liner. In the first test series the colorant was freshly prepared, while in the second test series the colorant was already used for many delta E tests and had aged for three month. In Figure 5-5 the spectra of these two test series are compared. The spectrum of the delta E test

performed in the second test series shows a higher absorption of light, which is reasoned by an absorption of a higher quantity of colorant to the paper. The measured delta E value for these trials is compared with the coloured area determined from the scanned delta E test image (see chapter 3.4.1) in Table 5-6. Although the coloured area is nearly equal for the both tests carried out on this release liner, the delta E test result is significantly lower for the first test series. The equation determined for the correlation between coloured area and delta E value for the test series (see Figure 3-5) where the paper from the second test is included (see Figure 3-5) is used to determine the delta E value. In Table 5-6 the coloured areas of both tests of the release liner were used to determine the delta E value with the added equation. The high accordance of the measured delta E value from the second test with the determined delta E value using the equation is to expect, as this test was part of the test series used to calculate the equation. A comparison of the measured delta E result of the first test with the calculated delta E result, shows a high deviation of 25 %. This is a further proof for the aging and the effect of reuse of the colorant.

Oxidation reactions are certainly taking place, as it is known that the colorant has low light fastness. Although the colorant is stored in darkness, it is exposed to light during the stain tests. The impact on the delta E result cannot be evaluated with the analysis carried out, because it was not possible to relate the change in delta E value directly to oxidation or directly to an increasing salt content of the colorant with this experimental setup. Supposedly both phenomena together cause the effect of the delta E increase, with the use of the colorant over a longer period of time on various papers.

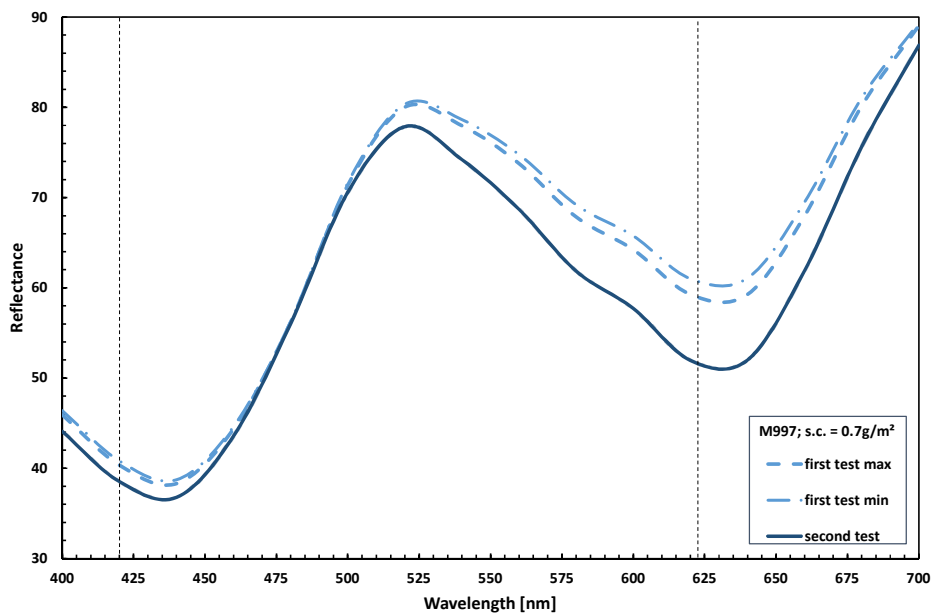


FIGURE 5-5: DIFFERENCES IN THE SPECTRA, WITHIN A MULTIPLE USE OF THE COLORANT SOLUTION

	Delta E test result	coloured area	delta E = 0.8598*x
first test max	15,8	24,0	20,6
second test	21,6	25,4	21,8

TABLE 5-6: COMPARISON OF THE COLOURED AREA, DELTA E RESULTS USING AN AREA EQUATION AND MEASURED DELTA E

Summarizing it can be said that:

- An increasing colour uptake of the paper is not only caused by aging (oxidation) of the colorant solution, but the delta E test results might be affected by an increasing salt content of the colorant, which is caused by the use of the colorant solution on too many papers.
- If the salt content of the colorant solution affects the delta E result, differences in paper conductivity might have an effect too.
- The comparison of the mean relative differences of the delta E values between two delta E test series of three different siliconizing trials, are showing different mean relative differences for each siliconizing trial. Therefore the delta E results of these different siliconizing trials are not comparable.
- The mean absolute difference of delta E values comparing two delta E test series is similar, independent of the silicone coat weight, given that the number of delta E tests done on the samples are equal for the compared test series.

pH value of the colorant

The pH value of the colorant solution might also affect the outcome like an increasing salt content. As the surface pH of the release base paper is normally below pH = 7, it is imaginable that the solution turns acidic when it is used for multiple testing. The effect would influence the result in the same way as the salt content.

But to be for sure that the pH value of the colorant is affecting the delta E test result, this influence has to be considered in a separate test series, excluding other influences, e.g. the salt content of the colorant or the multiple use of the colorant.

5.1.4. L*a*b* COLOUR SPACE AND L*a*b* MEASUREMENT:

Siliconizing

Siliconizing is changing the L*a*b* result compared to the release base paper. When pores are filled with silicone the refractive index and thus scattering changes which is causing the difference. Considering that only spots get stained, which are not covered with silicone, it is not correct to subtract the L*a*b* values of the stained paper from the L*a*b* values of the unstained paper. To evaluate the quantity of this influence the reflectance spectrum of a release base paper is compared to the release liners from this base paper (see Figure 5-6).

Differences in the spectra of the release liners and the release base paper are visible. As the spots where no silicone is present are affected most by the malachite solution an error is generated in theory. The differences between the three coat weights applied on the release liner are hardly noticeable and would result for the spectra plotted in Figure 5-6 in a delta E difference of 0.2 comparing the 1.3 g/m² liner with the 0.7 g/m² release liner. The difference between the siliconized liners is therefore negligible.

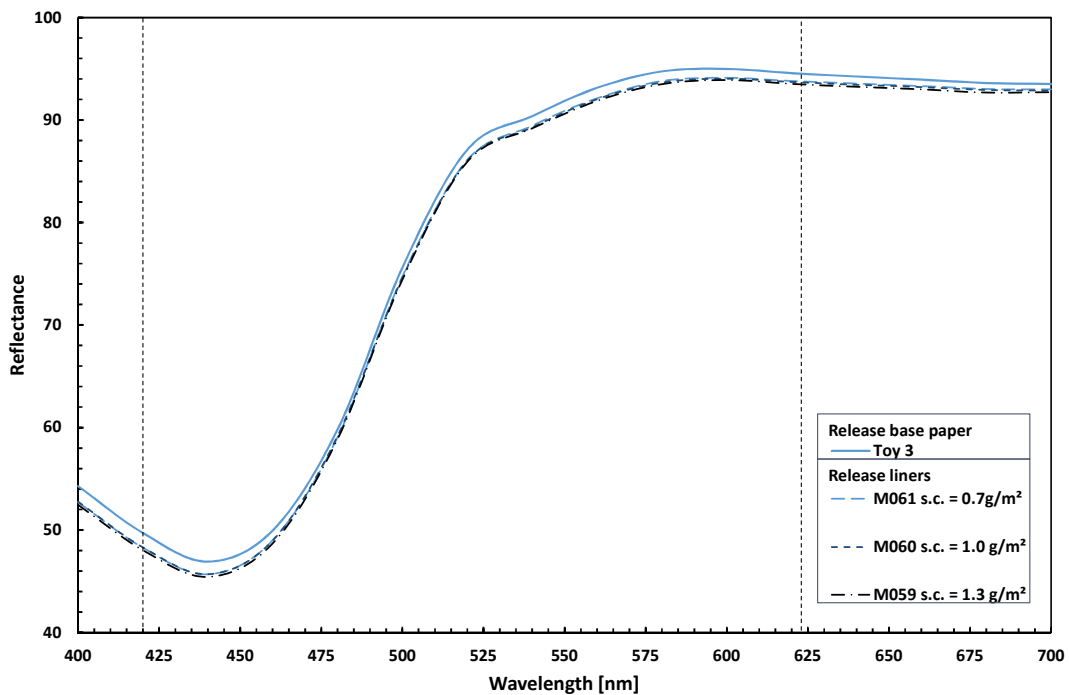


FIGURE 5-6: DIFFERENCES IN THE SPECTRA OF A RELEASE BASE PAPER AND A RELEASE LINER

Device settings

L*a*b* measurements are usually carried out with the light source D65 and an angle of 10°. Light sources D65 and C and 2° and 10° angle are compared by the calculation of the delta E values from the same stained liner sample (s.c. = 0.7 g/m²)

and s.c. = 1.3 g/m²) for these different settings. Figure 5-7 illustrates the deviation produced between the delta E results using the setting D65/2° compared to the delta E results using other settings. The differences in delta E resulting from different device settings are quite low with a maximum error of 3 %.

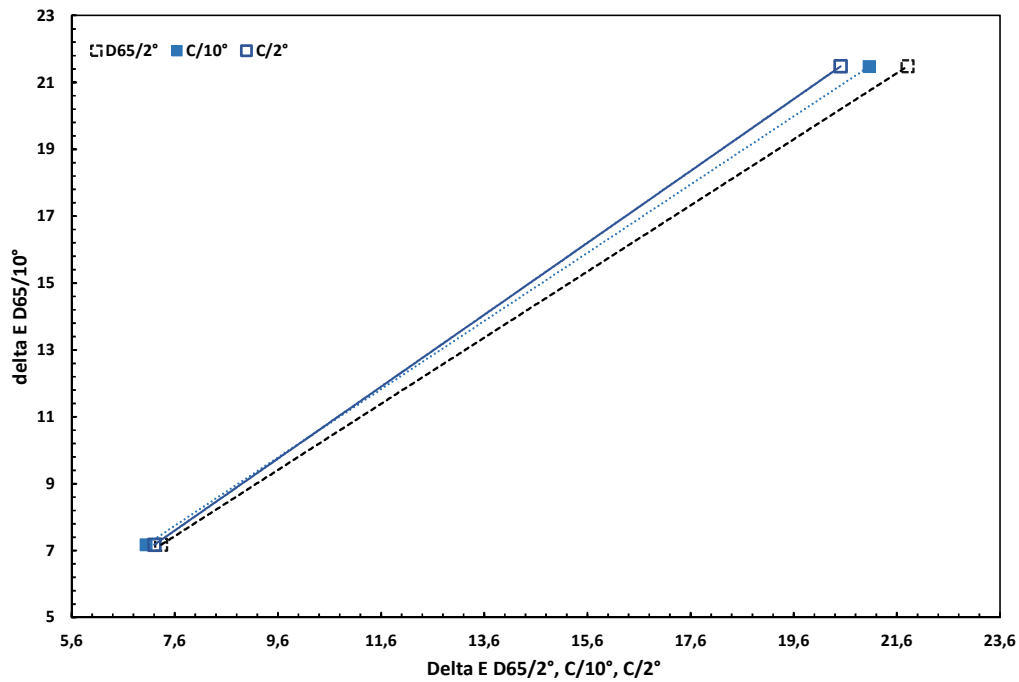


FIGURE 5-7: DIFFERENT DEVICE SETTINGS

5.1.5. EXECUTION OF THE DELTA E TEST.

Penetration time:

The influence of penetration time on the delta E test result is investigated in this section, in order to discuss the possible error produced when the penetration time is 5 seconds longer or shorter. This seems to be a possible variation in penetration time, considering the procedure how the test is carried out. In Figure 5-8 the curve development of the delta E test result with increasing penetration time for the same release base paper siliconized with the silicone coat weights of 0.7 g/m² silicone and 1.3 g/m² silicone is depicted. The mean values for the penetration times of 30 s, 60 s and 120 s are calculated from three delta E tests.

At a penetration time of 30 seconds where the delta E test is usually carried out, the curves have a steeper slope, while they are flattening out reaching a time of 120 seconds. This curve development is caused by the generation of additional stained areas, which can have two reasons. The colorant solution needs more time to penetrate

into smaller defects and so with increasing penetration time additional stained spots are created. The other issue is spreading of the colorant on the release base paper - silicone interface leading to an area increase of already stained spots. Both phenomena can be present, although the spreading of the colorant on already stained spots seems to take place predominately in the first 30 seconds, which is described in the following section where two different colorants are compared.

Assuming a difference in penetration time of five seconds the highest possible error occurs at the test time of 30 seconds, where the slope is steepest. For the analysed papers, which are coming from the same base paper a relative error of eight percent was determined for both silicone coat weights (see Table 5-7).

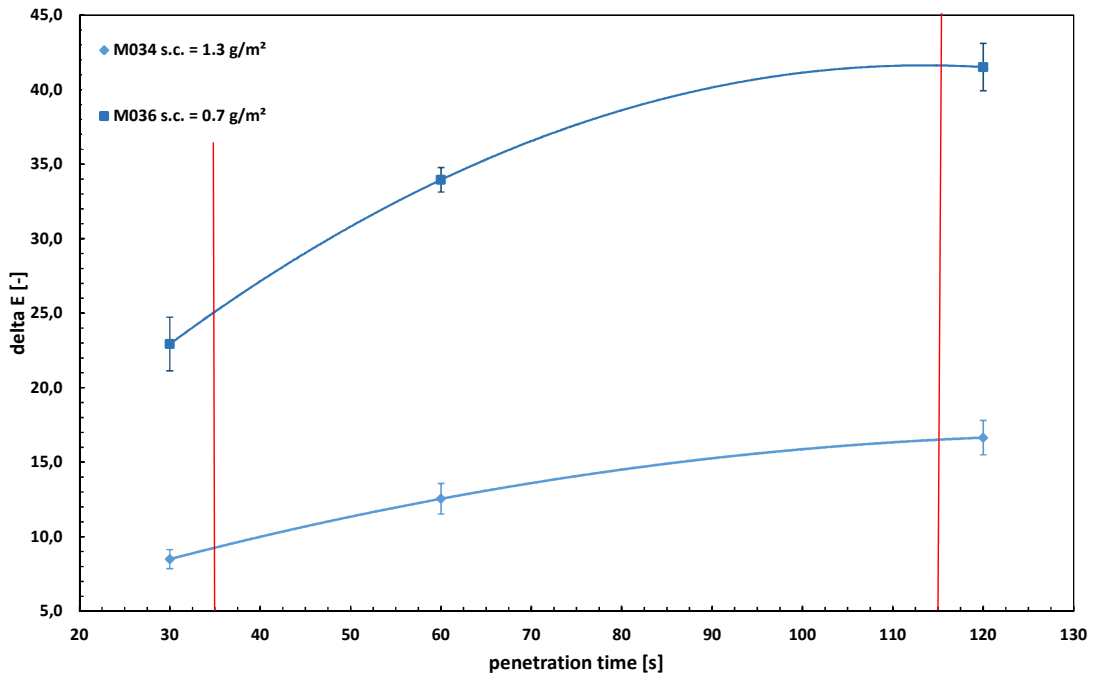


FIGURE 5-8: DEVELOPMENT OF THE DELTA E TEST RESULT WITH THE PENETRATION TIME

	M034 s.c. = 1.3 g/m ²	M036 s.c. = 0.7 g/m ²
30 sec	8,5	22,9
35 sec	9,2	24,8
Abs error	0,7	1,8
Rel error	7,9	8,0

TABLE 5-7: EXPECTED ERROR FOR A PENETRATON TIME DIFFERENCE OF 5 SECONDS

Summarizing it can be said that:

- The test carried out with a penetration time of thirty seconds provides the most instable conditions, because the slope of the curve is steepest at this penetration time.
- Instability occurs because of the generation of additional stained areas as already discussed in chapter 5.1.2 investigating spreading and absorption properties.
- Based on the finding (see chapter 5.1.2), that at a penetration time of 30 seconds small defects are not coloured, this penetration time is not sufficient.

Different colorants:

For malachite green it was already shown that the spreading and absorption properties of the colorant solution are dependent on the release base paper properties (see chapter 5.1.2). In this section the differences in spreading and absorption properties of malachite green and “Shirlastain A” are compared, including the development of stained areas with increasing penetration time. Therefore the delta E test was carried out on the same release liner with a silicone coat weight of 1.3 g/m² for the penetration times of 30 s, 60 s and 120 s for both colorants (see Figure 5-9).

As “Shirlastain A” is not only colouring the defect spots but also the silicone layer, using a colorimetric measurement for the determination of the delta E value would not be reliable for a comparison of its colouring properties with malachite green. Therefore instead of the delta E value, the determination of the coloured area is used for the comparison of these colorants. In the determination of the percentage of the coloured area colour intensity is neglected, which makes it possible to compare only the spreading properties of the colorant. On the left y-axis of Figure 5-9 the coloured area for malachite green is plotted, whereas the right y-axis displays the coloured area for “Shirlastain A”. Figure 5-10 shows the images of the scans of the malachite green and “Shirlastain A” delta E test papers for the penetration times of 30 s and 120 s where also the differences in colour intensity are visible. Only the coloured areas are depicted, to enhance the contrast. It is not possible to carry out the delta E test for both colorants at the exact same paper position. Therefore the location of the stained spots cannot be compared directly. The percentage of coloured areas for the entire scanned delta E test images (7.5 cm x7.5 cm) is shown in Table 5-8 to compare the influence of different penetration times. Relative and absolute differences between the coloured areas of malachite green and “Shirlastain A” delta E test papers are also determined.

In Figure 5-9 two y-axis were used to visualize, that the curve development with the penetration time is similar for both colorants, but totally different in the values.

The coloured area for a penetration time of 30 seconds is 17.6 % using malachite green, whereas it is only 2.5 % using “Shirlastain A”. The reason is the high spreading ability of malachite green, which is responsible for the growth of stained spots at the silicone base paper interface. “Shirlastain A” does not seem to have significant spreading properties. The coloured area for a penetration time of 120 s is at a similar level as the defect area determined with the method of the silicone negatives of release liners with a silicone coat weight of 1.3 g/m² (see Table 5-2). To verify, that “Shirlastain A” is detecting the real size of defect spots, silicone negatives for the papers treated with “Shirlastain A” would have to be taken and compared with the delta E test result.

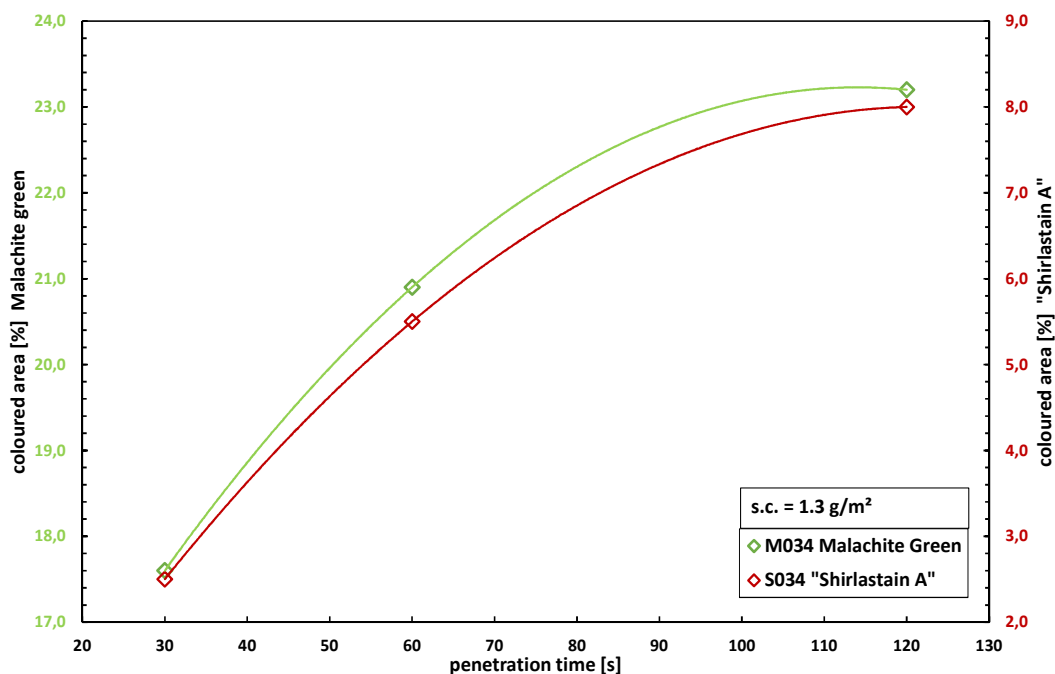


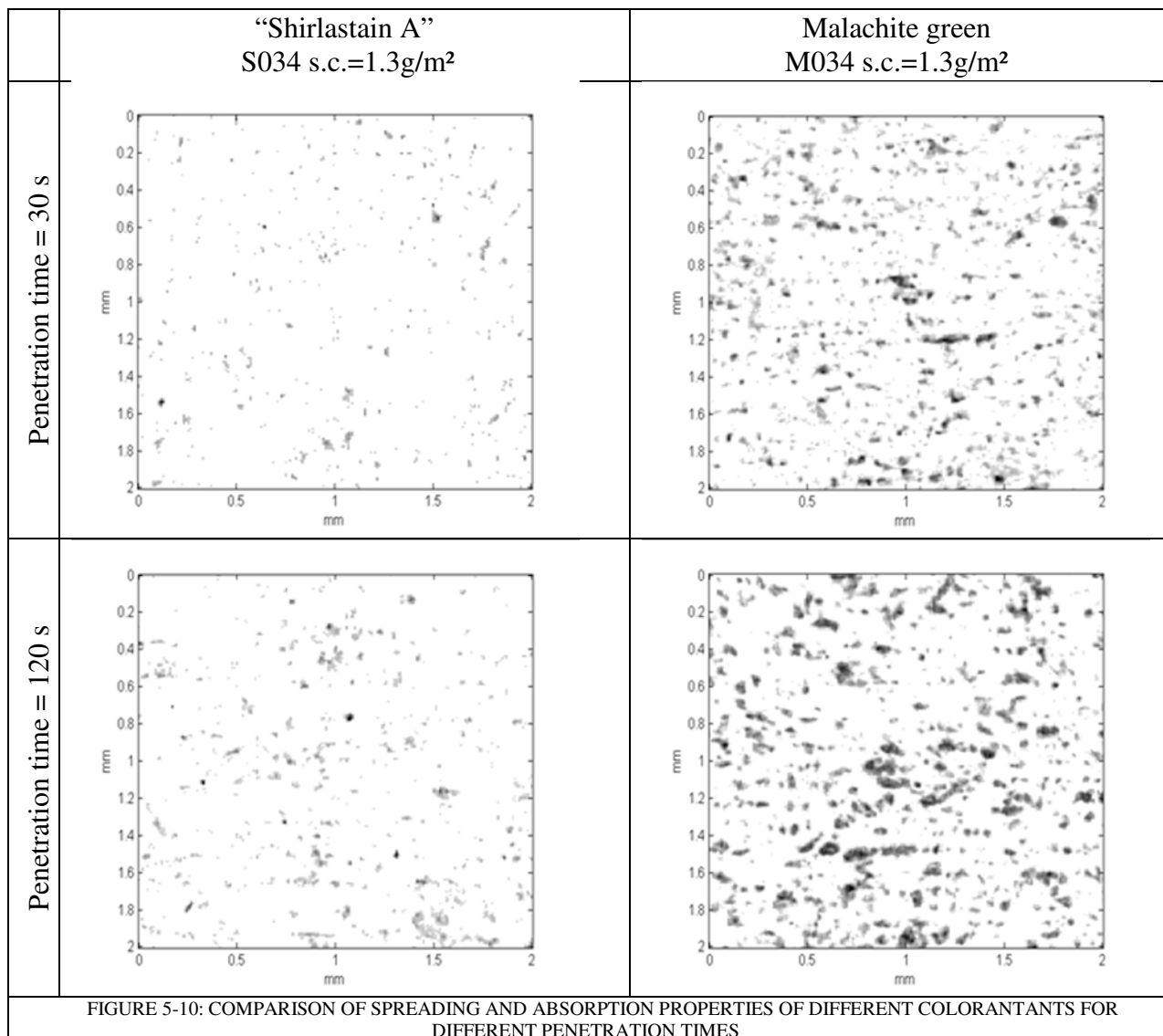
FIGURE 5-9: DEVELOPMENT OF COLOURED AREA FOR DIFFERENT COLORANTS WITH INCREASING PENETRATION TIME

"Shirlastain A"	coloured area [%]	Malachite green	coloured area [%]	rel difference (M/S)	abs difference (M-S)
S034_30	2,5	M034_30	17,6	6,9	15,0
S034_60	5,5	M034_60	20,9	3,8	15,4
S034_120	8,0	M034_120	23,2	2,9	15,2

TABLE 5-8: AREA DEVELOPMENT WITH PENETRATION TIME, USING DIFFERENT COLORANTSANTS

The absolute difference between the coloured area using malachite green and the coloured area using “Shirlastain A” is nearly constant at an average of 15.2 % (see Table 5-8). The slight increase of the absolute difference with higher penetration times, might be caused by the time dependence of the coloration of small spots. Malachite green seems to affect the spots, which need a higher penetration time to be stained, more, because of its spreading ability. Most of the influence of spreading has already

happened at 30 seconds, which can be argued with the already high coloured area of malachite green compared to “Shirlastain A”. Malachite green is diluted in water, which facilitates spreading on the hydrophilic fibres and PVA. “Shirlastain A” is a combination of chlorazol blue, crocein scarlet and picric acid diluted in water ([24]). Picric acid seems to reduce the spreading properties. The images depicted in Figure 5-10 visualize the spreading ability of malachite green compared to “Shiralstain A” for the same release liner samples compared in Figure 5-9. A penetration time of 30 seconds shows less coloured area in comparison to the penetration time of 120 seconds for both colorants. Spots, which are darker indicates a higher amount in colour uptake. Less fluctuations in colour intensity are visible for “Shirlastain A”, which is reasoned by a more constant paper - colorant interaction.



In (Table 5-9) the release liner with a silicone coat weight of 0.7 g/m² on the same base paper is included to discuss the influence of the colorants for different silicone coat weights. A penetration time of 120 seconds is chosen for this comparison as at this time all defects seems to be stained, indicated by the almost flat slope at 120 s in Figure 5-9. Due to the higher silicone coat weight the size of the defects will be smaller at 1.3 g/m² coat weight. Assuming that spreading itself is not affected by the size of the defects in the silicone layer, the area increase of a small defect caused by spreading will be relatively (compared to the defect size) larger, than the area increase of a large defect. This trend also shows in the relative difference of malachite green and “Shirlastain A”, which is higher at a silicone coat weight of 1.3 g/m², where the defects are smaller.

	s.c. = 1.3 g/m ²		s.c. = 0.7 g/m ²	
	S034_120	M034_120	S036_120	M036_120
coloured area [%]	8,0	23,2	20,8	39,7
rel difference (M/S)	2,91		1,91	
abs difference (M-S)	15,2		18,9	

TABLE 5-9: COMPARISON OF THE STAINED AREA FOR DIFFERENT SILICONE COAT WEIGHTS

Summarizing it can be said that:

- “Shirlastain A” has less spreading ability on the paper as the percentage of coloured area using “Shirlastain A” is similar to the defect area determined from the silicone negatives.
- Spreading of malachite green is almost completed at a penetration time of 30 seconds as the absolute difference between malachite green and “Shirlastain A” is nearly constant for the 3 penetration times investigated.
- Both colorants seems to need at least a penetration time of 120 seconds, to be able to stain small defects in the silicone layer.
- It is not reliable to compare a paper using malachite green with a penetration time of 30 seconds, with a paper stained with “Shirlastain A” with a penetration time of 120 seconds.
- For the reason that smaller spots needs more time to get stained, it is not reliable to compare a paper with small defects to a paper with large defects at a penetration time of 30 seconds, independent of the colorant used.
- “Shirlastain A” is attaching to the base paper more uniformly, as lower colour intensity fluctuations are noticed, than for malachite green (see Figure 5-10).
- The increase in coloured area caused by spreading has a higher effect on smaller defects.

Standard error and number of tested samples:

In this section the influence of the number of delta E test samples on the accuracy of the delta E value is discussed. Fluctuations in silicone coverage between different siliconizing trials are evaluated too.

Figure 5-11 shows boxplots, which represent the distribution of delta E values for five measurements per paper sample. Release liners with silicone coat weights of 0.7 g/m² and 1.3g/m² are compared. The first letter (F or M) stands for different siliconizing trials at different dates in which the same base papers are siliconized. The second number (1 or 2) indicates different base papers and (_07 or _13) refers the silicone coat weight applied. All delta E tests were performed on the same day in the laboratory of TU Graz.

Base papers from two different trials were chosen, to ensure that the distribution is not only caused by measurement errors related to the execution of the delta E test, but by fluctuations in the siliconizing process too. It is obvious that the width of the range of delta E values of the trial F is wider than for trial M, which indicates a rather non - uniform silicone coverage distribution. When only one sample of release liner F2_07 is measured, the resulting delta E value could be between 14.6 and 19.4 with a maximum relative error of 28.1 %. The more measurements are done the better the mean performance of the paper is described. The red line crossing the box marks the mean delta E value, determined for the five samples. Assuming a normal distribution the mean should divide the box in two equally sized parts, which is not the case for these plots. In theory a minimum of ten measurements are necessary to approximate a normal distribution. Therefore five measurements are not sufficient for the determination of the real mean. If there is a clear trend in silicone coverage caused e.g. by misalignments of the release liner, normal distribution cannot be assumed. The five delta E test samples were cut out in one meter distance from each other and numbered. A clear trend of delta E values of the five samples was not present. Comparing paper F1 and F2 with paper M1 and M2, where the only difference is the siliconizing trial date, the silicone layer has a more homogenous distribution for papers M1 and M2. Therefore the error in the delta E test results is reduced. The box plots of the same release liners of the different siliconizing trials (F1 and M1, F2 and M2), which should principally show the same delta E results, as the same release base paper was siliconized, are not even overlapping. This might be caused by a mistake during the silicone coating preparation or at the pilot coater. Another possible source might be an effect of the humidity of the release base paper on the siliconizing process. Comparing the width of the distributions of the two silicone coat weights of the same siliconizing trial, the delta E values at a silicone coat weight of 1.3 g/m² show a narrower distribution. Considering the low delta E values at 1.3 g/m² silicone coat weight the relative error is higher than for the 0.7 g/m² coat weight.

The comparison of the standard error of the delta E tests for papers from the two siliconizing trials including some additional papers is shown in Figure A-5. Papers starting with the numbers 45xxx were siliconized during trial F, whereas papers with the numbers 46xxx came from trial M. The mean standard error, including the papers of trial F (45534-45539) is at 11.4. The mean standard error determined for the identical papers in trial M (46019-46024) is 4.1.

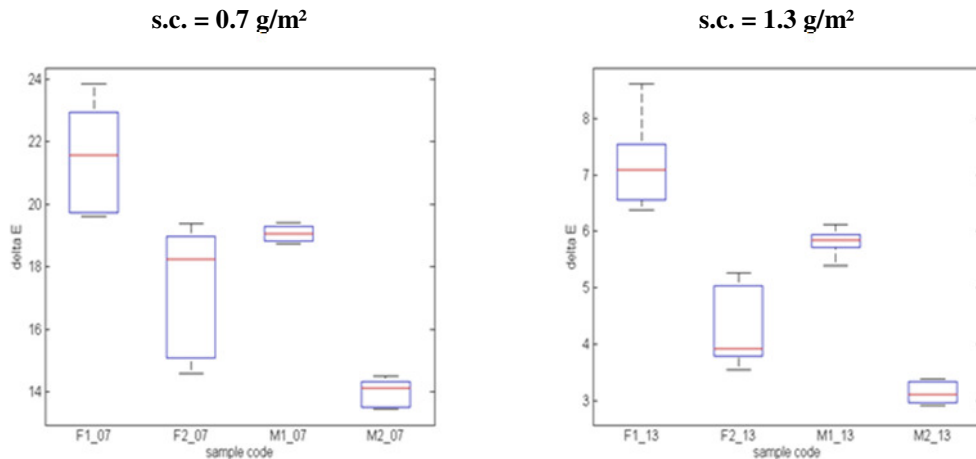


FIGURE 5-11: VARIABILITY OF THE DELTA E VALUES: COMPARISON OF TWO SILICONIZING TRIALS

Summarizing it can be said that:

- The width of the distribution is dependent of the applied silicone coat weight.
- The delta E values measured in trial F were significantly higher than in trial M. The distributions for the same papers siliconized in the different siliconizing trials are not even overlapping.
- Partly the resulting error is produced by the execution of the test, which in this case seems to be the minor source.
- In this comparison of trial F and trial M, the larger part of the error is affected by a non - uniform silicone coverage.
- In this evaluation the non - uniformity is caused by the siliconizing process, as the same base papers are compared.
- Multiple measurement allow to obtain information regarding large scale variations in the siliconizing process, which is a quality aspect too.

Climatised conditions:

It is known that absorption properties and especially water absorption is influenced by the humidity of the paper and the temperature. As malachite green is diluted in water, an effect on colour absorption may occur, when the humidity is changing.

5.2. DISCUSSION OF VARIABILITY OF MEASUREMENT DATA FOR THE USE IN MULTIPLE LINEAR REGRESSION ANALYSIS

The aim of this chapter is to analyse the quality of the measurement data for release base papers, which are going to be used as predictor variables in multiple linear regression analysis (MLR) in chapter 5.3. The variability of measurement data in combination with the measurement range of the data from the measurement series used in the regression analysis will be discussed. The mean values of the measurement series used in MLR are provided by Dunafin and Tervakoski. The data of the single measurements were not available. Therefore measurements carried out in the laboratory of TU Graz were used to evaluate the variability of measurement data. These tests were at first carried out for another purpose that is why the number of tested paper samples is not constant for the different quality parameters. Therefore this discussion is to be seen as a rough estimation, which should help to get a feeling regarding the prediction quality of release base paper quality parameters. Table 5-10 shows the number of measurements of the quality parameters, which were the basis for the determination of the variability of measurement data. All tested papers are from the siliconizing trial reels, which have a width of 25 cm.

	papers	tests/paper
Basis Weight	6	10
Thickness	8	20
Bekk W.S.	8	10
Cobb60 PVA	5	5
surface pH	30	3
dE_1,3	10	5
A_04	10	10

TABLE 5-10: BASIS FOR THE EVALUATION OF VARIABILITY OF MEASUREMENT DATA (SMALL SCALE)

Variability of measurement data

Variability of measurement data have three different sources:

- Accuracy of the testing method itself
- Fluctuations in the paper quality
 - Small scale (mm to cm scale)
 - Large scale (cm to m scale)
- Number of tested samples

Accuracy of the testing method

Especially for tests, where time is included as a factor and which are carried out by a human, high variability can occur. Another aspect is the execution of the tests in

different laboratories, using another equipment. As an example Cobb₆₀ measurements on the same release base paper samples were carried out in different laboratories (Lab A, Lab B and Lab TU Graz). Release base papers which were measured in Lab A or Lab B were compared with the measurements at TU Graz (5 tests/paper). Taking the measurements from the laboratory at TU Graz as basis the results of Lab A especially samples A1 and A2 are higher (see Figure 5-12), while the comparison of Lab B and TU Graz shows quite similar results. This might be explained by the use of a mini Cobb in Lab A. Another example for possible measurement faults is the Bekk value. All air leakage methods are dependent on the surrounding air pressure, which is determined by the location and the weather. To avoid errors the Bekk result have to be corrected to a defined pressure. As an example the Bekk value is about 5 % lower when the pressure is reduced by 50 mbar compared to the atmospheric pressure.

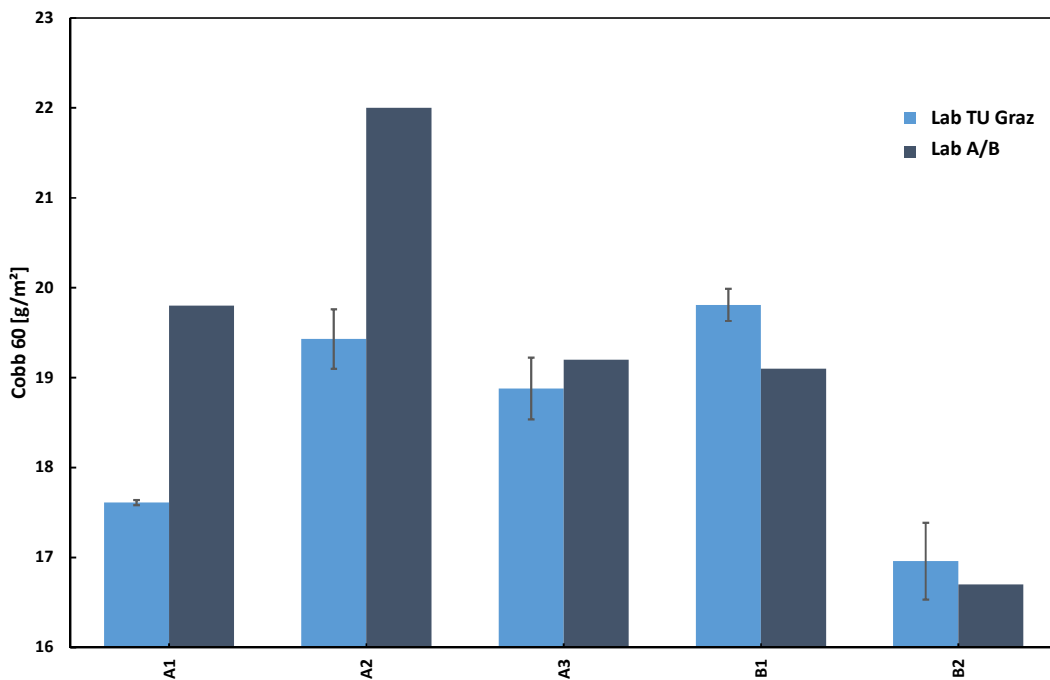


FIGURE 5-12: COMPARISON OF COBB VALUES FROM DIFFERENT LABORATORIES

Variations in the paper quality:

Large scale variations in the paper quality are caused by process stability issues, and can be separated into MD, CD and random variations. Small scale variations are defined as variations that occur within the size of the sample measured in the laboratory.

Variability of measurement data and significance – small scale:

The small scale variations are determined for the quality parameters listed in Table 5-11 and compared with the measurement range of the predictor variables used later in MLR. Following the measurement range of the release base papers with a basis weight of 58 g/m² tested in Dunafin is discussed and displayed in Table 5-11 and Figure 5-13. Small scale variability was estimated from the measurements of the quality parameters performed in the laboratory of TU Graz. As measure for the variability of measurement data the mean sigma value is determined as the arithmetic mean of the single sigma values of the different tested papers (see Table 5-10). The measurement range (MR) is determined by the difference of the maximum and minimum test result of the Dunafin test series, including 31 papers. To be able to compare the MR with the sigma value the MR is divided by 2 (½ MR). The relative ½ MR or relative sigma value (sigma_rel) are determined by dividing the ½ MR or sigma value with the mean test result of the Dunafin test series or the mean of the measured values at TU Graz. This was necessary because not exactly the same papers are used for the determination of MR and sigma and the absolute values are dependent from the mean value. A ratio indicating the reliability of a quality parameter with regards to its use in multiple linear regression analysis (MLR) is determined by the division of the relative ½ MR with the relative sigma value. This ratio describes how often the sigma value is contained within the ½ MR which is visualized in Figure 5-13 and listed in Table 5-11. A detailed list of measurement ranges is to find in the appendix for measurement data from Dunafin and also from Tervakoski (see Table A-2, Table A-3). A low ratio is an indication for a low significance of the measured property with regards to MLR. Variability of the measurement expressed by the sigma is very close to the range of measurement data. The release base paper quality parameters, thickness and contact angle (A_04), have a low significance as the MR is similar to the variability of measurement data expressed by the sigma value. The delta E value at a silicone coat weight of 1.3 g/m², which is used as a response variable in MLR (see chapter 5.3.1) was included to compare the range of delta E values with the variability caused by the execution of the delta E test. The measurement range of the delta E value is sufficient for a differentiation of the delta E results.

	Dunafin data			TU Graz data			½ (MR) _rel/ Sigma_rel
	Measurement range (MR)			Variability of measurement data			
	Mean	½ (MR)_abs	½ (MR)_rel	Mean	Sigma_abs	Sigma_rel	
'Basis Weight'	58,7	3,3	0,06	59,8	0,44	0,007	7,4
'Thickness'	51,7	1,8	0,03	51,7	1,19	0,023	1,5
'Bekk W.S.'	1622	779	0,48	1646	101	0,060	7,7
'Cobb60 PVA'	19,1	3,2	0,17	18,7	0,27	0,015	11,9
'surface pH'	5,4	0,5	0,09	5,4	0,04	0,007	13,3
'dE_1,3'	7,7	4,0	0,51	5,7	0,46	0,082	8,6
'A_04'	51,4	2,5	0,05	51,7	0,82	0,016	3,1

TABLE 5-11: MEASUREMENT RANGE AND VARIABILITY OF MEASUREMENT DATA (SMALL SCALE)

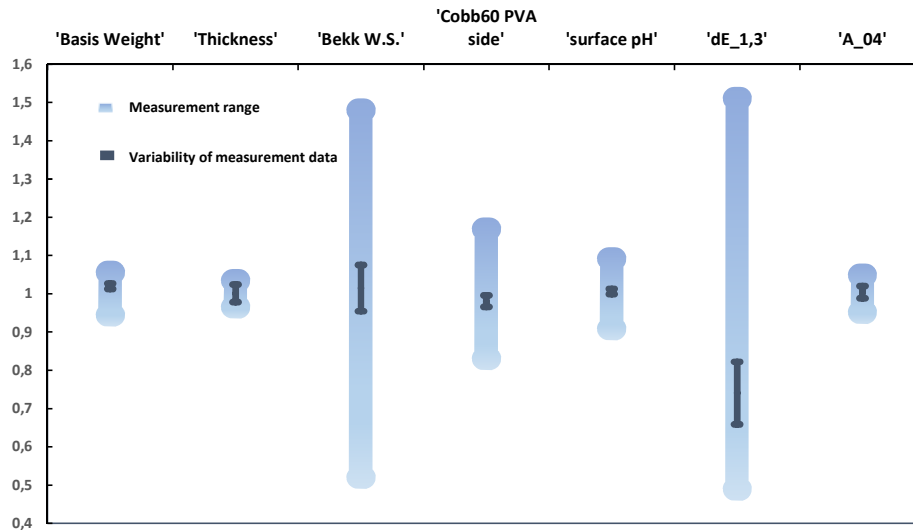


FIGURE 5-13: RELATIVE MEASUREMENT RANGE AND VARIABILITY OF MEASUREMENT DATA (SMALL SCALE)

Variability of measurement data and significance –large scale:

To get a feeling for the large scale variation of release base paper, the quality parameters from the siliconizing trial samples with a paper width of 25 cm are compared to the quality parameters, measured across the width of the paper machine of 430 cm for the same production. All data were measured in Dunafin. Only the mean values of the data over the whole paper width were available for 12 different release base papers. As a measure for variability the coefficient of determination (r^2) is determined between the mean value over the paper width and the mean value determined on the siliconizing trial reels (see Table 5-12). The mean value across the whole paper width is plotted on the x – axis against the result from the siliconizing trial reels on the y – axis in Figure A-6. The coefficients of determination are quite low which can be explained for some quality parameters by a few outliers. For each quality parameters the outliers are caused from different papers. The correlation is depicted in the regression plot in Figure A-6. The reason for the outliers, causing this poor correlation could not be identified. Neglecting them basis weight, Cobb 60 PVA side, Cobb Unger and Bekk provide a reliable correlation. IGT and delta E Shirlastain do not seem to be significant within the given measurement range. Despite a good correlation the porosity has to be excluded as a predictor variable in MLR, as the upper measurement limit is already reached for most of the measured samples.

Parameter	Correlation coefficient R ²
Basis Weight	0,39
Thickness	0,00
Density	0,12
Porosity	0,68
Bekk W.S.	0,01
Unger	0,47
Cobb60 PVA side	0,35
Cobb60 starch side	0,63
IGT	0,00
Transparency	0,48
delta E Shirlastain	0,06

TABLE 5-12: VARIABILITY OF MEASUREMENT DATA (LARGE SCALE VARIATIONS)

Additional measurements:

The additional measurements carried out at the laboratory of TU Graz with the aim to describe the release base paper quality concerning siliconability are discussed in this section separately in more detail.

Surface pH:

From a statistical point of view surface pH measurement is a reliable predictor. The question is whether the actual surface pH is measured or the pH of the whole paper, considering a water exposure time of the paper of 10 minutes. The pH of the paper can be different from the surface pH as PVA is applied. Nevertheless Figure 5-1 (see chapter 5.1.2) has shown a high correlation between surface pH and delta E value.

Contact Angle

The statistical evaluation has shown, that the contact angle and all related parameters are not reliable within this small measurement range of the tested samples. The number of data points per second would have to be higher in order to determine the exact time when the silicone oil is transferred to the paper more accurately.

As the same silicone oil as in the siliconizing trials is used for the determination of the contact angle and the contact angle difference, these parameters should be able to quantify spreading and absorption properties of the silicone oil on the paper substrate using a more precise device.

PVA coverage

A statistical evaluation of the method to determine PVA coverage was not possible within the time range of this thesis. As the characteristics of PVA are directly related to siliconability, it is useful to determine PVA coverage. Nevertheless the testing method has to be refined and evaluated as already discussed in chapter 4.1.

Summary:

Small scale variations only:

- Given the range of measured values, the thickness and the contact angle (A_04) are poor predictors for the use in multiple linear regression analysis (MLR). The variability of measurement data is nearly as high as the measurement range.
- Although the measurement range of the surface pH of the measured papers is rather small, the accuracy of the measurement method allows the use in MLR. As the contact time during the pH measurement is quite high, it has to be considered, whether only the surface pH is determined or the pH of the whole paper.
- The significance of the delta E value (s.c. = 1.3 g/m²) is quite good, when only the variability of the delta E test procedure is taken into account. Deviations caused by other reasons than the accuracy of the test methods (e.g. base paper – colorant interactions) are not considered here.

Large scale variations included:

- Considering also large scale variations basis weight, Cobb 60, Cobb Unger and Bekk are reliable predictors to use in MLR.
- Delta E Shirlastain has a low significance based on this rough evaluation.

5.3. PREDICTION OF THE DELTA E VALUE AND SILICONE COVERAGE USING MULTIPLE LINEAR REGRESSION ANALYSIS:

Multiple linear regression (MLR) is used to detect the influencing quality variables of release base papers concerning the delta E value and silicone coverage. The additional parameter parameter S_{cov} developed from the scanned delta E test images is also analysed in a separate MLR. This parameter should be an indicator for the ability of closing defects (actually of the reduction of the stained spot size) with increasing silicone coat weight (see chapter 3.4.2). The Durlac value which is an important release liner quality parameter for the description of silicone anchorage to the base paper will be discussed briefly.

As reliable predictor variables of release base papers the basis weight, Bekk, Cobb Unger, Cobb 60, IGT, surface pH and PVA coverage are chosen, because of the results of the statistical evaluation regarding the significance of these parameters (see chapter 5.2). The data measured in Tervakoski and Dunafin laboratory are considered separately. The regression analysis was mainly based on the data from the Dunafin

laboratory, with 31 different release base papers from different production runs. The other 21 papers from a PVA coating trial in Tervakoski are neglected in the MLR with the delta E value as a response variable, as the same release base paper was used in all trials, where only the PVA recipe was changed. So only rather low variations were found in the lab values and putting these rather similar quality data in the model would distort the result, as each measurement set has the same weight in regression analysis. The analysis routine will be described in detail for the prediction of the delta E value. For the evaluation of silicone coverage the analysis routine is the same.

5.3.1. PREDICTION OF DELTA E:

The first step is to include all possible predictor variables in the MLR model, as shown in Figure 5-14. The columns represent the shares on the coefficient of determination (r^2) of each predictor variable. The columns are parted in dark and light grey areas. The entire column represents the coefficient of determination, when the predictor variable is used alone in a single linear regression (SLR) to describe the response variable delta E. The dark grey area of the column (r^2 exclusive) is the exclusive share of the coefficient of determination (r^2) for the MLR model, displayed in the figure. This represents the information surplus of this predictor for the model, when all other predictors are present. Therefore the light grey area (r^2 redundant) is the redundant share which can be explained by one or more of the other prediction variables used in the MLR model and is thus an indication for the interrelation between parameters. In Figure 5-14 three MLR models for the prediction of the delta E value with the three different silicone coat weights are shown. The horizontally crossing red line in the plots shows the mean coefficient of determination (r^2) for all three models. On the left y – axes the coefficient of determination (r^2) is plotted. On the right y – axes the coefficients of the predictors ($\beta_{i=1..n}$) are plotted, which are displayed as black error bars. The error bars show the range of the predictor coefficient (β_i) in which each single value of β_i of the single datasets is localized. A narrow range means low fluctuations of the β_i of the single datasets. The level also tells whether the predictor coefficient is influencing the response variable positively or negatively and how high this influence is. If the error bars are crossing the zero line, it cannot be said for sure whether there is a positive or a negative influence by this predictor. E.g. for the model displayed in Figure 5-14 the predictor coefficient β_i for the Bekk value indicates that smoothness is not reliable as a predictor and has to be rejected. The influence of a predictor parameter, the exclusive share in the model can change, when some of the predictors are removed. This can have an influence on the location of β_i . A β_i where the prefix is not entirely positive or negative and therefore the predictor is not reliable in the model, can shift and become significant for a model reduced by

some predictors. Therefore the significance of β_i have to be crosschecked using stepwise regression. The stepwise regression analysis starts with the determination of the r^2 and statistical significance including only one prediction parameter and the response variable, like in single linear regression. This determination is carried out for all predictor parameters regarding the response variable (delta E) separately. The parameter with the highest significance is included in the model. In the next step the (r^2) and the statistical significance is determined for the remaining parameters. The parameter which bring the highest information surplus is added again to the model. If the newly added parameter is interacting with a parameter already present in the model, and its significance is reduced, this parameter is rejected from the model. This loop is carried out as long as a significance limit is reached. The final result is a MLR model, which includes all the significant predictors. In the case of the delta E value the significant predictors were not the same for the different silicone coat weights (s.c. = 0.7 g/m², 1.0 g/m², 1.3 g/m²). The surface pH was the most significant predictor parameter in stepwise regression for all of the coat weights. For the coat weights of 0.7 g/m² and 1.0 g/m² the Cobb Unger was suggested and the Cobb value for a coat weight of 1.3 g/m². As the overall r^2 for the whole model was the highest at a coat weight of 1.3 g/m², finally the Cobb value and the surface pH were chosen as predictors for the MLR model (see Figure 5-15).

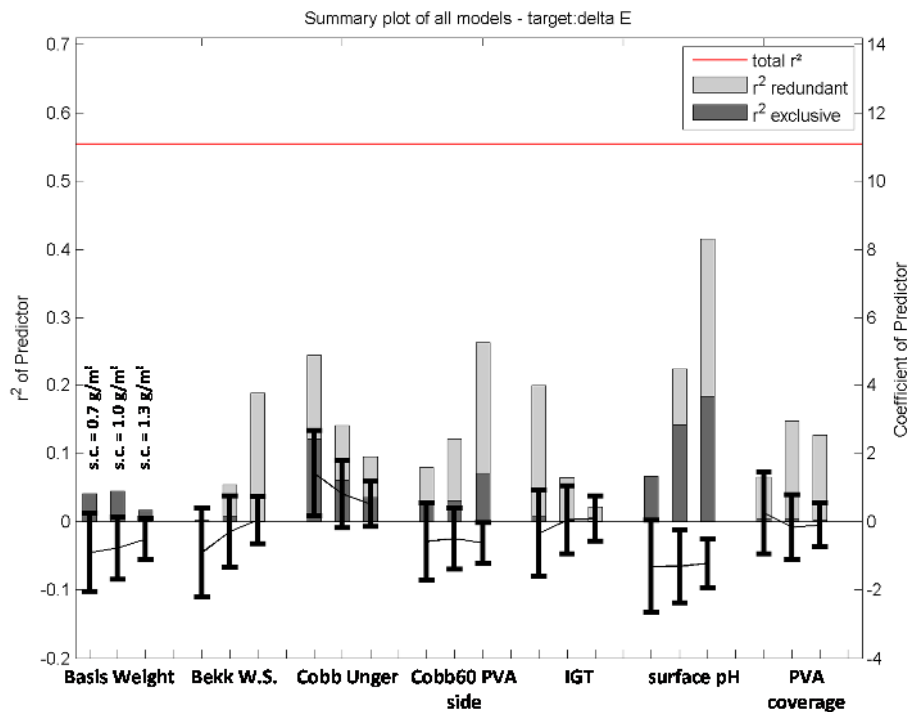


FIGURE 5-14: PREDICTION OF DELTA E WITH MLR (ALL PARAMETERS)

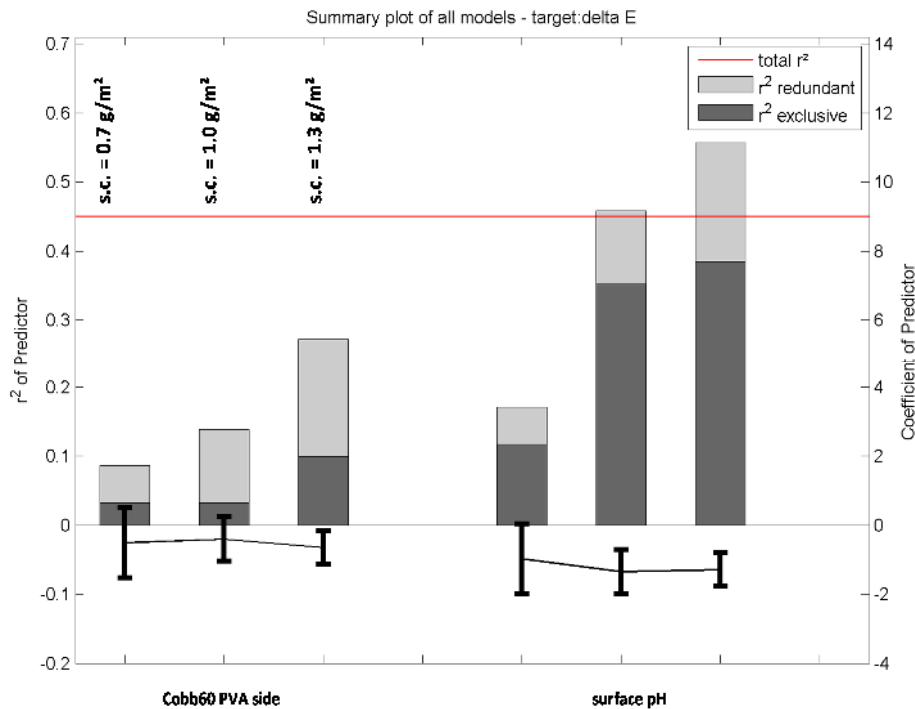


FIGURE 5-15: PREDICTION OF DELTA E WITH MLR (FINAL MODEL)

Both predictors, the Cobb value and the surface pH are significant for the delta E value at a silicone coat weight of 1.3 g/m², as the error columns are not crossing the zero line. The predictors have both a negative prefix, which results in a decrease of the delta E value with the increase of the predictor values or vice versa. This seems not to be the right conclusion considering a higher delta E value at a lower Cobb value. As depicted in Figure 5-15 the Cobb value and the surface pH shows an interaction, visible in the light grey parts of the columns. This has been considered by adding the interaction between surface pH and Cobb value to the model. The prefix of the Cobb value changes to positive for all three coat weights (see Figure A-7). The overall r² remains nearly the same. As the aim of the prediction of the delta E value was to be able to attribute the influence on the delta E result to a single parameter, the model depicted in Figure 5-15, which does not include the interaction term between the Cobb value and surface pH is chosen for further discussions. The r² between the measured and the determined delta E value using MLR is shown in Figure 5-16 for the three coat weights separately and for all coat weights using the three different models for the different silicone coat weights. The prediction coefficients β_i for the delta E value with the different silicone coat weights are also shown in the correlation plot.

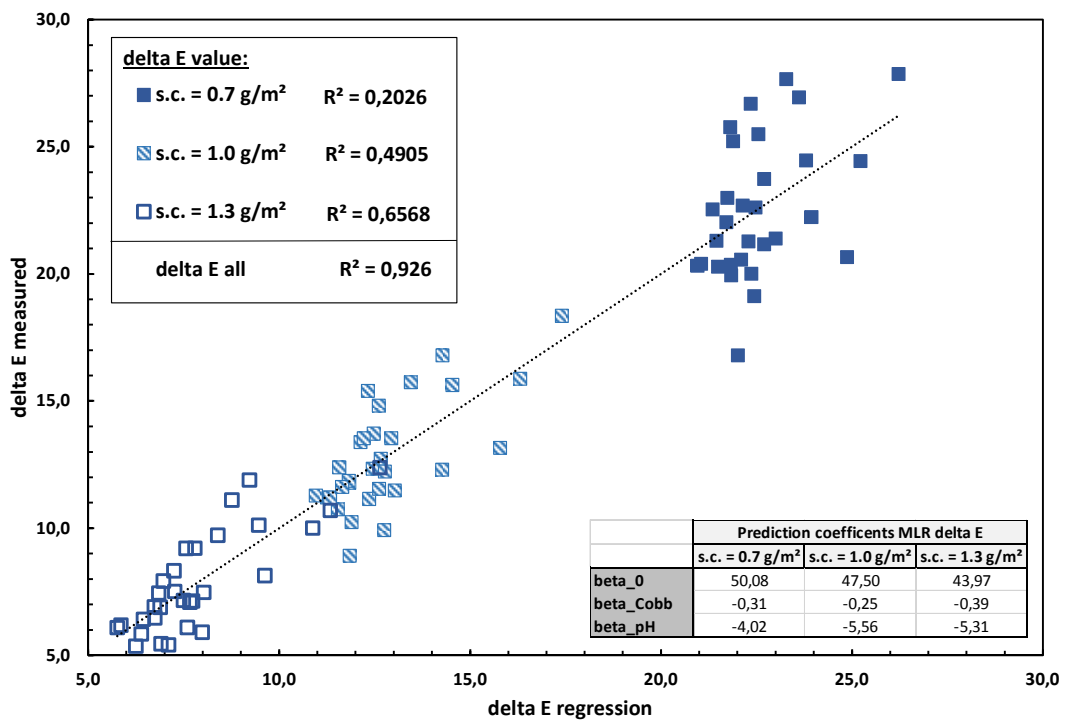


FIGURE 5-16: CORRELATION AND COEFFICIENT OF DETERMINATIONS (MLR DELTA E)

Considering the model for the coat weight of 1.3 g/m², which is displayed in equation (5-1), the influence of the surface pH of the base paper on the delta E result is about 3.5 times higher than the influence of the Cobb value. The Cobb value and the surface pH were already discussed as base paper properties influencing the colorant uptake of the defect spots in the silicone layer (see chapter 5.1.2). From that point of view it is reasonable that the explanatory power of the MLR model regarding the measured delta E values decrease with decreasing silicone coat weight. The delta E values are low at a silicone coat weight of 1.3 g/m² and therefore the influence of these parameters is higher.

$$\Delta E_{1.3} = 43.97 - 0.39 * Cobb - 5.31 * surf pH \quad (5-1)$$

In Figure 5-17 the number of stained spots (P_{total}) (see chapter 3.4.2) is used as an additional predictor variable. If the delta E value and the number of stained spots both would describe the same, which should be silicone coverage, adding the number of stained spots (P_{total}) to the regression model for the delta E value should not change the coefficient of determination in the models result. In other words, when both the delta E value and P_{total} would describe the same, the column indicating the share on the coefficient of determination (r^2) of the model should only have a redundant share (light grey). In this case the addition of P_{total} would not bring any information surplus. Figure

5-17 shows the opposite. The addition of the parameter P_{total} leads to an information surplus and equals the r^2 for the different silicone coat weights to the same level. Therefore the mean overall r^2 indicated by the red horizontal line increases from 0.45 without P_{total} to nearly 0.7 including P_{total} . As P_{total} is the number of stained spots, a high relation to silicone coverage is expected. Assuming that, four reasons can be brought up that the delta E value is a rather poor predictor for silicone coverage:

- Cobb and surface pH are expected to influence base paper colorant interactions and not silicone coverage. This parameters are able to explain the delta E value best.
- The addition of P_{total} , which is expected to predict silicone coverage, to the delta E MLR model results in an increasing correlation and equals the r^2 for the single silicone coat weights.
- A high share of the parameter P_{total} is exclusive.
- Considering the whole column of the parameter P_{total} the maximum r^2 is only 0.3, which means a poor correlation of the delta E and parameter P_{total} , which is expected to predict silicone coverage.

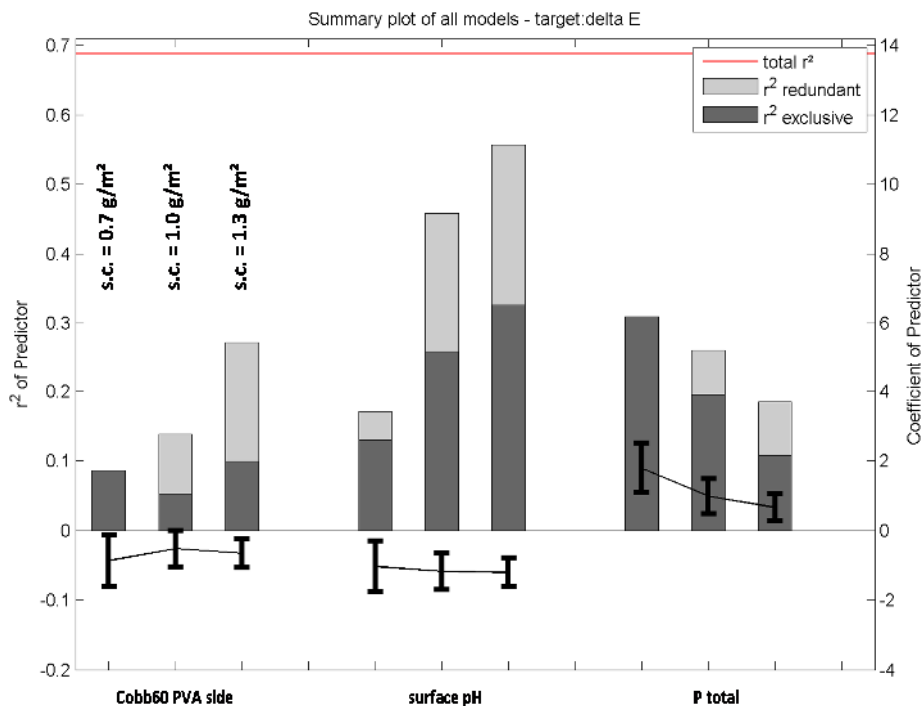


FIGURE 5-17: PREDICTION OF DELTA E WITH MLR (FINAL MODEL) INCLUDING P_{TOTAL}

5.3.2. PREDICTION OF SILICONE COVERAGE:

A good parameter to describe silicone coverage, is the number of stained spots, which is referred to as P_{total} . This parameter is determined from the scanned in delta E test papers, treated with malachite green (see chapter 3.4.2). The stained area (A_{total}) is not a reliable predictor for silicone coverage, as the spreading ability of malachite green is changing the real size of the defect spots depended on the base paper properties and the shape and size of defects. Taking the number of stained spots (P_{total}) as a parameter, no information regarding the size of defects is given at all. In Figure 5-18 the area distribution of the scanned delta E test image is compared to the area distribution of the silicone negative image. Both images originate from the exact same spot of the release liner. The base paper is the same and just the applied silicone coat weight is different for the two depicted liners. The share of the defect area respectively the stained area smaller than $100\ \mu\text{m}$ (indicated by the red vertical line) is determined. Taking the area distribution of the silicone negative as the true defect distribution, a high percentage of the defects is smaller than $100\ \mu\text{m}$. Therefore it seems justified to obtain an estimate for these small areas by using the number of stained spots calculated from the scanned delta E test images, as these small areas serve as an approximation for the number of defects in the silicone layer. An additional aspect is, that the distribution of defects, based on the silicone negatives, is quite similar for release liners of the same coat weight with a different base paper. This is shown by a comparison of Figure 5-18 and Figure 5-19, where the same procedure was carried out with a different base paper. As the structure size distribution of the defect area of the silicone negatives is similar, it seems to be not necessary to bring in the information about the size of the defects. Nevertheless an error is produced as the determination of the number of stained spots from the delta E test images using a bandpass filter is limited by the resolution of the scanner to the minimum structure size of $42.34\ \mu\text{m}$. Defects for papers siliconized with $1.3\ \text{g/m}^2$ silicone are smaller compared to a lower silicone coat weight, which also shows the area distribution of the scanned delta E test images. The percentage of area, which is smaller than $42.34\ \mu\text{m}$ is therefore higher for a liner with $1.3\ \text{g/m}^2$ silicone coat weight compared to a liner with a lower silicone coat weight. An estimation of the stained spot area, which is smaller than $42.34\ \mu\text{m}$ was not directly possible, but considering the area distribution functions of the papers with $1.3\ \text{g/m}^2$ about 10 % of the stained area is not captured and therefore the number of the stained spots in this region cannot be determined.

The similar distributions of defects visible in the silicone negatives, compared to the non - uniform distribution of the stained delta E test images for the different release base papers, is the reason why the area determined from the scanned delta E test images is not reliable to predict silicone coverage. Therefore the determination of the number

of stained spots, where the information of the size of the stained spots is excluded seems to be the most promising predictor to estimate silicone coverage.

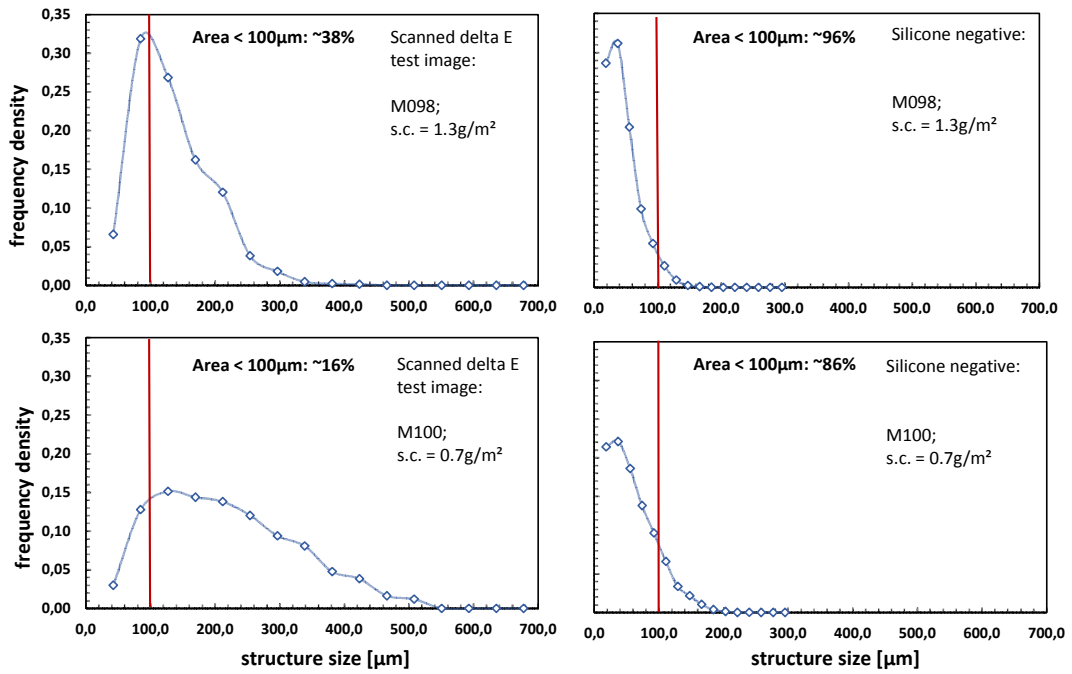


FIGURE 5-18: AREA DISTRIBUTION OF THE SCANNED DELTA E TEST IMAGE AND THE DEFECTS OF THE SILICONE NEGATIVES (SAME BASE PAPER)

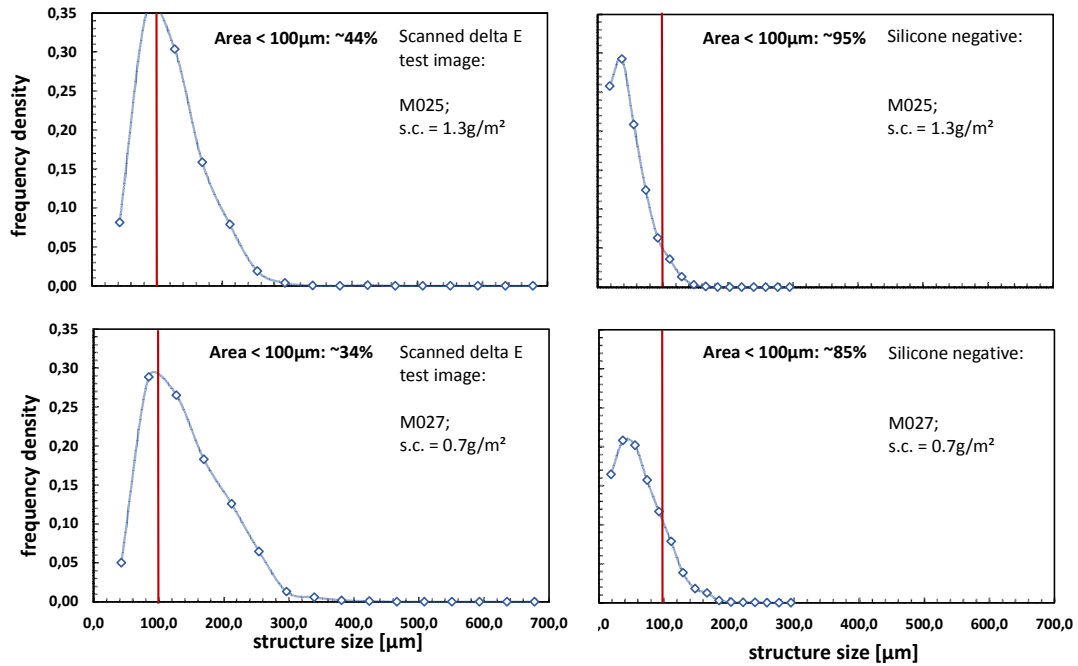


FIGURE 5-19: AREA DISTRIBUTION OF THE SCANNED DELTA E TEST IMAGE AND THE DEFECTS OF THE SILICONE NEGATIVES (SAME BASE PAPER)

MLR analysis with the use of the number of stained spots as a response variable for silicone coverage was performed in the same way as the MLR analysis using the delta E value as a response variable (see chapter 5.3.1). A MLR model including all predictor variables is displayed in Figure 5-24. On the basis of this model the Bekk value, the Cobb Unger and PVA coverage should be chosen as predictors. Stepwise regression was performed for each silicone coat weight (s.c. = 0.7 g/m², 1.0 g/m² and 1.3 g/m²) which resulted in the same predictors for the single coat weights as already expected from the MLR model including all predictor variables. Compared to the MLR model for the delta E value (see chapter 5.3.1) stepwise regression proposes the same predictors for all silicone coat weights.

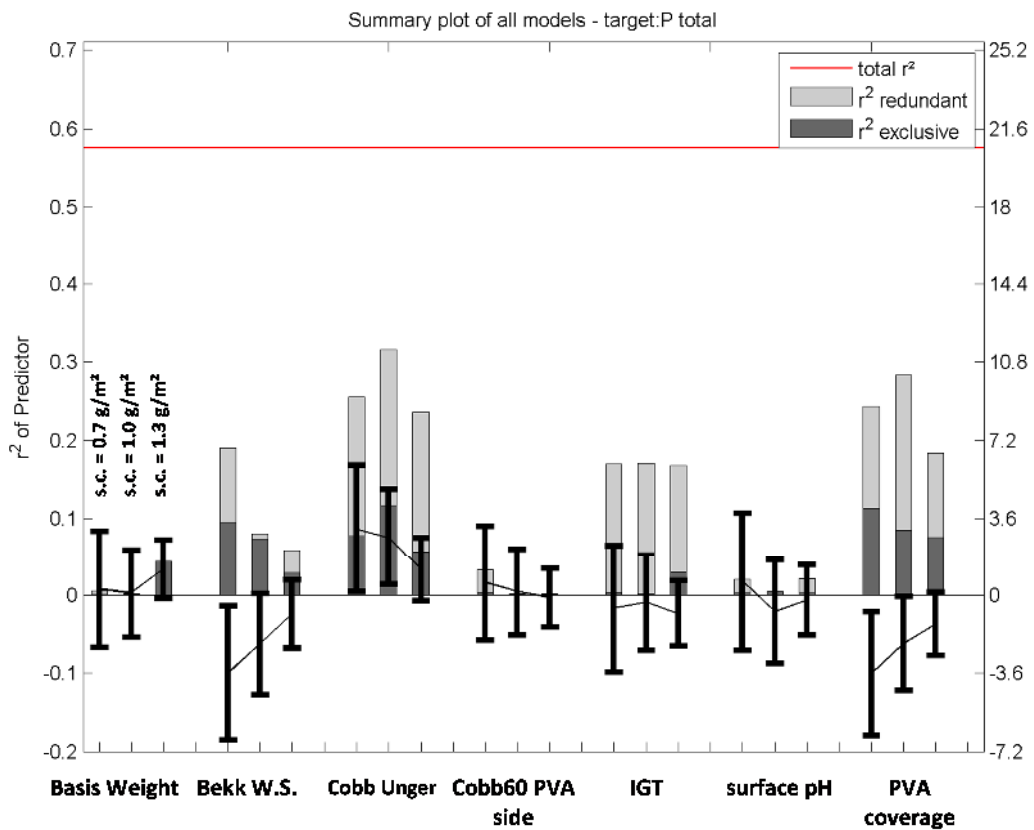


FIGURE 5-20: PREDICTION OF P_{TOTAL} WITH MLR (ALL PARAMETERS)

The final model, describing the number of stained spots (P_{total}) best is depicted in Figure 5-21. The correlation between the stained spots determined from the delta E test images (P_{total} “measured”) and the results from the MLR model (Figure 5-21) is plotted in Figure 5-22 for the single models with the different silicone coat weights. The prediction coefficients β_i of the MLR models are put in this figure. The correlation for the release liner with 0.7 g/m² silicone coat weight is the best, which is

explained by the wider range of the values for this coat weight. The model seems to be reliable for the description of silicone coverage. A possible explanation how the model parameters are related to the siliconizing process and therefore to silicon coverage will be introduced. Bekk smoothness is responsible for the initial contact area of the silicone and the release base paper, when the silicone is transferred from the steel cylinder to the paper. Afterwards the silicone has a time of two seconds to distribute uniformly on the paper surface, before the curing process is starting. It is expected that silicone is able to spread faster on PVA covered areas than on the cellulose substrate. Therefore PVA coverage is an important parameter, which has the highest influence of the predictors. Cobb Unger and PVA coverage are dependent from each other to a certain degree. This is shown by the light grey parts (redundant share) of the Cobb Unger and PVA coverage in Figure 5-21 and explained by the higher oil absorption capacity of areas, where the PVA does not cover the cellulose substrate. The exclusive share of the Cobb Unger might be explained by pores in the paper substrate, which silicone is not able to cover.

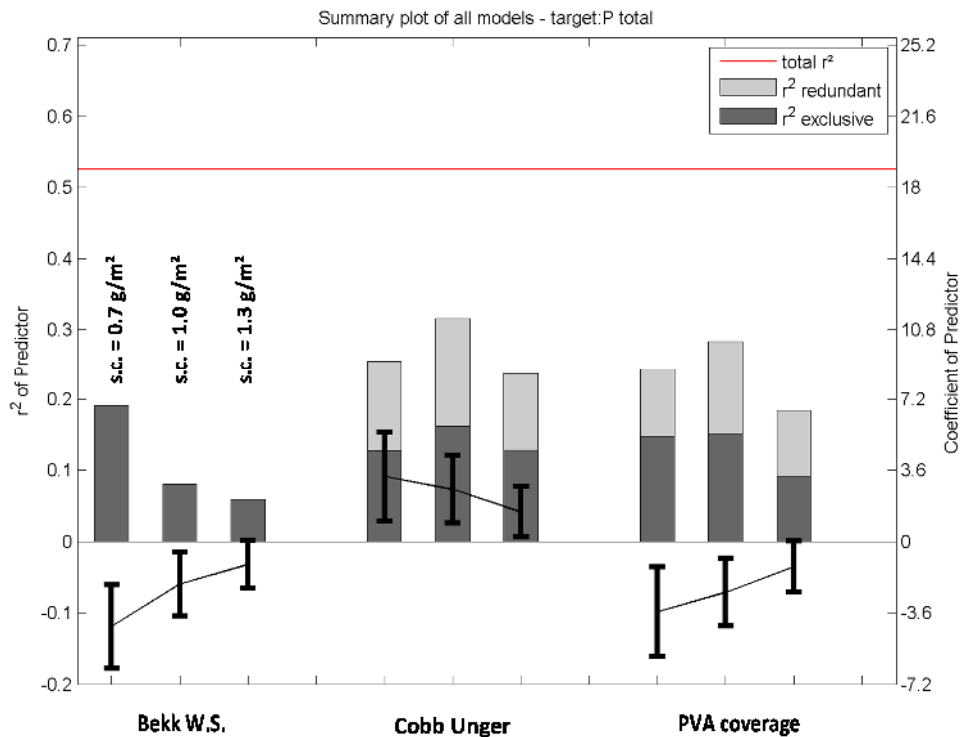


FIGURE 5-21: PREDICTION OF P_{TOTAL} WITH MLR (FINAL MODEL)

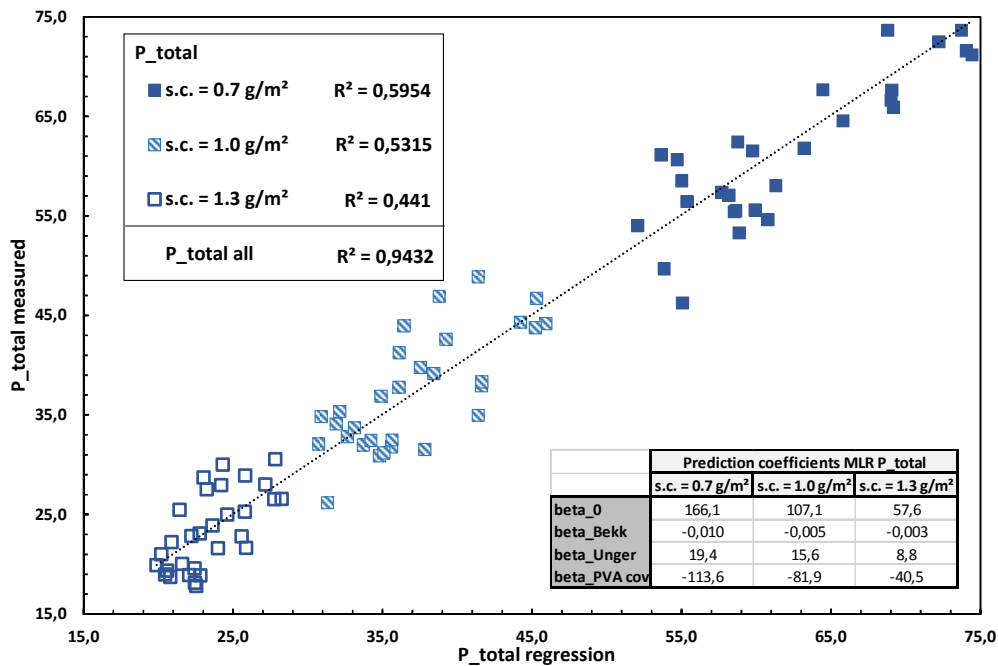


FIGURE 5-22: CORRELATION AND COEFFICIENTS OF DETERMINATION (MLR P_{TOTAL})

The predictors for the three different silicone coat weights only deviate from each other by a multiplicative factor of the coefficients. For this reason it is possible to describe the effect on silicone coverage without the need for three different regression models, by an equation valid for all silicone coat weights between 0.7 g/m² and 1.3 g/m². To determine this equation the predictor coefficients β_i are divided by the mean value of P_{total} separately for the different silicone coat weights (s.c. = 0.7 g/m², 1.0 g/m² and 1.3 g/m²). The results are quite similar coefficients β_i (see Figure 5-23). The mean value for each β_i over the different coat weights is determined. This mean values are used as mean β_i in the final model for all silicone coat weights. The silicone coat weight has to be added to the model as a multiplicative factor now. To determine this factor the mean values of P_{total} are plotted against the mean values of the silicone coat weights for the three different applied coat weights.

The decrease in the number of stained spots with the coat weight can be described best by a potential function (see Figure 5-23). This mathematical relationship may change, if the area of the defects are detected, but it can be assumed that the predictors and the coefficients will remain the same. Equation (5-2) is capable to predict silicone coverage by the number of defect spots, for every silicone coat weight between 0.7g/m² and 1.3 g/m² silicone.

		Prediction coefficients MLR P _{total}			
		s.c. = 0.7 g/m ²	s.c. = 1.0 g/m ²	s.c. = 1.3 g/m ²	
:	beta_0	166,1	107,1	57,6	
	beta_Bekk	-0,0105	-0,0052	-0,0028	
	beta_Unger	19,4	15,6	8,8	
	beta_PVA cov	-113,6	-81,9	-40,5	
=					
		norm			Mean_norm
	mean P _{total}	61,8	36,9	23,4	
	mean s.c. [g/m ²]	0,72	1,00	1,28	
	beta_0	2,69	2,90	2,46	2,68
	beta_Bekk	-0,00017	-0,00014	-0,00012	-0,00014
	beta_Unger	0,31	0,42	0,38	0,37
	beta_PVA cov	-1,84	-2,22	-1,73	-1,93

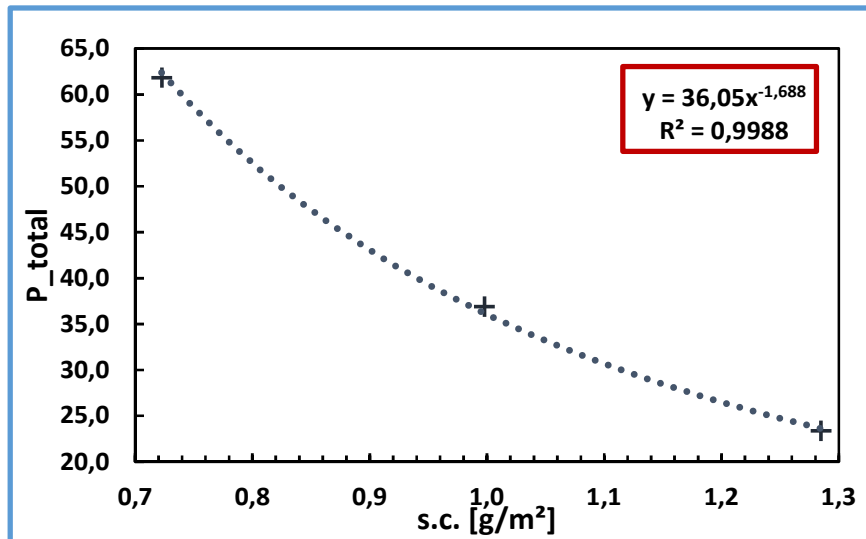


FIGURE 5-23: DETERMINATION OF A MODEL VALID FOR ALL SILICONE COATWEIGHTS BETWEEN 0.7 G/M² AND 1.3 G/M² BASED ON DUNAFIN DATA

$$\begin{aligned}
 P_{total} = & 36.05 * s.c.^{-1.688} \\
 & * (2.684 - 1.439 * 10^{-4} * Bekk + 0.371 \\
 & * Unger - 1.929 * PVA_{cov}) \quad (5-2)
 \end{aligned}$$

This equation is derived using the data of release base papers produced in Dunafin and may be only reliable for Dunafin papers, as not all possible influences of the production process are considered with the three prediction parameters. A good example for this is the correlation between the “measured” and the calculated number of stained spots (P_{total}) using equation (5-2). The correlation is depicted for release base papers produced, PVA coated and calandered in Dunafin and for release base papers produced in Dunafin and PVA coated and calandered in Tervakoski at the pilot

machine (see Figure 5-24). Both paper sets show a good correlation. The difference is in the slope, which is higher for papers finished in Tervakoski. Mathematically this is caused by the higher Bekk values measured for Tervakoski finished papers. Practically the reason might be the differences in the coating application and, in case of the Bekk value, the different calendering process conditions. These production process related aspects are not captured by this model. Considering the higher Bekk smoothness for the Tervakoski finished papers, which is still resulting in quite the same number of defects, there has to be an additional effect which cannot be evaluated by the Bekk smoothness and therefore has to be caused in this case by the PVA application procedure. This will be further discussed in chapter 5.4 where the 2D data maps for different release base papers are compared.

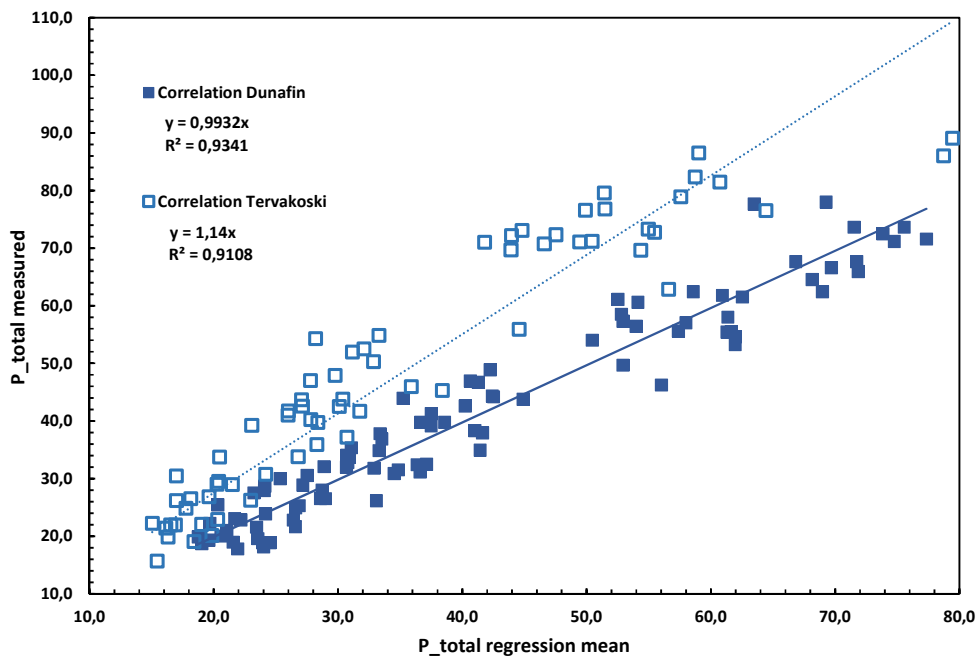


FIGURE 5-24: CORRELATION FOR THE PREDICTION MODEL (EQUATION (5-3))

Adding the delta E values to the MLR model for the different silicone coat weights, an increase of the r^2 can be observed. For the silicone coat weight of 0.7 g/m^2 a larger share of the delta E value can be explained by the other parameters in the model, visible in the high redundant share of the column. This share is decreasing with increasing coat weight, while the exclusive share brought in by the delta E value is nearly constant for all three coat weights between 0.15 and 0.2 r^2 . So the delta E value describes the number of stained spots only to a small extent, which was already discussed in chapter 5.3.1, where the parameter P_{total} was added to the MLR model for the delta E value.

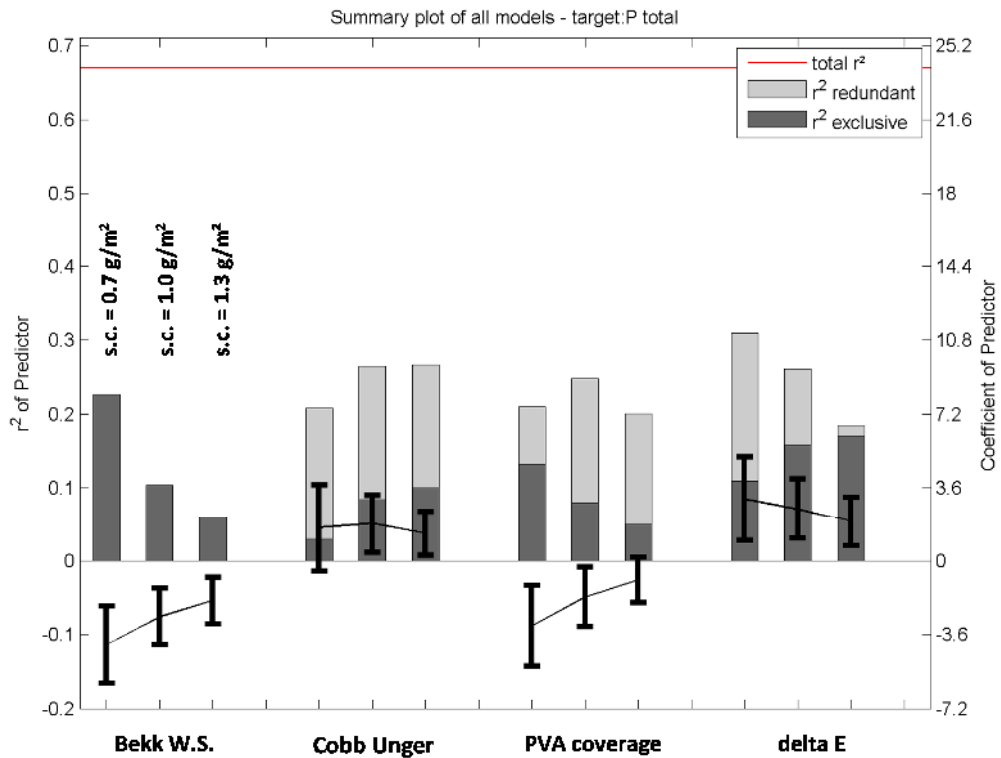


FIGURE 5-25: PREDICTION OF P_{TOTAL} WITH MLR (FINAL MODEL) INCLUDING DELTA E

5.3.3. ADDITIONAL RESPONSE VARIABLES:

Parameter S_{cov}

The parameter S_{cov} should indicate the decrease of the defect size with increasing silicone coat weight and is the slope of the ratios ($R = \frac{P_{total}}{A_{total}} * 10^6$) plotted against the silicone coat weights. The influence of the spreading of the colorant on the base paper – silicone interface is present as the stained spot area (A_{total}) is used in the determination of S_{cov}, why the MLR modelling result is not clear (see Figure A-8). The MLR analysis and stepwise regression was performed for Dunafin and Tervakoski data separately. The parameters PVA coverage and basis weight were chosen by the stepwise regression for Tervakoski and Dunafin data, but the coefficient of determination (r²) for both datasets is quite low with 0.35. Considering the MLR and the stepwise regression result, the Bekk value does not seem to have any effect on the decrease of the stained spot size with increasing silicone coat weight. As an error was brought in with the stained spot area influenced by spreading, this conclusion is not reliable. Nevertheless S_{cov} would be a promising parameter, if no spreading occur.

S_{cov} would then allow the separation of the influential factors on silicone coverage in a factor describing an initial level of silicone coverage and a factor showing the influence of the base paper on the ability of the silicone to form a closed layer with the increase of silicone coat weight.

Durlac value:

The Durlac value is a release liner quality parameter, which should describe the anchorage of the silicone to the base paper (see chapter 2.4), which is related to chemical properties. The Durlac value is expected to be influenced by the cure of the silicone. The silicone cure can be disturbed by substances, which interacts with the platinum catalyst (see chapter 2.2.2), used to speed up the reaction of the silicone with the crosslinker. MLR was again carried out with the Durlac value as response variable using Dunafin and Tervakoski data and a silicone coat weight of 1.0 g/m². Within the Tervakoski papers only PVA coating was changed, while within the Dunafin papers various process parameters were changed. MLR analysis with all variables showed different results for Dunafin and Tervakoski data (see Figure A-9). For some predictors even the prefix changed. The reason might be that for the Tervakoski papers only the PVA recipe had an effect on the Durlac value, while for the Dunafin papers many process variables were changed and the measured release base paper quality parameters does not cover chemical aspects sufficient.

In Table 5-13 the results for the prediction of the Durlac value using stepwise regression are shown. The Durlac values were modelled for the three different coat weights (s.c. = 0.7 g/m², 1.0 g/m² and 1.3 g/m²) for the Tervakoski and the Dunafin papers. Plus and minus (+/-) shows the prefix of the coefficients β_i , selected by the stepwise regression analysis routine. The coefficients of determination (r^2) are added for the single models. The Dunafin data show a low r^2 compared to the Tervakoski data. For both data sets the predictors for the silicone coat weight of 1.3 g/m² are different from the predictors for the lower coat weights. Considering the silicone coat weights of 1.0g/m² and 0.7 g/m² Bekk W.S. and Cobb₆₀ are present for both data sets, but the coefficients have a different prefix. An interaction with another prediction parameter for the Durlac value might be the reason. PVA coverage is a predictor for the Dunafin dataset, but not for the Tervakoski dataset. This might be explained by the higher variations in PVA coverage for the Dunafin data. The Durlac value of the Dunafin data does not seem to be explainable by the measured quality parameters. This is an indication that the Durlac value is highly dependent on variations in the papermaking process (e.g. refining, sizing...). This assumption is underlined by Figure 5-26 where the correlation between the Durlac value and the number of stained spots (P_{total}) is plotted. A rather good correlation exists for the Tervakoski papers, while the Dunafin papers do not show a connection between the Durlac value (silicone

anchorage) and P_{total} (indicates silicone coverage). The observation that lower Bekk values lead to higher Durlac values (better anchorage) in the stepwise regression result of the Tervakoski data, might be explained by the Durlac test itself. In the Durlac test a release liner is clued to a defined weight and rubbed against a felt, rubbing off the silicone layer from the release liner. The amount rubbed off from a less smooth release liner might be lower, as the contact area between the silicone layer and the felt is lower.

	Dunafin			Tervakoski		
	s.c. = 1.3g/m ²	s.c. = 1.0g/m ²	s.c. = 0.7g/m ²	s.c. = 1.3g/m ²	s.c. = 1.0g/m ²	s.c. = 0.7g/m ²
'Basis Weight'				-		
'Bekk W.S.'	+	+	+	-	-	-
'Unger'	-					
'Cobb60 PVA side'		+	+	-	-	-
'IGT'	-					
'surface pH'	+					
'PVA coverage'		+	+			
r ² model	0.51	0.37	0.37	0.63	0.58	0.58

TABLE 5-13: RESULTING INFLUENCE PARAMETERS ON THE DURLAC VALUE (STEPWISE REGRESSION)

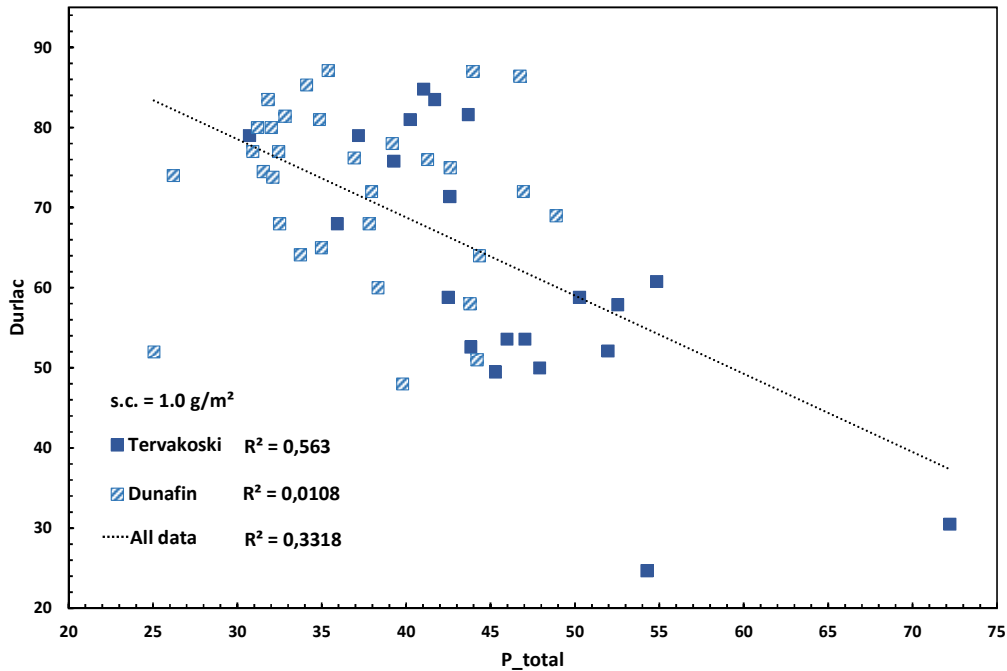


FIGURE 5-26: CORRELATION BETWEEN P_{TOTAL} AND THE DURLAC VALUE FOR DUNAFIN AND TERVAKOSKI DATA

5.4. EVALUATION OF SILICONE COVERAGE BY THE COMPARISON OF 2D DATA MAPS:

Originally the plan in this chapter was to evaluate the influence of the base paper on silicone coverage locally. A square area of 15 x 15 mm on selected release base papers was marked with a laser cutter (see chapter 4.3.1). Silicone negatives (see chapter 4.2.1) were made from the marked areas. The release base papers were siliconized and silicone negatives were taken again afterwards. The negatives of the release base papers and release liners were to be measured with the IFM device (see chapter 4.2.2). The resulting topographical and image maps from the liners and release base papers would have been locally compared after registration (see chapter 4.3.2). Unfortunately the silicone layer was not fully cured when the negatives of the release liners were taken and the silicone layer partly dissolved again in the silicone used for taking the negatives. As the silicone negatives of the release liners were destroyed the comparison of local paper properties could not be carried out. Still some possible local quality aspects will be discussed in this chapter, which might be of use for a future testing. For this purpose three release base papers from three different paper mills were chosen to visualize possible local quality aspects (D3, D4, E2). Negatives were taken from the corresponding release liners with a silicone coat weight of 1.3 g/m². A local comparison is not possible as the negatives of the release liners do not have the same paper position as the negatives of the release base paper.

With the IFM device it is possible to measure topography and in addition an optical image of the sample. From the resulting 2D maps the following aspects can be analysed:

- Roughness: max structure size 100 µm
- Waviness: structures from 500 µm to 2500 µm
- Total topography: max structure size 2500 µm
- Surface area of the total topography
- Topography distributions
- Pores and high z-variations

First the 2D maps will be discussed. The images from the silicone negatives show a variation in lightness. This is based on differences in reflection caused by micro roughness. The lightness difference in the images makes it possible to select smoother and therefore brighter PVA covered areas from the images of the release base papers and smoother siliconized areas from the images of release liners. The images (4x4 mm) of the silicone negatives for the release base papers and the release liners (s.c. = 1.3 g/m²) for the papers D3, D4, E2 are depicted in Figure 5-28. It has to be pointed

out again, that the negatives from the release base papers and release liners do not taken at the same paper position. Comparing the release liner and base paper for each paper separately it seems that PVA coverage has an effect on silicone coverage. In sample D3 PVA is more uniformly distributed than in sample D4. The image of the release liner also shows smaller defect for sample D3 compared to sample D4. The observation that a more uniform PVA coverage leads to a better silicone coverage was already found in the MLR model (see chapter 5.3.2). A local comparison of PVA coverage to silicone coverage is an opportunity to quantify the impact of PVA coverage and PVA distribution and might help to improve the PVA coating application. Based on the lightness of the PVA coating in the image a distribution can be calculated (see Figure 5-27) using grey levels. On the x-axis a gradation of grey levels is plotted. At the zero position the average grey level is located. The more the distribution function shifts to positive values on the x-axis the better is the PVA coverage. The shape of the curves of the three paper samples shows large differences. Sample D3 shows the most uniform distribution, which is visible comparing the distribution with the image in Figure 5-28. E2 has a high percentage of lighter areas compared to D4 and E2. Lighter areas indicates better PVA coverage. Sample D4 shows a random distribution with no distinct peak. This kind of comparison might be useful in the development of a PVA coating recipe to be able to quantify which PVA distribution results in the best silicone coverage. The compared papers are coated using different application systems. The high differences in the distribution might also result from these different PVA application systems. As PVA is often used in combination with clays and starch, the PVA coverage from the silicone negatives is actually the coating coverage.

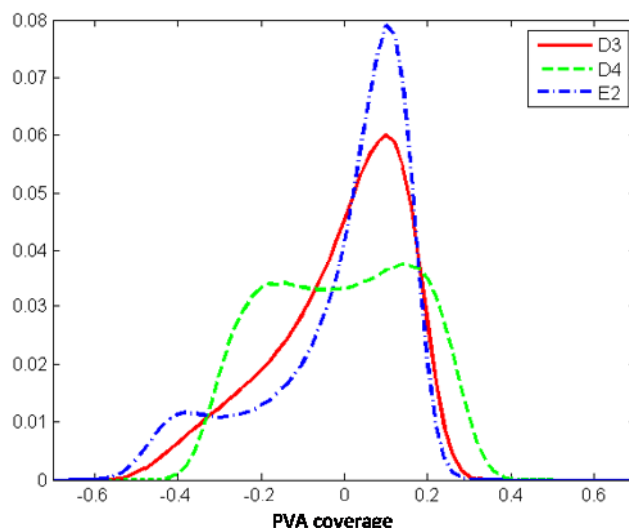


FIGURE 5-27: DISTRIBUTION OF PVA COVERAGE BASED ON GREY LEVELS OF THE SILICONE NEGATIVE IMAGES

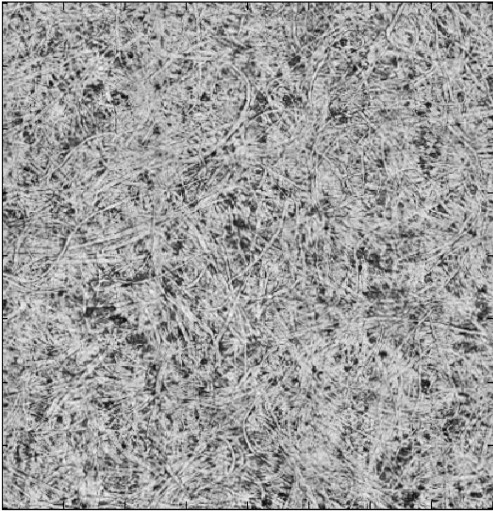
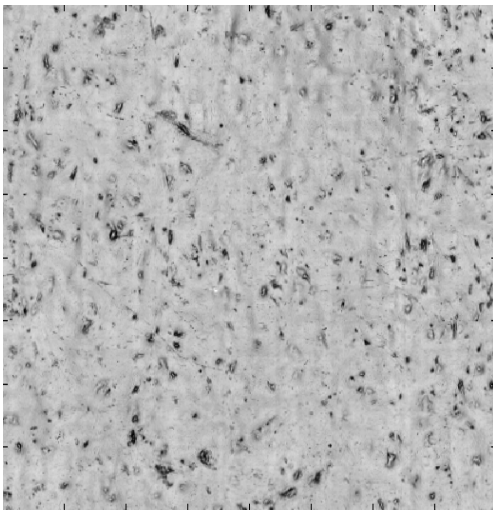
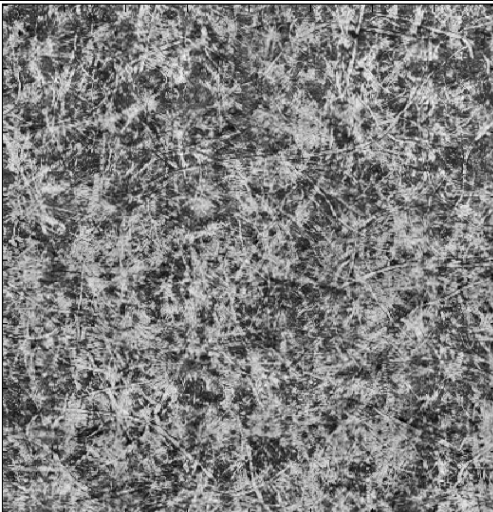
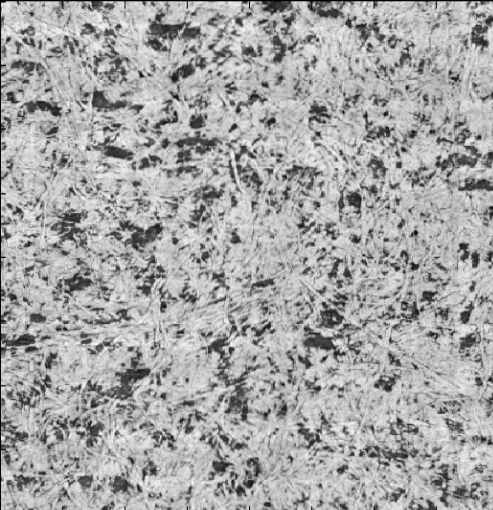
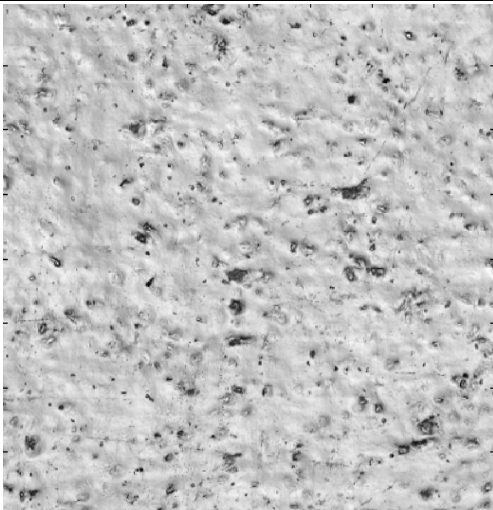
	Release base paper	Release liner
D3		
D4		
E2		

FIGURE 5-28: IMAGES FROM SILICONE NEGATIVES (BASE PAPER AND LINER (4X4MM))

Additionally to the images the topography of the silicone negatives can be analysed. Exemplary the topography maps from the release base papers negatives are discussed. The same analysis procedures can be used for the topography maps of the release liners as well. Topography can be separated into different structure sizes by the use of filters. For the samples discussed in this thesis, roughness is defined by a maximum structure size of $100\ \mu\text{m}$, whereas waviness is determined for structures bigger than $500\ \mu\text{m}$ up to $2500\ \mu\text{m}$. It is also necessary to use a filter for the total topography as the specimen stage on the IFM device cannot be adjusted in plane with the high precision, needed. For the total topography all structures larger than $2500\ \mu\text{m}$ were rejected. Figure A-11, Figure A-12 and Figure A-13 illustrate the roughness profiles, the waviness and the distribution of topography for sample D3, D4 and E2. In Figure A-10 topography maps for the release base paper samples are depicted. Visually and also comparing the distribution functions only small differences between the three papers can be observed. Trying to find a correlation between the topography and the PVA coverage visible in the images (see Figure 5-28) using different structure sizes, which might be responsible for the PVA coverage was not successful. This is caused by the very high smoothness of the release base papers, which were measured after calendering. Further topography measurements using a higher resolution in the z – direction should be carried out in the future. The local basis weight (formation) might be a better descriptor for PVA coverage as the topography for these very smooth papers.

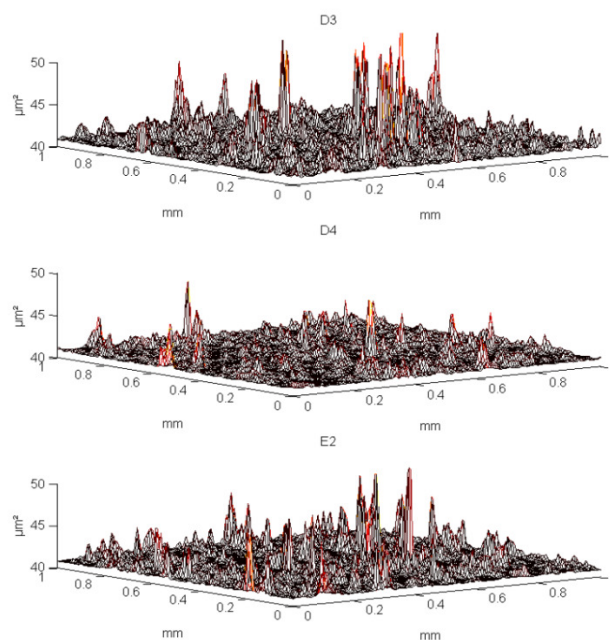


FIGURE 5-29: LOCAL SURFACE AREA

For the determination of the surface area, finite areas which include four neighbored data points from the topography map are calculated for each position. The sum of all finite areas is then the surface area. The ratio of the surface area to the projected area is the portion of additional area caused by the topography of the paper. Finite areas are higher in regions where pores and high z-position fluctuations (e.g. caused by pores) are located. In Figure 5-29 the surface areas for the release base papers D3, D4 and E2 are plotted.

Derived average parameters can also be determined from the local paper properties. PVA coverage from the release base paper and silicone coverage from the release liner negatives is determined using a threshold value. From the topography data the arithmetic average and the root mean square roughness (Ra and Rq) can be determined. The determination of the surface area, which might be related to the quantity of silicone needed to cover the surface was already discussed. Exemplary these parameters were calculated for the samples D3, D4 and E2 for an area of 14 x 14mm (see Table 5-14). To be able to use the full potential of 2D maps, it is necessary to compare the same paper position. As this was not possible no further conclusions can be made from these 2D data analysis. Nevertheless the method is an opportunity to obtain more knowledge regarding the silicone - paper interaction with the analysis of only a small quantity of samples. In comparison to the overall quality parameters, where each paper is representing one data point, the local analysis provides, depending on the resolution, 10⁶ data points and more per paper sample. The opportunity is therefore to need fewer samples to estimate the influential parameters.

The parameters that turned out to influence silicone coverage in the regression analysis can also be evaluated using local properties. In addition local compressibility, local basis weight (formation) and local density may be of interest for further analysis.

	PVA coverage [%]	Silicone coverage [%]	Ra [μm]	Rq [μm]	Additional area [-]
D3	79,6	98,4	1,34	1,72	1,0090
D4	74,3	97,2	1,50	1,93	1,0063
E2	79,0	97,5	1,53	1,95	1,0092

TABLE 5-14: AVERAGE PARAMETERS CALCULATED FROM 2D MAPS

6. CONCLUSIONS:

It turned out that the delta E value determined from the stain test using malachite green as a colorant and actual silicone coverage are different issues. The conclusion is therefore summarized separately for the delta E value and for the silicone coverage.

6.1. DELTA E VALUE:

At the start of this thesis, it seemed to be the right conclusion that the delta E value determined using malachite green describes silicone coverage. The only possibility how the colorant is able to stain the paper is a defect in the silicone layer. Therefore the more defects, the higher the colour difference measured by the delta E value. The problem is that the delta E results as a measure of silicone coverage is only poorly explainable by the measured quality parameters describing the release base paper. The first possible reason for this observation is that a parameter is missing in quality control of the release base paper, which cannot be described by the standard quality parameters. The second possibility is, that the delta E value does not describe silicone coverage only. Considering the potential weaknesses of the test, it turned out that the delta E value has to be questioned as a measurement for the description of silicone coverage, for several reasons. The sources for the errors brought in by the delta E test procedure are explained in detail in chapter 5.1 and are summarized in Figure 6-1. Reasons written in italic letters in Figure 6-1 could not be evaluated in this thesis, but are expected to have an effect on the delta E test results.

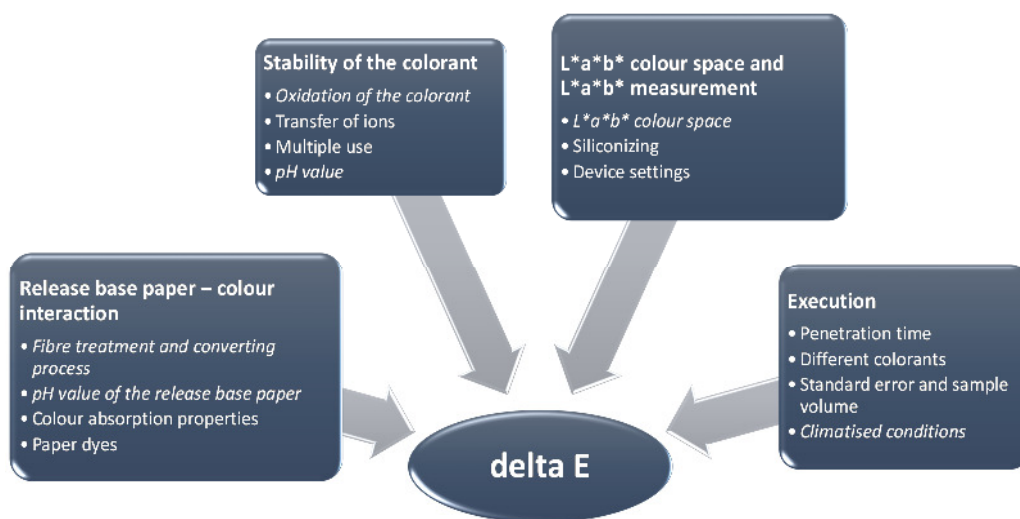


FIGURE 6-1: INFLUENCES ON THE DELTA E VALUE

Consequences of the errors are an incomplete detection of defects, caused by a too short penetration time, a change in colour intensity influenced by the base paper and the multiple use of the colorant over longer periods. Another issue are the spreading properties of the colorant solution at the base paper – silicone interface especially for malachite green, which are effected by the base paper properties. Even though base paper properties are constant, spreading does have more impact on smaller defects and is dependent of the defects shape. The influence caused by the determination using the $L^*a^*b^*$ colour space was not determined. Nevertheless the $L^*a^*b^*$ colour space interprets the colour difference based on humans sensation. The variability of measurement data is quite high and influenced additionally by large scale variations in silicone coverage which cannot be detected with only one measurement per release liner sample.

6.2. SILICONE COVERAGE:

Multiple linear regression analysis was performed for two different parameters, which were considered to predict silicone coverage. The first parameter was the delta E value. It was not possible to show a relationship between the delta E value and parameters like e.g. the Bekk value, IGT and Cobb Unger, expected to influence silicone coverage. The two parameters which were able to be related to the delta E value were the Cobb value and the surface pH of the release base paper. As already discussed in chapter 5.1 these two parameters are influencing the colorant - base paper interaction. The other parameter used for the prediction of silicone coverage is the total number of stained spots, which was determined for the same stained papers, where the delta E value was measured. To take the number of defects was the only way to neglect most of the influences brought in by the spreading and absorption properties of the malachite green solution and the test method. Multiple linear regression analysis showed reasonable models for all three silicone coat weights. The predictors for the number of defects are the Bekk smoothness, Cobb Unger and PVA coverage. PVA coverage does have the highest impact of the three predictors. It was possible to combine the three models to one and to obtain a relationship for all silicone coat weights with only one model. Considering this, it seems not to be necessary, to coat the release base paper with three different silicone coat weights to be able to predict silicone coverage. Applying this model to papers where the manufacturing process is different, also resulted in a good correlation, but the slope was different. Although the prediction of silicone coverage by the number of defects is only a rough estimation, it leads to clearly more reasonable results, compared to the delta E value.

The IFM device measures topography and simultaneously the optical image. Using the IFM to evaluate silicone negatives taken of the release base paper and the release liner surface promising local properties such as number of defects in the silicone layer or PVA coverage were derived. A final conclusion from the local measurements, could not be obtained, because the negatives of the release liners could not be taken at exactly the same paper position due to experimental reasons. A visual comparison of the image maps from the release base paper and the release liner shows that the defect size and size distribution seems to be caused by the PVA coverage and distribution. The assumption is that this is caused primarily by the higher affinity of silicone to PVA than to cellulose and to a lower degree because of silicone absorption on paper areas not covered by PVA.

7. OUTLOOK

This thesis offers the basis for further detailed analysis. Three new test methods were developed:

- Visualisation of PVA coverage and distribution by a colour reaction of PVA with boric acid and KI – I₂ solution.
- Image analysis of delta E stain tests using a scanner and an image analysis software
- Silicone negatives, which can be qualitatively evaluated under a standard light microscope or quantitatively under an optical topography system.

These methods could be implemented with relatively low budget and effort in the laboratory at the mill. All of these methods help to improve the understanding regarding the interaction between release base paper and silicone. The method to evaluate PVA coverage and distribution is a promising method for the quality control of release base papers, but has to be optimized further before an implementation in this field.

Regarding the evaluation of silicone coverage and its relation to quality parameters of release base papers, a new method should be developed, as the delta E test method with malachite green is not fully reliable. Instead of malachite green, another colorant should be found. “Shirlastain A” is promising, as it seems to have negligible spreading properties. This can be crosschecked by taking silicone negatives and compare them with the stain test as was shown in this thesis for malachite green. The disadvantage of “Shirlastain A” is the coloration of the silicone, which makes it more difficult to separate the stained areas using image analysis. A colorimetric measurement is not possible, because the coloured silicone is measured too. If there is a possibility, the colorimetric measurement should be supported by image analysis, as image analysis colorimetric measurement is creating additional information. The image analysis software can be used for the determination of PVA coverage too. Powders as solid or pigment colorant solutions might be additional possibilities for a replacement of malachite green in the delta E test. To be really sure that all defects are stained the contact time of the release liner and the colorant solution have to be at least 120 seconds using malachite green or “Shirlastain A”. The results of the regression analysis showed that PVA coverage has the highest influence concerning silicone coverage. Therefore the PVA type, additives, PVA cooking, storage and application should be considered. Coating rheology at high shear rates is important for the development of coatings. Bekk smoothness is also a quite important issue, which may be considered to improve. For further quality development 2D mapping methods and local paper

property analysis can be helpful and give more detailed information than the standard siliconizing trials alone. It turned out that it might not be necessary at all to apply three different silicone coat weights. A coat weight of 0.7 g/m² is to be preferred as the widest range in silicone coverage occurs. With the pilot silicone coater it is possible to change other settings than the coat weight. For example the machine speed, which can help to identify the source, which is causing defects in the silicone layer, as dynamic factors also play a role regarding silicone coverage.

A.APPENDIX:

A.1. NEW METHODS: DETAILED TEST PROCEDURE:

A1.1. METHOD TO CHARACTERIZE PVA COVERAGE AND DISTRIBUTION:

Purpose and scope:

A method to evaluate the uniformity of PVA application on the base paper was developed, to investigate the influence of PVA coverage on the siliconability and to examine PVA coating faults.

Principle:

This method is a modification of a qualitative method for PVA identification, based on a Tervakoski test method. Under presence of boric acid, a colour reaction of PVA with a potassium iodide (KI) – iodide (I₂) solution appears. Bluish color indicates the presence of pure PVA. In the case that PVA is used together with starch, the colour shifts to a more purple region, while starch alone is indicated only by a purple coloration. This shift allows to determine PVA coverage also for PVA and starch coated samples (see Figure 4-1).

Equipment:

- 2x100ml flasks
- Mortar
- 2xBeaker glasses
- 2x aerosol cans
- Cone
- 5 ml pipette
- 2 ml pipette
- Heating plate
- 50 x50 cm cardboard box
- Tissue
- Copy paper as fixation frame
- Cardboard stand
- Cutter

Chemicals:

- Potassium iodide (powder)
- Iodine (granulate)
- Boric acid (powder)

Method:

Preparation of test liquids:

For the preparation of a 40 g/l boric acid solution 4.0 g boric acid are weighed in a beaker glass and funnelled in the 100 ml flask. The dissolution is done with distilled water on a heated plate. The solution then has to be cooled down to ambient temperature and filled up to the 100 ml mark on the flask with distilled water.

For the preparation of the KI – I₂ solution 2.5 g KI and 0.1 g I₂ is crushed and mixed in a mortar. To dissolve the crushed KI – I₂ mixture, 5 ml of distilled water are added in the mortar slowly. 2 ml of this solution are pipetted in a 100ml flask and filled up with distilled water to the mark.

Application:

A window (20 cm x 6 cm) is cut out of an A4 copy paper, for the fixation of the release base paper sample.

The release base paper sample (25 cm (CD) x 8 cm (MD)) is fixed with a tape to the backside of the A4 sheet in the region of the cut out window. The A4 sheet is taped to the cardboard stand and put in the cardboard box as depicted in Figure A-1. The boric acid solution and the KI – I₂ solution are filled in two separate spray cans. First the KI – I₂ solution is sprayed onto the release paper sample in the box. Immediately the boric acid solution is sprayed onto the wetted surface. The reaction occurs spontaneously. The sample is taken out of the box and dabbed dry with a tissue.

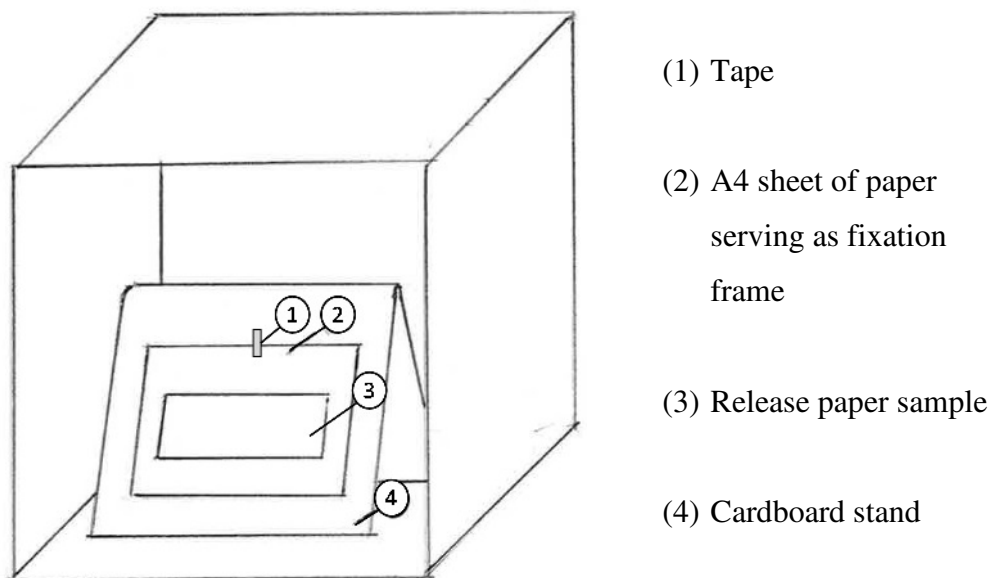


FIGURE A-1: SCHEMATIC DRAWING OF THE EXPERIMENTAL SETUP

Results:

Due to the colour reaction with the PVA this test allows an evaluation of PVA coverage and uniformity of PVA distribution. The resulting images can be evaluated visually. Another possibility is to evaluate the distribution using a suitable image analysis software after scanning the image in order to determine the PVA covered area as a percentage. In Figure 4-1 some examples showing the differences in PVA coverage are given.

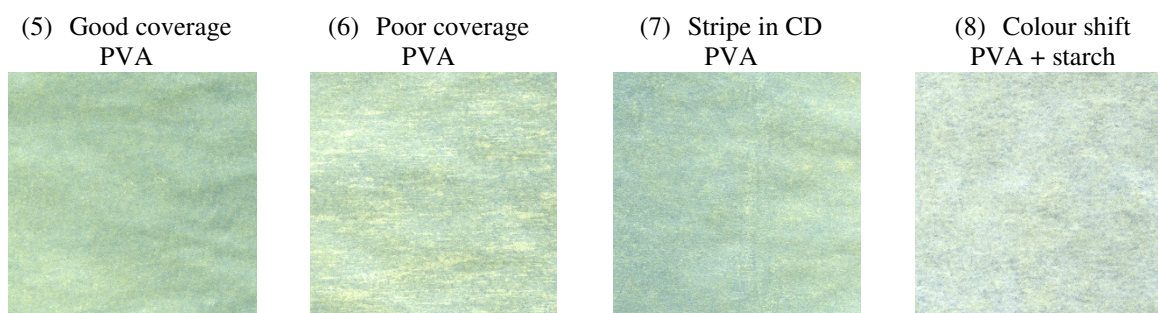


FIGURE A-2: EXAMPLES SHOWING DIFFERENCES IN PVA COVERAGE

Remarks:

Because of the given time frame of this thesis the PVA coverage test was only carried out as described above. Although the results are promising, this test method needs to be optimized, since a uniform application of the test liquids on a larger area is difficult to achieve with the aerosol cans. Due to the poor wetting behaviour of boric acid, KI – I₂ solution is applied first, followed by the boric acid solution. The possibility to mix the two test liquids together should also be evaluated. A further option would be to wet the paper surface with distilled water first, before the test liquid application with the aerosol can. Another possibility would be to execute this test using a Cobb device under the condition, that the test liquids can be mixed. Attention has to be paid as the PVA can dissolve in the test liquid. Saturation of the air with the test liquids in a climate box is another possibility to consider in the optimization of this test.

A1.2. METHOD FOR SILICONE NEGATIVES FROM BASE PAPER AND RELEASE LINER SURFACES:

Purpose and scope:

ESCA (electron spectroscopy for chemical analysis) and AFM (atomic force microscopy) are usually used to detect the topography and the silicone coverage of release liners. These methods have their advantages in the high resolution that can be

achieved, but only very small areas can be analysed with a rather high effort. Optical topography methods for release base papers and release liners are generating questionable results, as these papers are transparent and vary in local opacity. Mechanical topography methods can be used, but are time consuming when high resolutions are required and the measuring head is in direct contact with the test sample. This can cause variances from the real topography, as it is necessary to apply a minimum force on the paper. Taking a negative of the paper surface, using silicone, creates an optical homogeneous surface, which can be analysed using optical topography methods.

Principle:

Due to its low surface energy and its freedom of rotation, silicone is capable to creep into small pores and to wet all kind of surfaces. These properties are needed to achieve a negative which includes all the topographical information from the original.

Equipment:

- Sample frame (polymer sheet, thickness 0.2 cm)
- Counter plate
- Plastic (glass) beaker (100 ml)
- 2x spatula

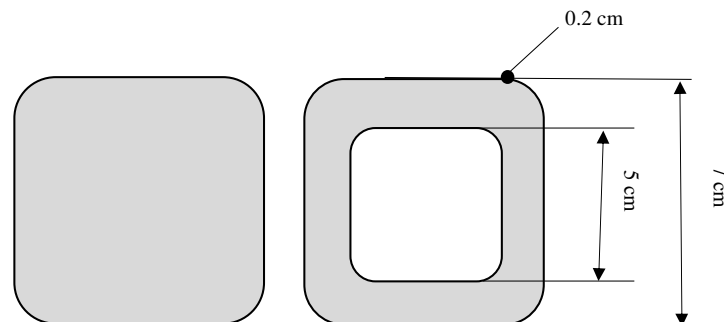


FIGURE A-3: COUNTER PLATE AND SAMPLE FRAME

Chemicals:

- Silicone
- Hardener
- Colour - paste (black)

Method:

The counter plate and the sample frame are cut out of a polymer board preferably using a laser cutter. Other materials than polymers can be used too, if they fulfil the requirements of high smoothness and evenness. The counter plate has the function to provide an even and smooth sample holder for the paper sample. The sample can be fixed to the counter plate with a double – faced adhesive tape, if the paper tends to curl or has an uneven, wavy surface. The sample frame is put on top of the paper and can be fixed with a tape to the counter plate, to prevent the leakage of silicon later on. For release base papers with a high smoothness it is not necessary, to connect the sample frame with the counter plate.

The silicone is weight in a plastic beaker together with 10 % hardener (based on the mass of silicone) and homogenized with a spatula. A small quantity of the black paste is mixed with the already homogenized components with a spatula until the mixture reaches a homogeneous black colour. It is of importance to follow the preparation procedure, as the black paste cannot be bonded sufficient to the silicone when the silicone and the hardener are not homogenized before its addition. With a different mixing order the colour paste can attach to the cellulose substrate. The liquid silicone compound is then poured onto the paper sample in the sample frame. After three hours the silicone is cured and can be separated from the frame and the paper.

Results:

The silicone negative replicates the topography of the paper, which could not be evaluated directly via optical topography systems due to the transparency of the paper, of the applied PVA and, in case of the release liner, due to the transparency of the silicone layer. The black silicone negative however can be analysed using optical methods. Defects in the silicone coating, formation of the base paper and the quality of the PVA coating are visible under a standard light microscope for a fast qualitative analysis and a comparison of different papers. Image and topographical mapping of quite large areas compared to the methods working on the basis of the chemical composition of the silicone or the PVA is possible for the silicone negatives using e.g. the optical infinite focus method (IFM).

Remarks:

It is not possible to take silicone negatives of release liner surfaces shortly after siliconization of the release base paper, as the not fully cured silicone layer can dissolve in the silicone used for the negatives. This phenomenon does not occur with release liners with a fully cured silicone layer. The minimum curing time needed for the silicone layer was not evaluated, as most analysed samples, where siliconized at least one month before taking the negatives and do not show a dissolution of the

silicone layer. Only in one case silicone negatives were produced three days after siliconization and these showed the problem mentioned above.

A.2. RELEASE BASE PAPER COLORANT INTERACTION:

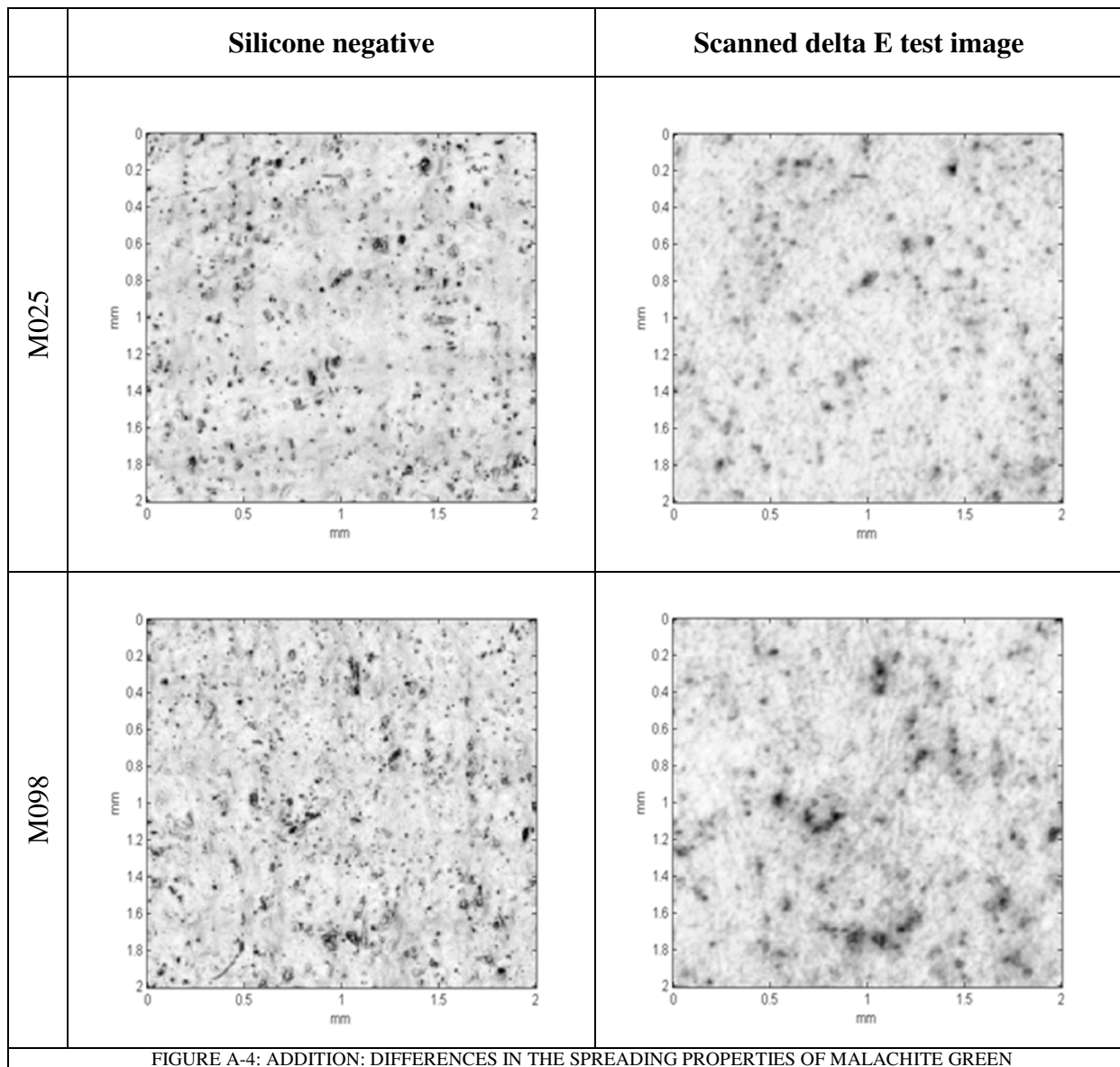


FIGURE A-4: ADDITION: DIFFERENCES IN THE SPREADING PROPERTIES OF MALACHITE GREEN

A.3. STABILITY OF THE COLORANT:

sample code	determined delta E values						relative difference (Trial 3.1 : Trial 3.0)			absolute difference (Trial 3.1 - Trial 3.0)		
	s.c. = 1,3 g/m ²		s.c. = 1,0 g/m ²		s.c. = 0,7g/m ²		delta E (s.c.=1.3 g/m ²)	delta E (s.c.=1.0 g/m ²)	delta E (s.c.=0.7 g/m ²)	delta E (s.c.=1.3 g/m ²)	delta E (s.c.=1.0 g/m ²)	delta E (s.c.=0.7 g/m ²)
	Trial 3.0	Trial 3.1	Trial 3.0	Trial 3.1	Trial 3.0	Trial 3.1						
5.1	5,2	6,9	11,2	11,8	23,1	22,0	1,33	1,05	0,95	1,7	0,6	-1,1
5.2	5,1	6,1	10,5	11,2	20,0	20,3	1,19	1,07	1,02	1,0	0,7	0,3
5.3	5,3	5,5	10,5	11,2	19,8	20,4	1,03	1,06	1,03	0,2	0,7	0,6
5.4	6,1	7,5	12,1	13,5	22,1	23,7	1,23	1,12	1,07	1,4	1,4	1,6
5.5	4,7	6,1	10,2	9,9	19,5	20,0	1,30	0,97	1,03	1,4	-0,3	0,5
5.6	7,0	7,9	13,2	13,5	24,0	25,2	1,13	1,03	1,05	0,9	0,3	1,2
5.7	6,6	7,1	10,9	12,2	23,2	22,6	1,08	1,12	0,97	0,5	1,3	-0,6
6.1	5,5	6,4	10,8	12,4	19,7	20,3	1,17	1,15	1,03	0,9	1,6	0,6
6.2	6,4	5,8	11,6	10,7	21,5	21,3	0,91	0,93	0,99	-0,6	-0,9	-0,2
6.3	5,5	7,5	11,4	11,9	21,7	25,8	1,35	1,04	1,19	2,0	0,5	4,1
6.4	5,5	6,2	10,6	11,3	21,2	20,4	1,13	1,06	0,96	0,7	0,7	-0,8
6.5	4,3	5,4	9,1	11,2	20,5	22,5	1,24	1,23	1,10	1,1	2,1	2,0
6.6	5,1	6,5	10,5	11,6	20,7	23,0	1,27	1,11	1,11	1,4	1,1	2,3
6.7	4,9	5,9	9,8	11,5	19,7	21,2	1,21	1,18	1,07	1,0	1,7	1,5
6.8	4,1	5,4	8,6	8,9	16,3	16,8	1,32	1,04	1,03	1,3	0,3	0,5
7.1	4,1	4,5	6,4	5,7	13,4	13,9	1,09	0,89	1,04	0,4	-0,7	0,5
						Avg	1,19	1,07	1,04	0,95	0,70	0,82

TABLE A-1: DETERMINATION OF MEAN RELATIVE AND ABSOLUTE DIFFERENCES OF DELTA E VALUES

A.4. STANDARD ERROR AND SAMPLE VOLUME:

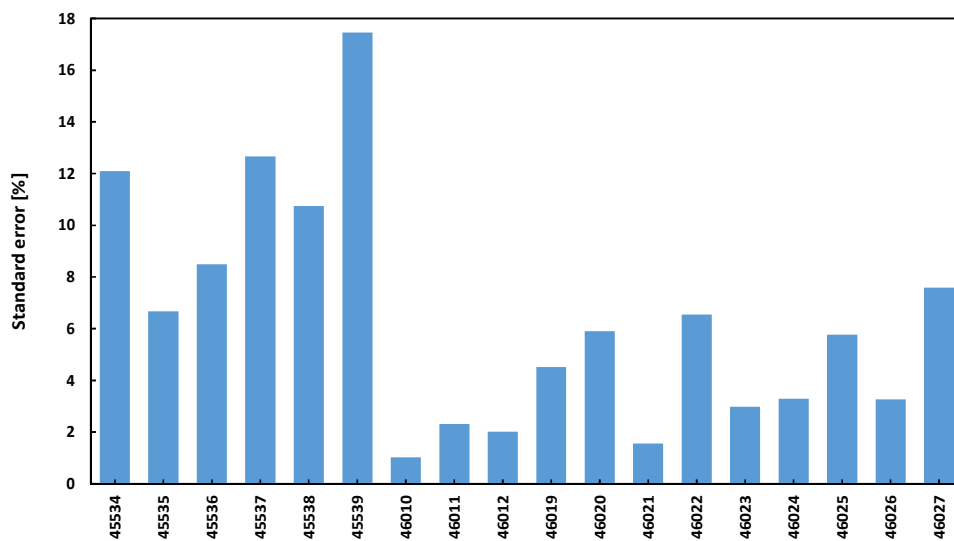


FIGURE A-5: STANDARD ERRORS OF DELTA E VALUES (FIVE MEASUREMENTS PER SAMPLE)

A.5. VARIABILITY OF MEASUREMENT DATA AND PROCESS
FLUCTUATIONS:

	Mean	Max	Min	½ (MR)_abs	½ (MR)_rel
'Basis Weight'	58,7	63,6	57,1	3,3	0,06
'Thickness'	51,7	53,8	50,3	1,8	0,03
'Density'	1,1	1,2	1,1	0,0	0,04
'Porosity'	39844	42300	20950	10675	0,27
'Bekk W.S.'	1622	2771	1213	779	0,48
'Unger'	0,8	1,2	0,5	0,3	0,44
'Cobb60 PVA side'	19,1	22,8	16,3	3,2	0,17
'Cobb60 starch side'	22,7	31,8	16,8	7,5	0,33
'IGT'	163	176	150	13	0,08
'delta E Shirlastain'	29,2	40,4	21,9	9,3	0,32
'surface pH'	5,4	5,7	4,7	0,5	0,09
'A_04'	51,4	54,3	49,3	2,5	0,05
'd_A'	32,4	34,9	30,4	2,3	0,07
'd_Acorr'	0,6	0,7	0,6	0,0	0,06
'd_V'	1,3	2,5	0,3	1,1	0,82
'd_Vcorr'	0,2	0,5	0,1	0,2	0,84
'PVA coverage '	0,9	1,0	0,8	0,1	0,06
'dE_1,3'	7,7	12,4	4,5	4,0	0,51
dE_1,0'	12,6	18,4	5,7	6,3	0,50
dE_0,7'	22,3	27,9	13,9	7,0	0,31

TABLE A-2:DETERMINATION OF THE MEASUREMENT RANGE INCLUDING 31 PAPERS (DUN LAB)

	Mean	Max	Min	½ (MR)_abs	½ (MR)_rel
'Basis Weight'	62,6	65,6	60,7	2,5	0,04
'Thickness'	55,1	58,8	53,2	2,8	0,05
'Density'	1,1	1,2	1,1	0,0	0,02
'Porosity'	41933	42300	37320	2490	0,06
'Bekk W.S.'	2578	2977	1960	509	0,20
'Unger'	0,7	1,4	0,4	0,5	0,70
'Cobb60 PVA side'	21,3	26,4	19,2	3,6	0,17
'Cobb60 starch side'	20,6	23,4	18,0	2,7	0,13
'IGT'	134	144	124	10,0	0,07
'delta E Shirlastain'					
'surface pH'	5,6	5,9	5,5	0,2	0,04
'A_04'	52,8	54,3	51,6	1,4	0,03
'd_A'	32,5	33,8	31,3	1,3	0,04
'd_Acorr'	0,6	0,7	0,6	0,0	0,04
'd_V'	0,8	1,9	0,2	0,8	1,06
'd_Vcorr'	0,1	0,3	0,0	0,1	1,07
'PVA coverage '	0,9	1,0	0,8	0,1	0,06
'dE_1,3'	10,1	13,7	7,5	3,1	0,31
dE_1,0'	16,4	23,3	12,1	5,6	0,34
dE_0,7'	29,2	36,5	21,6	7,5	0,26

TABLE A-3: DETERMINATION OF THE MEASUREMENT RANGE INCLUDING 21 PAPERS (TOY LAB)

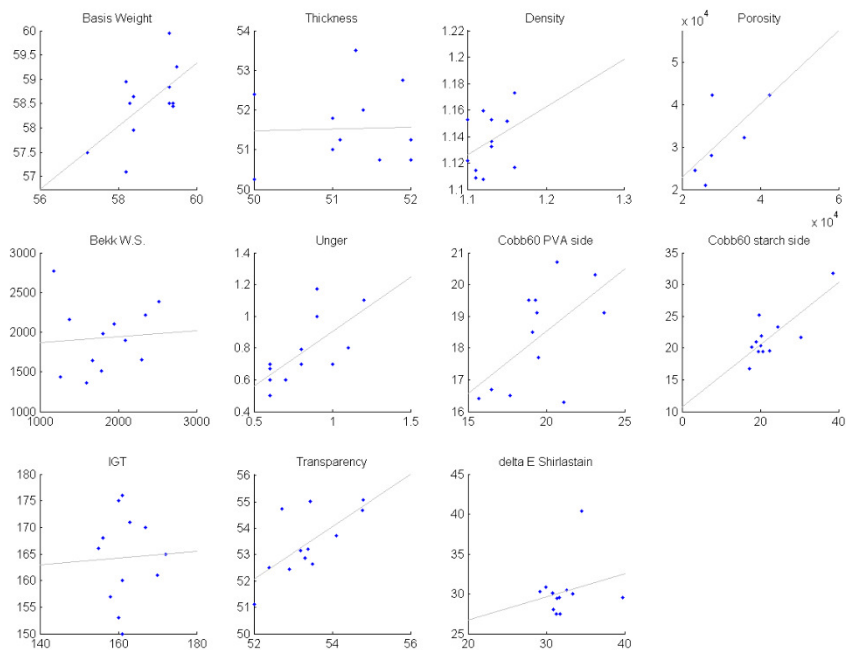


FIGURE A-6: VARIABILITY OF MEASUREMENT DATA (LARGE SCALE VARIATIONS)

A.6. PREDICTION OF SILICONE COVERAGE AND DELTA E USING MULTIPLE LINEAR REGRESSION ANALYSIS:

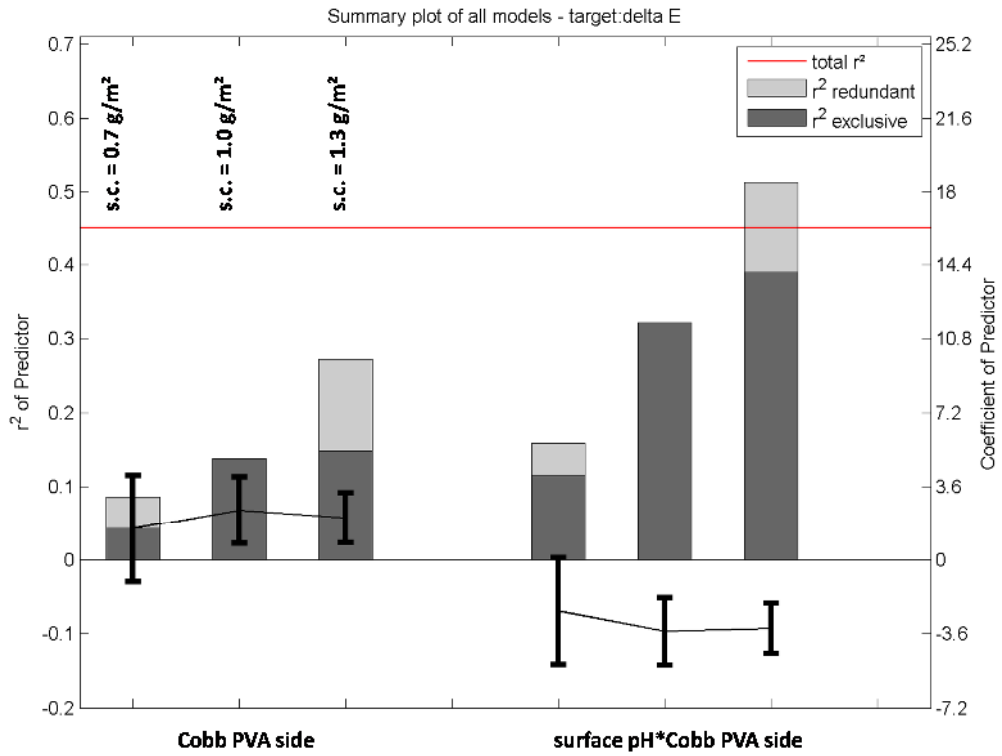


FIGURE A-7: PREFIX CHANGE CAUSED BY THE INTERACTION COBB*SURFACE PH (MLR DELTA E)

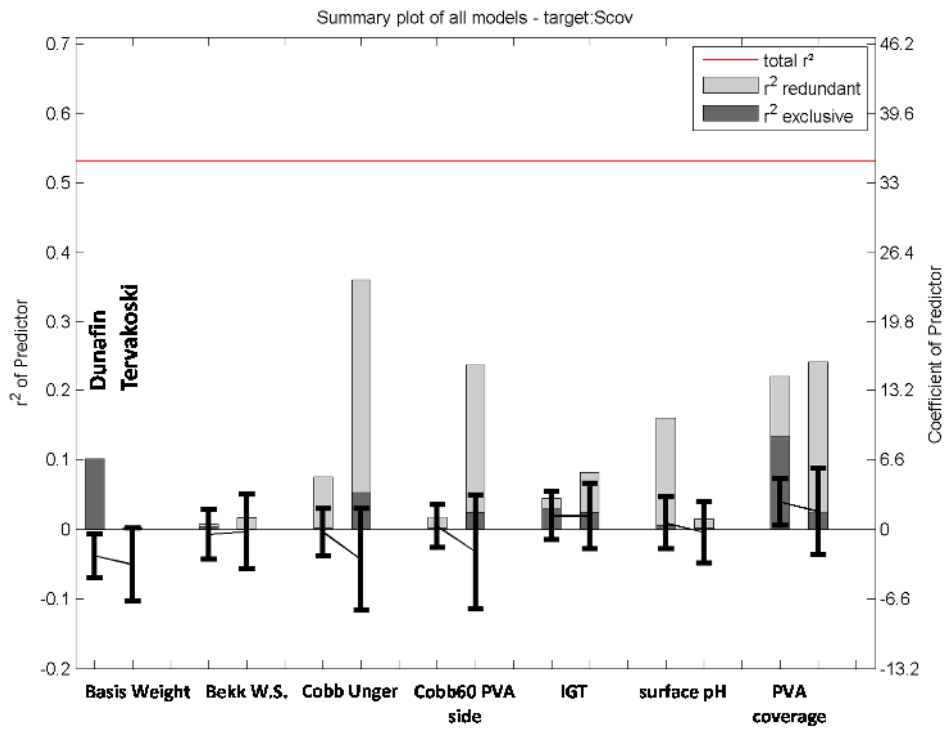


FIGURE A-8: PREDICTION OF S_{cov} WITH MLR (ALL PARAMETERS)

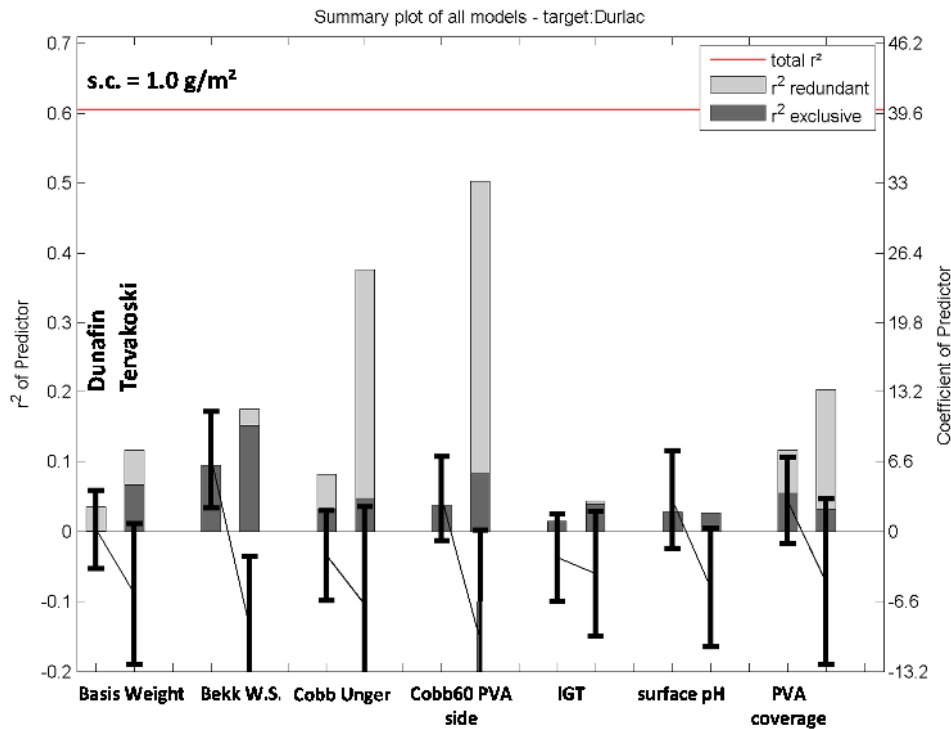


FIGURE A-9: PREDICTION OF THE DURLAC VALUE WITH MLR (ALL PARAMETERS)

A.7. EVALUATING QUALITY ISSUES OF SILICONE COVERAGE BY THE COMPARISON OF 2D DATA MAPS:

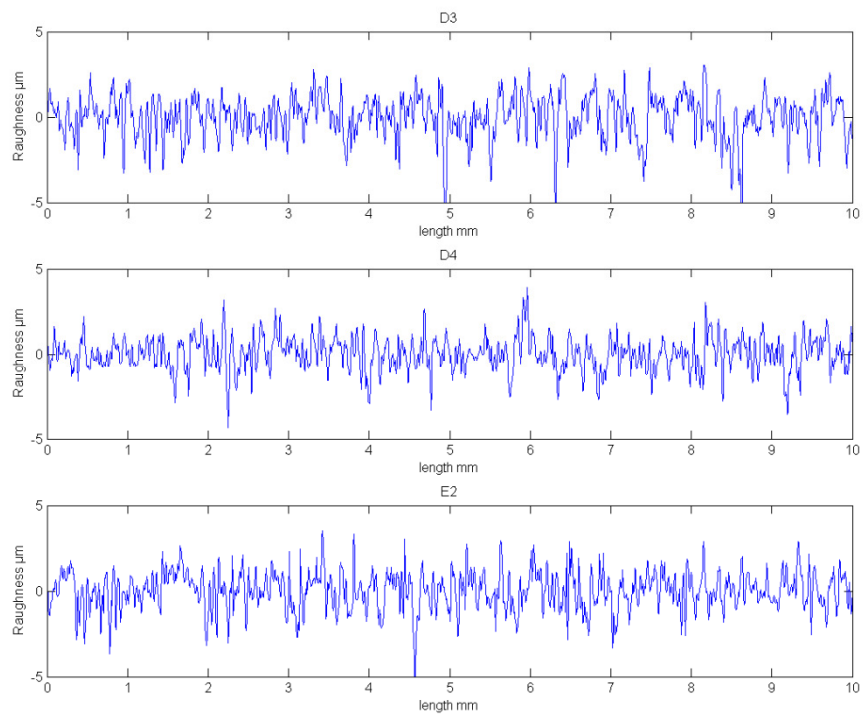
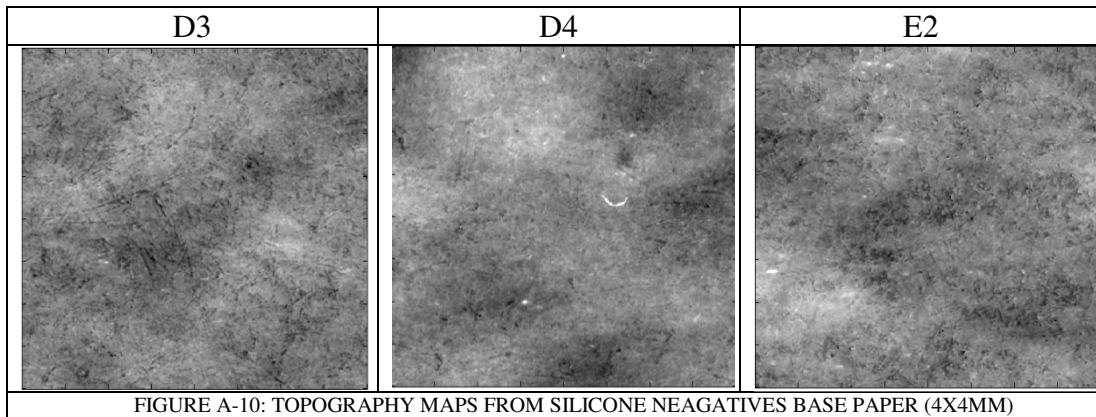


FIGURE A-11: COMPARISON OF ROUGHNESS (MAX STRUCTURE SIZE 100µM)

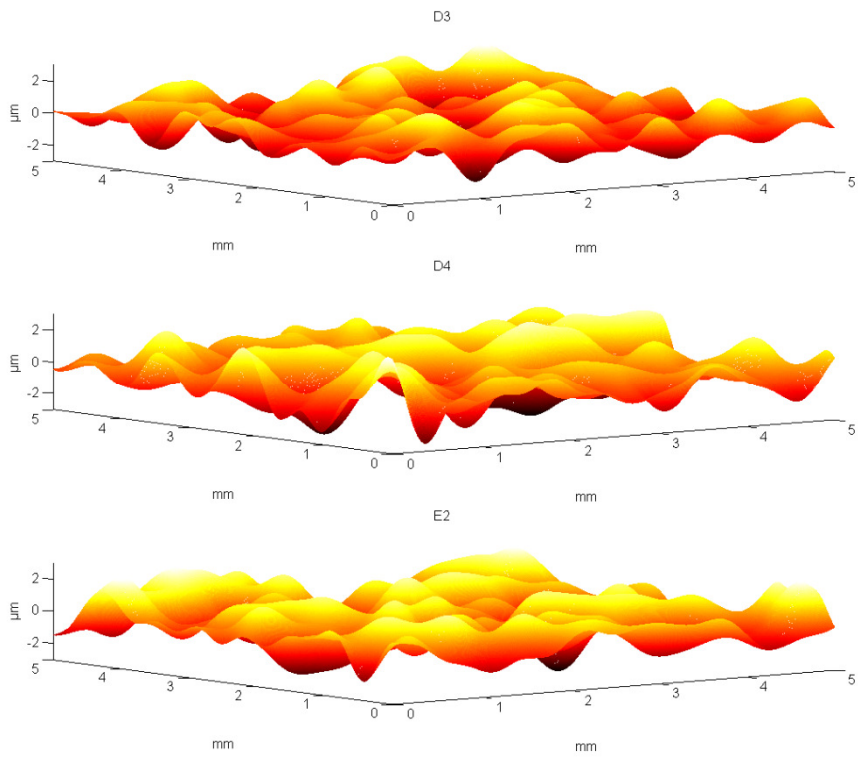


FIGURE A-12: COMPARISON OF WAVINESS (STRUCTURES BETWEEN 500 – 2500μM)

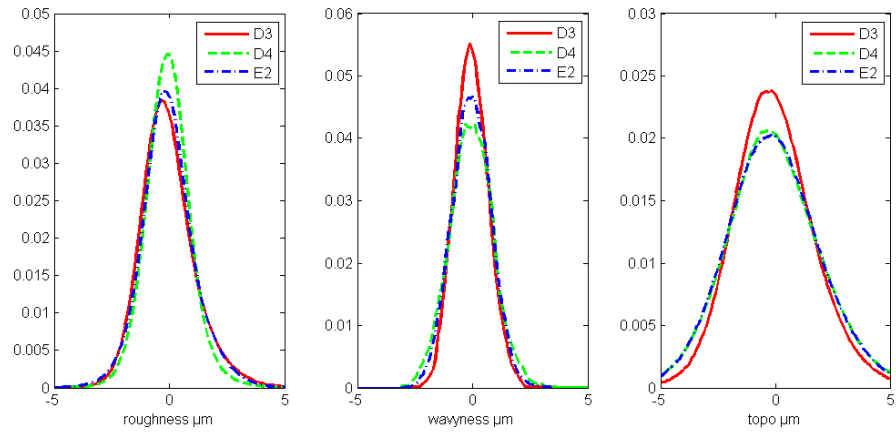


FIGURE A-13: DISTRIBUTION OF ROUGHNESS, WAVINESS AND TOTAL TOPOGRAPHY

BIBLIOGRAPHY

- [1] Kuo, A.C.M.; *Silicone Release Coatings for the Pressure Sensitive Industry - Overview and Trends*. Dow Corning Corporation, <https://www.dowcorning.com/content/publishedlit/30-1069A-01.pdf>, 29.08.2013
- [2] Kuo, A.C.M.; *Understanding Release Force*. Dow Corning Cooperation, <http://www4.dowcorning.com/content/publishedlit/30-1069c-01.pdf>, 29.08.2013
- [3] Orlych, G., M.; *Silicone-Adhesive Interactions in Release Liner Applications.*, <http://www.pstc.org/files/public/Orlych.pdf>, 02.10.2013
- [4] Lewis L., Stein, J., Gao, Y., Colborn, R., Hutchins, G; (1997); *Platinum Catalysts Used in the Silicones Industry*, *Platinum Metals Rev.*, 1997, 41, (2), S67
- [5] Andriot et al; *Silicones in Industrial Applications, Characterization of Silicones*, S10-11, Dow Corning, <http://www.dowcorning.com>, 06.09.2013
- [6] Döhler, H.; (1997); *Release coatings in the Printing Industry*. TEGO RC Silicones., http://www.tego-rc.com/product/tego_rc/en/about/papers-publications/Documents/pub_1997-12_sicoatings_hd_e.pdf, 06.09.2013
- [7] Döhler, H., Hamann, W.; (2003); *Alternative low cost release liner for label laminates*, AWA Conference, Brüssels, http://www.tego-rc.com/product/tego_rc/en/about/papers-publications/Documents/pub_2003-09_awa_hd_e.pdf, 30.08.2013
- [8] Gordon, G.V., Perz S.V., Tabler R.L., Stasser, J.L., Owen, M.J. and Tonge, J.S.; (1998); *Silicone Release Coatings: A Closer Look at Release Mechanisms*. Dow Corning Corporation, <http://www.dowcorning.com/content/publishedlit/26-016.pdf>, 29.08.2013
- [9] *Polydimethylsiloxane*, <http://ihome.cuhk.edu.hk/~b111516/PDMS.html>; 20.09.2013.
- [10] Lautenschlager, H.; (2009); *Crosslinking reactions of silicones; From fluid to rubber* Wacker Chemie AG, personal information, 27.02.2013
- [11] Hagemeister, T.; (2010); *DEHESIVE Release Coatings*. Wacker Chemie AG, personal information, 27.02.2013
- [12] Lautenschlager, H.; (2013); *More or less silicone*. Wacker Chemie AG, http://www.wacker.com/cms/media/documents/markets_brands/paper_films/dehesive_moreorless.pdf, 03.09.2013
- [13] *Homepage, Delfort Group*, <http://www.delfortgroup.com/index.php?id=43>, 08.10.2013.

- [14] Gaiero, F., (2013), *Background info*. Delfort Group, personal information, 27.02.2013
- [15] Patent CA 2786827 A1 (19.11.2011); *Cellulose fibre - based support containing a modified PVA layer and a method its production and use*, Ahlstrom
- [16]. Takács, G., Kollár, Z., Csókai, V., Szilágyi, A.; (2012); *PVA and silicone films on surface of the release paper*. iTechnologies K+F Nonprofit KFT, internal information, 07.03.2013
- [17] *Römpp online*; (2009); *Polyvinyl alcohols*, <https://roempp.thieme.de/roempp4.0/do/data/RD-16-03644>, 03.09.2013
- [18] *Römpp online* (2004), *Malachitgrün* <https://roempp.thieme.de/roempp4.0/do/data/RD-13-00311>, 03.09.2013
- [19] Bach, H., Pfeil, E., Philipp, W., Reich, M.; (1963); *Molekülaufbau und Haftung substantiver Farbstoffe*, *Angew. Chem./75.Jahrg.1963/Nr.9*.
- [20] *L*a*b* colour space*, <http://www.mappe.de/blog/fachbegriff-der-woche-2.html>, 09.11.13.
- [21] Hirn, U., Lechtaler, M., Bauer, W.; (2008); *Registration and point wise correlation of local paper properties*. *Nordic Pulp and Paper Research Journal* Vol 23 no. 4/2008.
- [22] Wind, E. (2011) *Untersuchung der Ursache für kleinräumige Druckbildstörungen im Heatset Web Offset Druck an ungestrichenen Papieren*, S 61, Graz, University of Technology, Paper, Pulp and Fiber Technology, Diss., 2011
- [23] Hirn, U., Lechtaler M., Wind E., Bauer, W.; (2009); *Linear regression modelling of local print density in gravure printed SC papers*. *Papermaking research symposium*, 2009
- [24]. *Test method 31*; (1997); *Determination of silicone coverage with "Shirlastain A"*, Rhone - Poulenc silicones UK test method for paper release products.
- [25] *Tappi T529 om-99*; (1999); *Surface pH measurement of paper*
- [26] *Determination of the delta E value*, internal test method, Dunafin, 22.10.2013
- [27] *PVA in paper*, internal test method, Tervakoski, 30.07.2013
- [28] *IFM Manual IFM 2.2 EN 23.01.2008*. (2008)
- [29]. FINAT, <http://www.finat.com/en/Knowledge/FINAT-publications/Technical-Handbook.aspx>; 10.09.2013